AN ABSTRACT OF THE THESIS OF

Douglas James Hunsaker for the degree of Master of Science

in Agricultural Engineering presented on February 27, 1984

Title: An Investigation of Furrow Advance Rates

_____Under Surge Flow Irrigation_____

Abstract Approved: ## Redacted for privacy

Marshall J. English

The intermittent or cyclic application of water to furrows or borders, a method known as "surge flow irrigation", can significantly improve the advance characteristics of surface irrigation. Numerous field studies have shown that the advance of furrows is considerably more rapid when irrigated by surge flow than by the conventional, continuous flow method. In addition, the advance rates of surge flow have been found to be less variable among furrows than by those of continuous flow. Furthermore a large difference between surge and continuous flow is generally seen in the volume of water required to complete the advance phase. These facts have led researchers to conclude that surge flow may be capable of significantly improving the efficiencies of surface irrigation.

Two field experiments were conducted in southern Oregon during the 1983 irrigation season to investigate advance rate differences between surge flow treatments

involving three different on-off time ratios and a contin-
uous stream with an equal instantaneous discharge rate.
Field data were used to construct power functions for
each individual treatment relating advance time and
advance distance. The derived power functions formed the
primary basis from which the treatments were compared.
The average advance-time and standard deviation for each
treatment at designated stations along the furrow run
were used in evaluating the variation in advance rates
among treatments.

The results of the field experiments, which were
consistent with findings of other surge flow researchers,
indicated that surge flow increased advance rates,
significantly reduced water use in advance, and improved
the advance uniformity among furrows. The experimental
results will be submitted to others involved in surge
flow research.

To support the experimental studies, a computer
model was developed and programmed to simulate both
surge flow and continuous flow advance. The model was
run for a continuous and a cycled flow with the model
input based on the conditions during the second field
experiment. In both cases the model underestimated the
observed field advance. However, the infiltration input,
which has a tremendous effect on the model results, had
to be estimated from the observed field advance data
rather than experimentally evaluated.

AN INVESTIGATION OF FURROW ADVANCE RATES UNDER SURGE FLOW IRRIGATION

by

Douglas James Hunsaker

A THESIS

submitted to

Oregon State University

in partial fulfillment of
the requirements for the
degree of

MASTER OF SCIENCE

Completed February 27, 1984

Commencement June 1984

APPROVED:

Redacted for privacy

_____
Associate Professor of Agricultural Engineering
   in charge of major

Redacted for privacy

_____
Head of Department of Agricultural Engineering

Redacted for privacy

_____
Dean of Graduate School

Date thesis is presented: February 27, 1984

Typed by Lyn Hunsaker for Douglas James Hunsaker

ACKNOWLEDGEMENT

CONTENTS

LIST OF FIGURES

LIST OF TABLES

AN INVESTIGATION OF FURROW ADVANCE RATES
UNDER SURGE-FLOW IRRIGATION

I. INTRODUCTION

Surge flow is a new and promising surface irrigation
technique capable of significantly improving the water
advance characteristics of furrow irrigation. Numerous
field studies have shown that the advance in furrows is
considerably more rapid when irrigated by surge flow than
by the conventional, continuous flow method; and thus
surge flow can reduce the intake opportunity time differ-
ences between the upper and lower ends of the furrow run
(Bishop, et al., 1981). In addition, the advance rates of
surge flow have been found to be less variable among
furrows than by those of continuous flow. Equally impor-
tant, a large difference between surge and continuous flow
is generally seen in the volume of water required to com-
plete the advance phase. In some of the cases reported,
the volume of application for surge flow to complete
advance was from 38% to 56% of the volume used by contin-
uous flow (Coolidge, et al., 1982).

The implications of initial surge studies are that
surge flow offers an opportunity to increase surface
irrigation efficiencies; possibly to levels normally
associated with sprinkler and drip irrigation. However,
surge flow systems, which can be fully automated, would
not require the high energy costs associated with the

operation of pressurized systems and might not involve the high capital costs of drip systems (Walker, et al., 1982).

The surge flow technique consists of applying water intermittently to the furrow, rather than continuously. A complete on/off cycle, i.e., the time from the beginning of one surge to the next, is typically from 10 to 60 minutes long. The ratio of the on-time to the complete on/off cycle can be any desired value, although the ratio used in previous field studies has generally been between 0.25 and 0.75 (Bishop, et al., 1981; Coolidge, et al., 1982).

The exact mechanisms responsible for the surge flow phenomenon have not been clearly identified and the subject is under current investigation. Nevertheless, researchers have generally agreed that the cyclical application of water to the furrow decreases the permeability of the soil surface layer and thereby reduces the soil intake rate (Bishop, et al., 1981). Apparently the infiltration characteristics are altered during the off portion of the surge cycle following a short drainage period of at least five minutes (Coolidge, et al., 1981; Walker, et al., 1982). Because of the reduction in intake rate at previously wetted furrow sections, subsequent surge applications of water can advance in the furrow at increasingly greater rates.

To date, a large number of surge flow experiments have been carried out in Utah, Idaho and Colorado which,

by and large, have demonstrated the superiority of surge flow over conventional surface irrigation. However, surge flow performance varies widely from location to location since its effects are dependent not only upon the surge flow parameters (furrow inflow rate, field length, slope, on-off durations), but also upon the soil intake characteristics and field conditions at the particular location (Walker, et al., 1982). As a result surge flow research has been expanded on a regional scale in a cooperative effort to provide surge flow data from experimentation conducted over a wide range of conditions from which optimum design criteria can be established. Currently, the regional project includes many western and mid-western states which are expected to conduct field investigations under typical cropping and physical conditions in each locality.

This thesis project represents Oregon State University's initial surge flow research involvement in that regional project. Two field experiments, carried out during the 1983 growing season at a test site near Medford, Oregon, were focused on advance time differences between surge flow treatments involving three different on-off time ratios and a constant stream with an equal instantaneous discharge rate. The experimental results will be submitted to other researchers involved in the regional project, along with the advance-time relationships derived from the field data for each treatment.

To support the experimental studies, a computer model based on the kinematic-wave approximation method was developed and programmed to simulate the advance, recession and infiltration processes for both continuous and surge flow regimes. The model was run for a continuous and a cycled flow with the model input based on the conditions (physical, flow rate, cycle time) during the second field experiment. However, the infiltration input, which was not determined at the time of the experiment, was estimated from the actual observed advance data.

The results of the two field experiments were consistent with the findings of other surge flow researchers. In the second experiment, advance was considerably faster in furrows irrigated by surge flow than in furrows irrigated continuously. Surge flow advance was also faster in the first experiment, although the difference was not as pronounced as in the second. In all trials, advance was accomplished with less water using surge flow than with continuous flow. A comparison of the advance variation within treatments of the second experiment showed that the advance rate differences were substantially less under surge flow than under continuous flow.

The observed continuous and surge flow advance from the second experiment and the model predictions of advance were generally consistent. However, the model underestimated advance in both cases, although more so in the case of continuous flow. Nevertheless, the results of the

model runs are encouraging in view of the fact that the infiltration function parameters were derived from the field advance observations rather than experimentally determined.

II. LITERATURE REVIEW

Introduction

Surface irrigation is the most widely used method of irrigation in the United States. Currently, surface methods constitute approximately two-thirds of all irrigated land in the U.S., and it is used to an even greater extent in other parts of the world (Jensen, et al., 1980). Most likely the use of surface irrigation, even with the rise in popularity of sprinkler and drip system, will not decrease. Inherently, surface systems are the least energy intensive of all methods, and thus the desireability of surface irrigation becomes increasingly evident in light of the foreseeable shortages and high cost of energy (Stringham and Keller, 1979; Jensen, et al., 1980).

Unfortunately, most surface irrigation systems at the present time are inefficient, with typically 50 percent or more of the applied water lost in the forms of surface runoff and deep percolation (Strelkoff and Katopodes, 1977). However, the associated inefficiencies are not directly attributable to the surface irrigation method, but rather are often the result of an inferior system design or poor management practices (Stringham and Keller, 1979). This is particularly true where water is relatively inexpensive and labor demands are high. Because current non-automated surface systems require a great deal of time and labor in the field, many farmers with a tight overall farm labor

schedule are simply unable to maintain a positive control on the irrigation operation (Bondurant and Humpherys, 1962). As a result irrigation efficiency suffers.

Highly correlated with the poor efficiency record of surface irrigation is the problem of non-uniform water distributions. In many cases the non-uniformity results from an inadequate system design, though variable soil intake rates can contribute significantly. Often in surface irrigation adequate water application at the lower end of the field requires excessive applications at the upper end of the field, some of which is eventually lost through deep percolation. On many occasions, particularly in soils of relatively high intake rates, overland flow may not even reach the lower end of the field.

For the past two decades considerable attention has been given to the design of surface irrigation systems which would improve the uniformity and efficiency of irrigation. More recent attention has been focused not only on water utilization, but also on minimizing labor requirements through automation. Ultimately, continued energy savings gained from surface irrigation may well depend on the ability to produce fully automated surface systems (Stringham and Keller, 1979).

The Surge Flow Concept

The time during which water advances from the upper
end of an irrigated run to the lower end is that portion
of the total surface irrigation known as the advance phase
(Jensen, et al., 1980). Because of its bearing on the
intake opportunity time (the time water is available for
infiltration) at any point along the run, the advance phase
greatly influences the uniformity, and thereby the efficien-
cy, of the irrigation (Bishop, et al., 1981). However, in
the past the advance phase has presented serious problems
to many irrigators. Exceedingly slow advance rates and
wide variability in advance rates across the irrigated area
are two primary examples. An inability to complete the
advance phase has been a major difficulty encountered by
some irrigators. For these reasons much attention has been
given to the study and understanding of the advance phase.

For many years cutback systems have been used in furrow
irrigation to achieve quicker advances. A large inflow
stream is applied during the advance phase to minimize in-
take opportunity differences between the upper and lower
end of the run. Upon the completion of the advance phase
the stream size is then reduced (intake phase) to minimize
surface runoff and deep percolation losses. Incorporating
tailwater recovery systems such as those developed by Bon-
durant (1969) and Stringham (1975) has increased the capa-
bility to virtually eliminate runoff losses during the

intake phase. It is now widely recognized that properly designed and managed cutback systems can attain high uniformities and application efficiencies (Nicolaescu and Kruse, 1971). However, since the optimal design of a furrow irrigation cutback system may involve several inflow stream size reductions, the improvement in efficiency and uniformity is gained at the expense of increased labor and flow regulation complexities (Jensen, et al., 1980). Therefore, automatic control as a further improvement to the furrow irrigation cutback system has been a concern of many investigators over the past twenty years.

Bondurant and Humpherys (1962) presented an automated open ditch surface irrigation method consisting of mechanized gates controlled by either a timing or moisture-sensing device. Garton (1964) and his co-workers designed an automated furrow cutback system involving mechanically operated check dams located in a concrete lined head ditch which was constructed as a series of level bays. Within each bay furrow-outlet tubes were set at the same elevation. The difference in elevation between each bay was equal to the head required on the inlet tubes at initial and cutback flow. By mechanically inserting or removing a check dam, the head in the bay could be regulated to produce either initial or cutback flow to the furrows.

Perhaps the most important innovation produced by all previous automated furrow irrigation research has been the successful development by both Fischbach (1970) and

Humpherys (1975) of pneumatic control valves for surface irrigation pipelines. These control valves attached to a closed conduit (gated-pipe) system can be opened and closed with air pressure actuated by electrically controlled solenoids. Thus by automating the valves the gated-pipe system could distribute water to individual furrows, or when the valves are closed, transport water through the pipeline.

Research in 1978 to improve automated furrow cutback irrigation led Professors Glen Stringham and Jack Keller at Utah State University (USU) to the concept of surge flow irrigation. It had been found that automated valves could be effectively operated fully opened or closed, but did not operate well when partially opened. They concluded that the cutback stream might be reduced on a time basis by cycling the valves on and off. They anticipated, for example, that the furrow streamsize produced from a continuously full-open valve could be reduced by one-half if the valve was alternated between fully open and fully closed for equal time durations. A prototype automated gated-pipe system was installed at USU using commercially available components and an electronic controller developed in conjunction with the USU Electrical Engineering Department. High pressure sprinkler valves modified for low pressure operation were attached to the gated-pipe and served as the furrow control valves. Subsequent tests of cycled flows to the furrows demonstrated that almost any desired average

stream size could be achieved by varying cycle times any-
where from a few seconds to hours (Stringham and Keller,
1979).

The most striking and surprising observation encounter-
ed during these tests was the impact that the cycled flows
had on the furrow advance rates. In a series of prelimin-
ary tests, Stringham and Keller recorded advance times for
three separate flow treatments consisting of four furrows,
each 660 ft (201 m) in length. Within each treatment were
two compacted furrows denoted as "wheel furrows" and two
furrows which were not compacted, denoted as "non-wheel
furrows." Valves for all three treatments were set to give
an instantaneous discharge of 13 gpm (0.82 l/s) with one
treatment allowed to flow continuously at that discharge
rate. The second treatment was cycled on and off at eight
second intervals, while the third treatment was cycled at
a rate of 16 seconds on and eight seconds off. Thus,
treatments two and three had time averaged flow rates of
approximately 50 and 67 percent of the continuous flow rate,
respectively.

Figure 1 shows the plotted advance times for the non-
wheel furrows. Although less apparent, the wheel furrow
advance data indicated the same general trend as the non-
wheel data (Stringham and Keller, 1979). Of particular
interest, as observed by Stringham and Keller, was that
the advance of the 16-8, on-off cycled flow was markedly
faster than the continuous flow advance. Not only did this
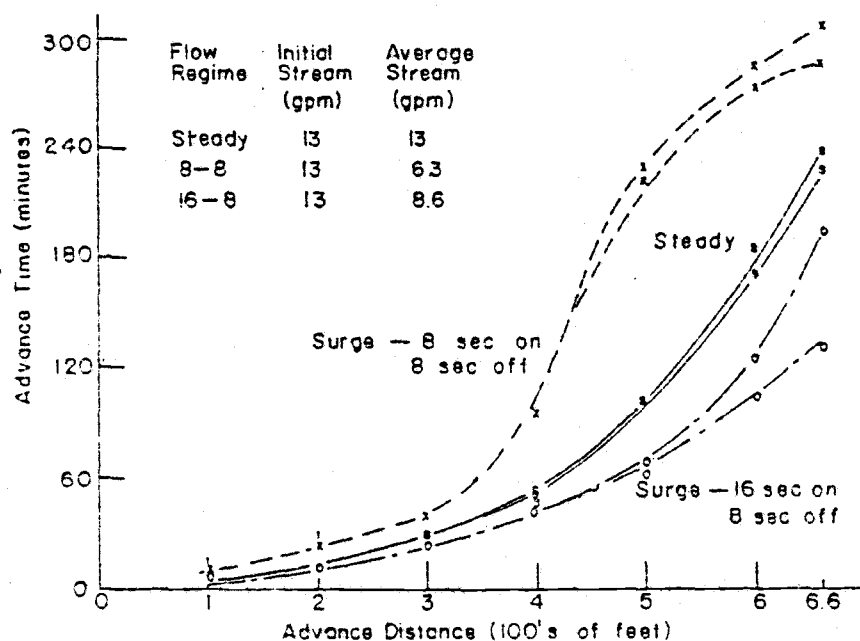
Figure 1. Advance data for steady flow, surge flow
cycled at 8 seconds on and 8 seconds off,
and surge flow cycled at 16 seconds on
and 8 seconds off (from Stringham and
Keller, 1979).

cycled flow wet the entire furrow length in less time, it required less than 67 percent of the volume of water required by the continuous flow stream. Also noteworthy was the performance of the 8-8 cycled flow. Although having an average flow rate half as great as the continuous flow stream, it maintained nearly the same advance rate over the first 300 ft (91.5 m) of furrow length as the two other flow regimes.

Stringham and Keller, recognizing the profound effect cycling inflows had on advance rate, called the technique 'surge flow' to distinguish it from all other surface irrigation methods. They felt that if subsequent testing could replicate the surge flow phenomenon, the technique might have the potential to dramatically improve furrow irrigation uniformities and efficiencies. Furthermore, they concluded that with surge flow it might be possible to significantly increase furrow length, thus decreasing to some degree the number of irrigation sets and the associated labor requirements of many operations.

Research Progress

Between the time in which the idea was first conceptualized by Stringham and Keller and the present time, some progress has been made towards the understanding and development of surge flow irrigation. The initial studies of surge flow raised many questions. Some of the key questions asked were:

1. What are the effects of surge flow on advance
    rate? Will surges separated by short time inter-
    vals be more effective in increasing the advance
    rate than surges separated by longer time spans?
    What cycle ratio and duration will optimize the
    system? What should be the instantaneous inflow
    rate?

2. What are the effects of surge flow on the infil-
    tration process? How does it affect the permeab-
    ility of the soil?

3. What is the hydraulic geometry and behavior of the
    surge wave as applied to surge flow irrigation?

4. How does surge flow affect soil erosion?

Questions such as these and others formed the basis
for ongoing surge flow research at Utah State University.
A full-scale research program was launched at USU during
the cropping season of 1979. By the end of the 1981 crop-
ping season, many additional field tests had been conducted
by USU researchers. The testing was designed primarily to
compare surge flow applications to conventional furrow
irrigation, and it was later broadened to cover a wider
range of soil types, slopes, and inflow rates common to
surface irrigation in that locality. During this period
numerous measurements of advance, infiltration, recession,
and runoff were recorded and evaluated. All USU field
testing through 1981 indicated considerable advantages for
surge flow over the conventional continuous flow method

(Bishop and Walker, 1981).

Allen and Poole, in separate tests at the USU Dairy Research Farm conducted field experiments focused on advance times. The site was planted to corn in soil classified as a silt loam. Test furrows spaced 30 in (0.76 m) apart, 600 ft (183 m) long, and which sloped 1.46% on the average were alternatively wheeled and non-wheeled. In both tests time-averaged flow rates for the surge furrow streams were the same as the instantaneous flow rate of the continuous stream furrows. This was achieved by adjusting the instantaneous flow for the surge furrow streams to the appropriate rate depending on the desired cycle ratio[1] (Bishop, et al., 1981).

In Allen's tests a continuous stream size of 10 gpm (.63 l/s) and three surge stream sizes of 15 gpm (.95 l/s), 20 gpm (1.26 l/s), and 30 gpm (1.89 l/s) at cycle ratios of two-thirds, one-half, and one-third, respectively, were applied simultaneously to the furrows. Thus, an equal volume of water was applied to each furrow over a given time. The cycle time (the time from the beginning of one surge to the next) for all of Allen's tests was 10 minutes. Similarly, Poole tested a 10 gpm (.63 l/s) continuous stream with surge streams of 20 gpm (1.26 l/s) at a cycle ratio of one-half. However, in this case the surge flow

---

1 The cycle ratio is the ratio of the on time to a complete on/off cycle.
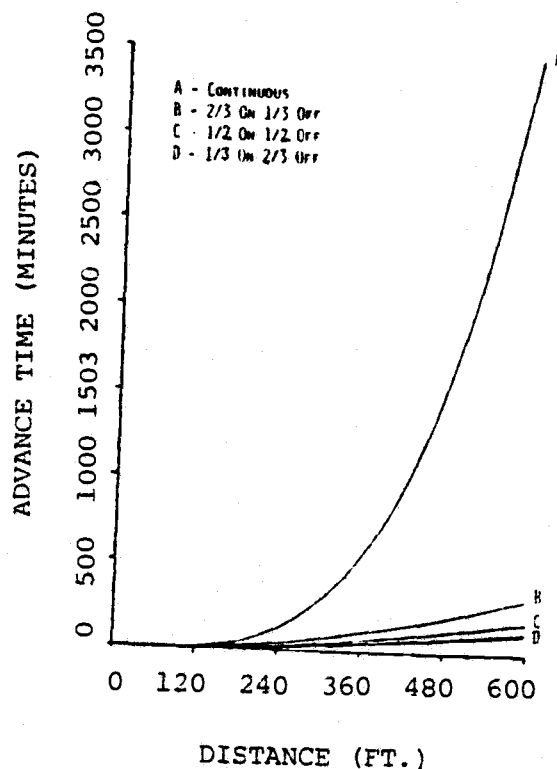
Figure 2. Advance rates under continuous and variable cycle ratio surge flow treatments of newly formed non-wheel furrows during first irrigation (from Bishop, et al., 1981).

cycle times were varied at 2, 5, 10, and 20 minutes. As in Allen's test, all furrows received an equal quantity of water during the test (Bishop, et al., 1981).

The various treatments were applied to randomly selected furrows and replicated several times over the field to eliminate spatial variability. Linear regression was used to fit power functions to advance data for each replication within a treatment. A mean relation for each treatment was determined by numerically averaging the logrithmically transformed power function coefficients. Figure 2 shows the plotted advance curves for non-wheel
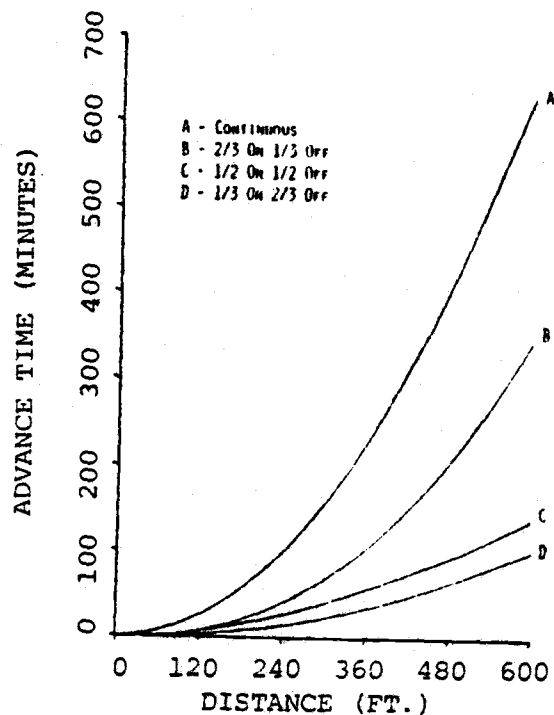
Figure 3.   Advance rates for continuous and variable
cycle ratio surge flow treatments of
non-wheel furrows during second irrigation
(from Bishop, et al., 1981).

furrows from the experiments conducted by Allen during

the first irrigation, and Figure 3 shows the advance

curves for the same test of the second irrigation.   A

decisive advantage for all surge flow treatments over the

continuous flow was evident, especially during the first

irrigation where the time required to complete the advance

phase for the continuous stream was nearly ten times

greater than for the surge streams.   The results of the

second irrigation indicate that the advantage for surge

flow was not as significant in this case.   The results

from Poole's tests demonstrated the same advantage for

the surge flow treatments (Bishop, et al., 1981).

Perhaps equally significant, as observed over the course of the 1979 growing season by both Allen and Poole, was the large variation in time required by the continuous flow streams to complete the advance phase, and the relatively small time differences for the surge flow streams regardless of irrigation number, field location, or compaction history. Including all experiments by Poole and Allen, advance times ranged from 270 - 3,490 minutes for the continuous flow furrows, whereas for the 20 minute cycled flow of Poole's tests, the advance time ranged only from 60 - 130 minutes; a remarkable difference in advance time variation between the two treatments (Bishop, et al., 1981).

The results of the 1979 field tests caused considerable excitement. It was felt that this was a major development in surface irrigation. Consequently, surge flow research at USU was intensified in 1980 and 1981. As the field testing undertaken during 1979 had involved the same time-averaged streams for all treatments, one important unanswered question remained; whether the differences in advance rates were due to the cyclical applications or to the higher instantaneous discharge rates of the surge flow treatments. Subsequent tests therefore addressed this question by comparing continuous streams with surge streams having the same instantaneous discharge rate (Walker, et al., 1982).
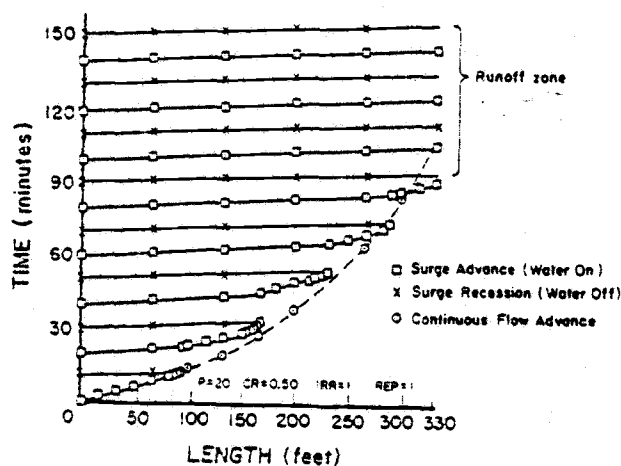
Figure 4. Advance length and recession with time for surge flow for cycle period of 20 minutes and cycle ratio of 0.5 with comparison to continuous flow advance (from Bishop and Walker, 1981).

In 1980, surge tests were carried out by Coolidge on a field of silt loam soil having an average slope of 1%. All furrows received an instantaneous discharge rate of 5 gpm (.32 1/s) and continuous flow was compared to surge flow using on-times of 5, 10, and 20 minutes, and off-times of 5, 10, 20, and 40 minutes. The resulting field data indicated that the surge flow streams advanced faster than the continuous streams even at the same instantaneous flow rate. Figure 4 illustrates a typical furrow advance test from the 1980 growing season, and shows that the amount of time required for a 20-minute cycle time, one-half cycle ratio surge to complete the 330 ft (100 m) of advance was 83 minutes. The continuous stream completed the advance in 108 minutes while using two and one-half times the water required for the surge to complete the

advance (Bishop and Walker, 1981).

It became increasingly obvious to those conducting the USU research that the surge flow technique affected the infiltration characteristics of the soil differently from continuous flow (Bishop, et al., 1981). Therefore, along with advance and recession data, the 1980 tests included runoff measurements intended to more clearly define soil intake differences among the furrows irrigated by the two methods. The runoff hydrograph for the 20-minute cycle time surge flow furrow of Figure 4 was compared with that of the continuous flow furrow. The hydrographs indicated that the surge flow method was able to produce runoff at a rate slightly greater than 3 gpm (.19 l/s) within three surges after reaching the end of the furrow run. The continuous flow furrow, however, yielded runoff at a rate never greater than 1 gpm (.06 l/s) (Bishop and Walker, 1981). This and other field data evaluations led to the conclusion that the infiltration rate was not only affected, but significantly reduced by the surge flow technique (Walker, et al., 1982).

It has been theorized by Bishop, Walker, and others conducting the USU Research that it is during the off portion of the surge cycle that the infiltration process is effected. During this interval following a short drainage period, previously dispersed soil particles and sediment in the furrow bottom rapidly consolidate under tension forces, progressively developing a surface seal,

thereby reducing the soil layer permeability (Bishop, et al., 1981; Walker, et al., 1982). Other mechanisms may be responsible for the intake reduction characteristic of surge flow, such as air entrapment between surges. Another suggestion has been that infiltration between surges may reduce the furrow roughness thus lowering the intake during the next surge (Coolidge, et al., 1982). Whatever the exact mechanisms are, the affects of surge flow on the infiltration rate of the furrow has been most apparent.

An interesting qualitative observation of the intake rate reduction of surge flow occurred to researchers while examining the furrow advance characteristics of the two flow regimes. In a dry, rough soil the first surge stream exhibits the same advance behavior as the continuous stream. Referring again to Figure 4, it is seen that during the first surge cycle (dry advance) both streams advanced at nearly the same rate. However, the second surge advanced relatively fast over the previously wetted section of the furrow. As the wetting front crossed the wet-dry interface, the second surge stream advance declined to an advance rate essentially the same as that during the initial surge cycle. In fact, all subsequent surges contacting a dry section of furrow demonstrated this general trend; advancing quickly over a previously wetted furrow section and maintaining the initial surge advance rate over the dry section. By comparison, the

advance rate for the continuous stream furrows declined steadily over time (Bishop and Walker, 1981).

In 1981 USU expanded research to three new test sites outside of Logan, Utah. This additional testing revealed more favorable evidence of surge flow superiority. The new locations, which provided a wider range of slope, soil type, and field length, broadened the studies to a greater extent. Since previous field testing had been concentrated in one location, researchers were concerned with the applicability of surge flow to more diverse field conditions. As in previous work, the 1981 field research involved the advance, recession, infiltration, and runoff measurements of both irrigation methods. However, a much greater emphasis was now given to precise infiltration measurements resulting in the development of a small recirculating infiltrometer at USU. This new apparatus (described by Walker, Malano, and Replogle, 1982) provided researchers with the capability to accurately measure furrow intake under conditions truly representative of the actual flow regimes and field conditions (Bishop and Walker, 1981).

Of the three new locations, perhaps the most significant results occurred near Flowell, Utah during a first irrigation on a sandy loam soil planted to corn. Surge and continuous flow treatments were applied to moderately sloping, non-wheel furrows 1180 ft (360 m) long, at an instantaneous flow rate of 32 gpm (2 l/s). One set of

furrows, which received a 20-minute on/20-minute off surge cycle, completed the advance phase in about an eight hour time period during which water infiltrated to an average equivalent depth of just over 2 in (5 cm). By contrast, the continuous flow furrows not only failed to complete the advance within this time period, but had essentially stopped advancing at 800 ft (244 m), or about three-quarters the length of the field. More notably, an average equivalent depth of 6 in (15 cm) had been applied to the furrows irrigated by the continuous flow method (Bishop and Walker, 1981; Walker, et al., 1982).

The infiltrometer data collected at all three test sites during the course of the 1981 season were evaluated and the results verified earlier assessments that surge flow improved advance time by reducing furrow infiltration rates. In all cases it was found that the cycled water applications decreased the rate of infiltration. A typical result from the Flowell location is shown in Figure 5 depicting the intake differences between surged and continuous flow applications. The dimensionless intake rate, defined as the ratio of the average intake rate to the average intake during the first surge cycle, when plotted as a function of intake opportunity time dramatically illustrates the intake reducing effect of surge flow (Walker, Malano, and Replogle, 1982).
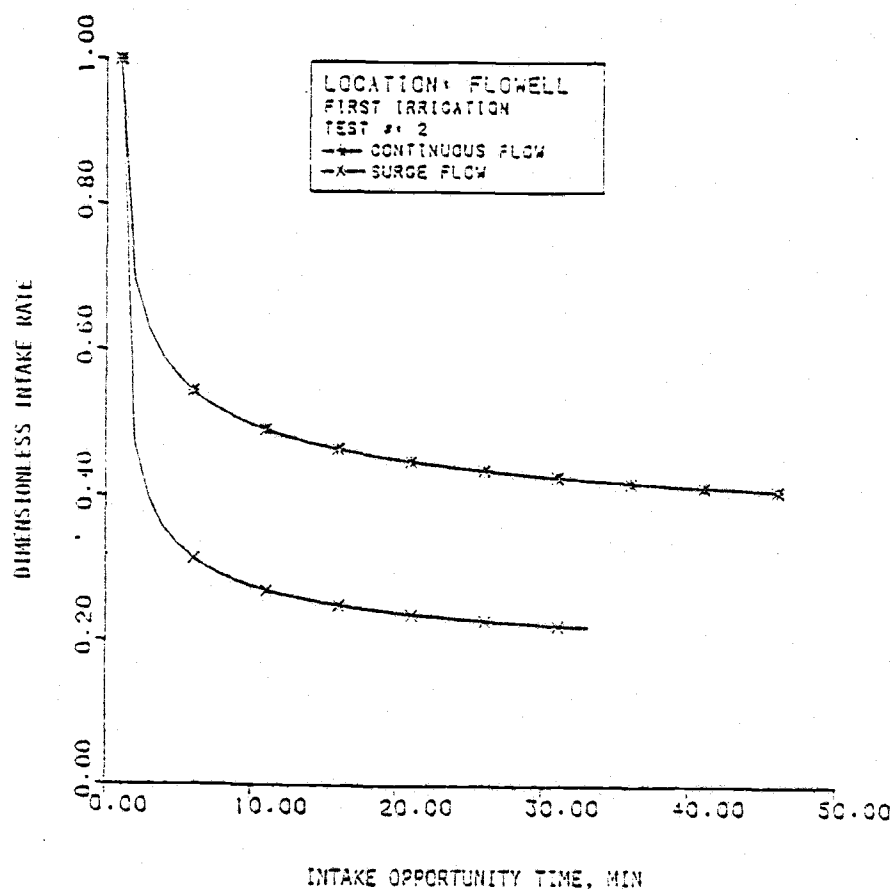
Figure 5. Dimensionless intake rate curves for
Flowell experiment, test No. 2, first
irrigation (from Walker, Malano, and
Replogle, 1982).

Regional Expansion

Since its conception, surge flow irrigation, through intense research efforts at USU, has demonstrated a number of significant advantages over conventional surface irrigation practices. Studies have indicated that surface irrigation by surge flow may substantially reduce the time required to complete the advance phase, increase the uniformity of advance across the field and throughout the season, and improve the uniformity of water penetration in the soil. During the advance phase, water requirements have been shown to be greatly reduced by surge flow.

Although much has been learned concerning the surge flow process many questions remain unanswered. Preliminary field studies undertaken in Colorado, Washington, and Idaho during 1981 have shown a wide variation in the performance of surge flow irrigation. Other important aspects of surface irrigation practices such as erosion, fertilizer leaching, and crop yields have received only a limited amount of attention. Design criteria, implementation, economic feasibility, and farmer acceptance are just some of the many concerns to those involved with the development of the surge flow technique (Walker, et al., 1982).

Therefore, in the fall of 1981 plans were formulated to broaden and intensify surge flow irrigation research on a regional scale. The regional project now includes many western and mid-western states participating in

efforts to add field and laboratory research to the existing programs. It is anticipated that the regional project will provide a large data base of surge flow experimentation applied over a wide range of soils and field conditions from which optimum design criteria (flow rates, length of run, cycle times, and cycle ratios) can be selected.

All states participating in the regional project are expected to conduct field investigations under various cropping and physical (soil, slope, length of run) conditions at locations in the respective states. Some will conduct laboratory studies directed at understanding the principles involved in intake processes under continuous and surge flow applications. Another objective of the regional study is the development and verification of models incorporating the processes of surface and sub-surface hydraulics associated with the continuous and surge flow regimes. The development of automated equipment and control systems for the implementation of surge flow systems will be undertaken by those with expertise in this area, while others will assess and evaluate the economic feasibility and operational effectiveness of surge flow systems in commercial applications. The final phase of the project will begin following the conclusion and evaluation of all previous work. At this time the principle effort will be on the formulation of system design criteria and procedures based on the translation of

the regionalized field data, laboratory studies, model generation, etc. (Walker, et al., 1982).

Development plans for this thesis, which represents Oregon State University's (OSU) initial participation in the regional project, began in spring, 1982. Over the next 12 months work was directed towards the preparation of the experimental surge flow studies to be carried out in 1983. This included the acquisition of a test site in Oregon suitable to the study purposes, the purchase, design, and installation of a gated-pipe distribution system, and the establishment of the experimental operations and procedures to be used. To support the experimental studies, a computer model capable of simulating advance times, recession and infiltration for both the continuous and surge flow regimes was developed.

Furrow advance time comparisons between the two flow treatments were the primary concern in the 1983 field experimentation. The test results will be contributed to the regional project.

III.   EXPERIMENTAL METHODS

The purpose of this experiment was to investigate advance time differences between furrows irrigated by surge flow and those irrigated by continuous flow. As the most pronounced effects of surge flow have occurred during a first irrigation, all experimentation was conducted under a representative initial irrigation field condition.

Preparations

The experimental study includes two separate field tests performed on the same test site during the 1983 growing season. The first, Experiment A, was conducted in mid-June with the field cropped in barley planted the previous fall. At the time of the test, the average height of the barley was about 36 in (91 cm). In May furrows were formed in the existing barley stand. During the furrowing operation plant residues were deposited in the furrows making it necessary to hand clean all furrows prior to running advance trials.

Because Experiment A represented the first attempt at conducting advance-time trials, there was some uncertainty as to how the system would perform. Also, there was some question as to whether the condition of the test site was suitable for the experimental purposes. For these reasons it was decided that Experiment A would serve as a trial

run of the experimental procedures.

In conducting Experiment A, it was found that furrow advance was affected to some extent by a depression located near the middle of the furrow runs. The depression, about 50 ft (15 m) long and extending across the width of the field, required the advancing front to move up a slope of roughly 0.005% for 25 to 30 ft (7.6 m to 9.2 m); a rise of about 1.25 to 1.8 in (3.18 to 4.57 cm).

Also during the first experiment it became evident that the method to determine furrow inflow rates by measuring the amount of time required for a stream to fill a two-gallon (7.5 l) bucket was inadequate. The method proved not only to be a slow and tedious process, but also did not measure inflow rates with the accuracy required for the experimental purposes.

Although advance time measurements were recorded in Experiment A, only limited attention is given to that experiment because of the difficulties encountered and their bearing on the validity of the experimental results. However, Experiment A provided information concerning the design and operation of the experiment which served as a guideline in formulating the second experiment.

In August the barley crop was harvested and the remaining plant debris was disked into the ground shortly afterwards. Over the next 40 days the test site was allowed to dry out in this condition. In mid-September additional topsoil was brought in to fill the depression

and the ground was re-leveled over the entire area of the test site. The field was then cultivated with a spring-tooth harrow and this was followed by the formation of new furrows. However no crop was planted.

In late September, following the field preparations, a second set of advance-time trials (Experiment B) was performed with the field in a fallow condition. Also in Experiment B a new flow measuring device was used which enabled the furrow inflows to be measured more quickly and precisely. These changes, along with the experience gained from the first test, significantly improved operations during Experiment B.

The remainder of this chapter pertains exclusively to the events of Experiment B, except where otherwise noted.

Site Description

The experimental site is a one acre (0.4 ha) plot of land located within the Southern Oregon Agricultural Experiment Station in Central Point, Oregon. The site, which is a long and narrow rectangular field 80 ft (24 m) by 570 ft (174 m), is located in the northeast section of the experiment station property adjacent to the northern boundary. A vehicle access road bounds the north and west sides of the field plot, while the south and east sides are bounded by fruit orchards (see Figure 6). Normally in the past, winter barley was planted each year on the field

Orchard

Hydrant

Gated-Pipe

S

E ← → W

N

Roadway

Unplanted

Test Plots

Orchard

Orchard

Orchard

Scale

0   40   80 ft

0   11   22m

Unplanted
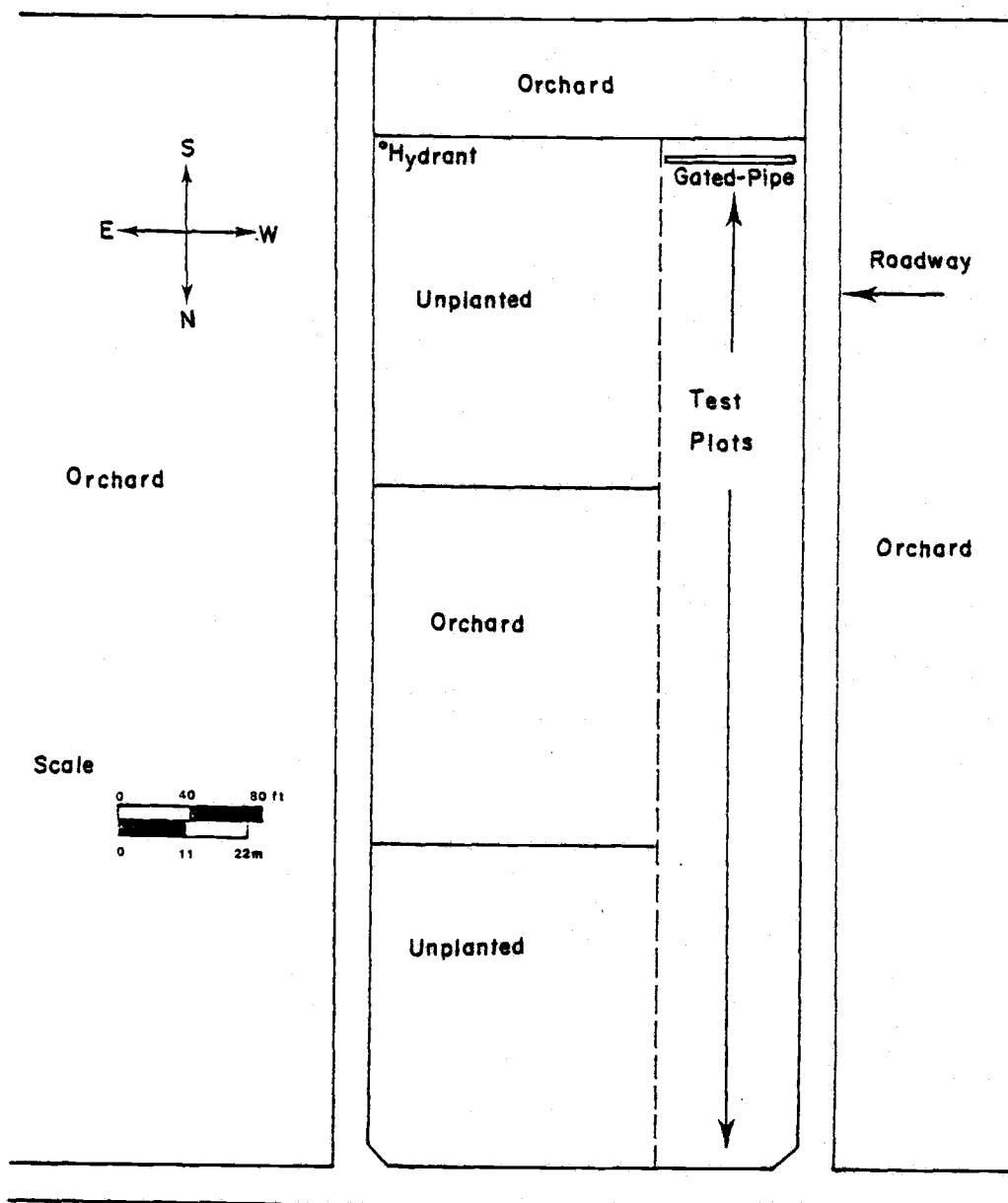
Figure 6.   Location of test plots on the Southern Oregon
Agricultural Experiment Station in Central
Point, Oregon.

site and was sprinkler irrigated beginning in mid-May.
However with the cooperation of the experiment station
supervisor the only water applied to the field site in
1983 was for the purposes of the surge flow experiment
described here. Water and pumping for the experiments
were provided by the station, as well as the tractor and
accessories used in preparing the test site. Experiment
station personnel also provided a considerable amount of
labor for the field preparations and system installment.

A topographic survey of the test site was made in May
1983 and again the following September just before the
furrow advance trials of Experiment B. A contour map
drawn from the second survey (Figure 7) illustrates the
slope characteristics of the test site.

The field slopes lengthwise from south to north with
a drop in elevation over the 570 ft (174 m) length of
5.65 ft (1.7 m) along the western boundary to 6.0 ft (1.8 m)
along the eastern boundary. The field has a near uniform
slope of 1.10% over the upper 70% of the field, after which
the slope tends to decrease over the remainder of the field.
The slope reduction is most extreme along the western
boundary while becoming more uniform across the field from
west to east.

The field also slopes slightly from west to east. At
the upper field boundary, the location at which water was
delivered to the field, the slope is 0.25%. Down the field
length the crosswise slope tends to gradually increase to
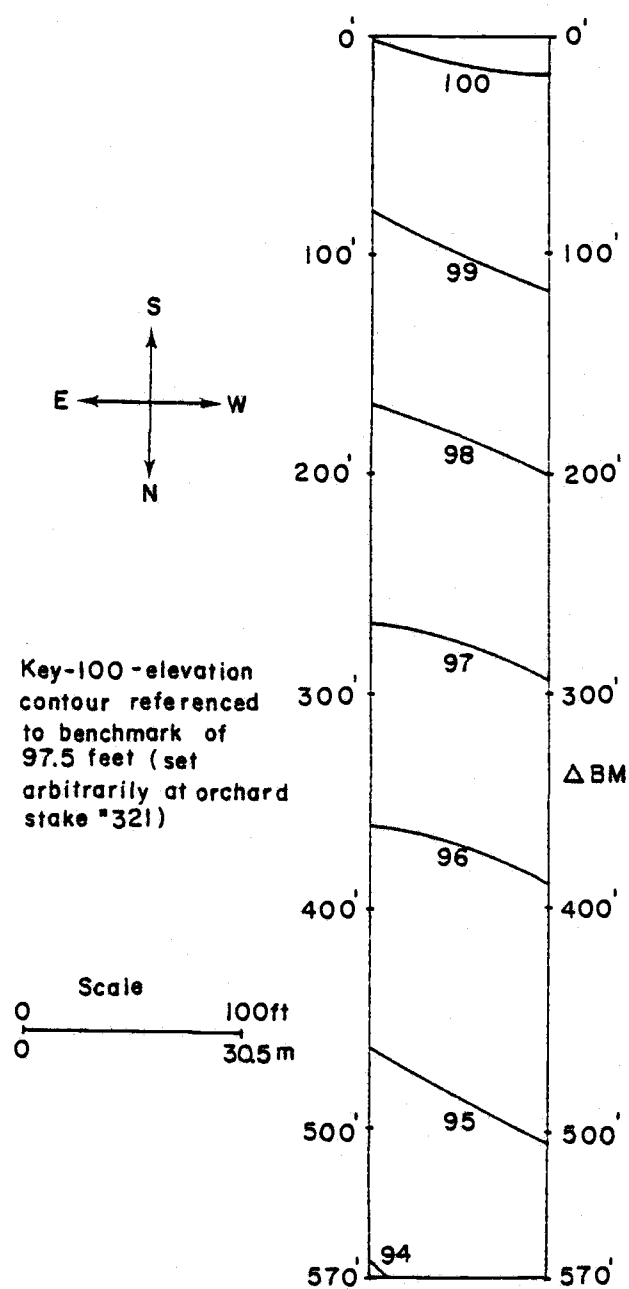
Figure 7. Topographic survey of field experiment
site.

nearly 0.8% at the lower end.

The soil on the experiment station property is classified as Central Point sandy loam, a member of the Central Point series, and belongs to the Pachic Haploxerolls, coarse-loamy, mixed, mesic family (USDA Soil Survey, 1979). The soil is typically a black sandy loam in the surface layer to 17 in (43 cm), becoming a dark brown sandy loam in the subsoil, and a very gravelly sandy loam from 49 in (124 cm) to 60 in (152 cm) or more in the substratum. The moist soil bulk density varies from 1.39 g/cm^3 in the A horizon to 1.52 g/cm^3 in the B and C horizons. Generally throughout the profile, the soil is slightly acidic (ph 6.5), hard, friable, nonplastic, and has a low shrinkage and swelling potential.

Commonly, Central Point sandy loam is a high intake soil and is excessively drained. Water movement is moderately fast in the surface layer and the rate increases in the substratum where the permeability can be as high as 20 in/hr (1.4 x 10^{-2} cm/sec) (USDA Soil Conservation Service, 1974). As a result surface irrigation water is subject to rapid percolation and on slightly to moderately sloping fields irrigation runoff is generally quite low.

At the time of Experiment B there were 33 furrows in the field, extending the 570 ft (174 m) length and spaced every 30 in (76 cm) across the field width. All furrows were wheel furrows (compacted by tractor wheels), parabolic in shape, and nearly uniform in size. Typically,

the furrow dimensions were 6 in (15 cm) across the top width and 3 in (7 cm) in depth.

Gated-Pipe System Layout

A gated-pipe water delivery system was installed at the upper end of the field aligned perpendicular to the furrows. The system consisted of three 30 ft (9 m) sections of 8 in (20 cm) diameter PVC irrigation pipe, each section having 12 rectangular port openings, 1.25 in (3 cm) by 2 in (5 cm), spaced every 30 in (76 cm) along the pipe. The pipe sections were connected and positioned across the uppermost end of the field with the ports facing in the downslope direction.

Inserted into each port were adjustable sliding gates which could be adjusted to regulate the area opening of the individual ports. Once the gated-pipe system was pressurized the opened ports each discharged a stream of water into a single furrow.

Water was pumped to the gated-pipe system from the station pumphouse located approximately 1500 ft (457 m) southwest of the field site. A 15 HP (11.2 kw), 400 gpm (25.2 l/s) rated capacity pump transported water from a large storage pond, located below the pumphouse, to a hydrant near the field site. The hydrant, 150 ft (46 m) east of the gated-pipe entrance, was connected to the system by approximately 165 ft (50 m) of 4 in (10 cm) diameter aluminum pipe. A steel expansion section joined
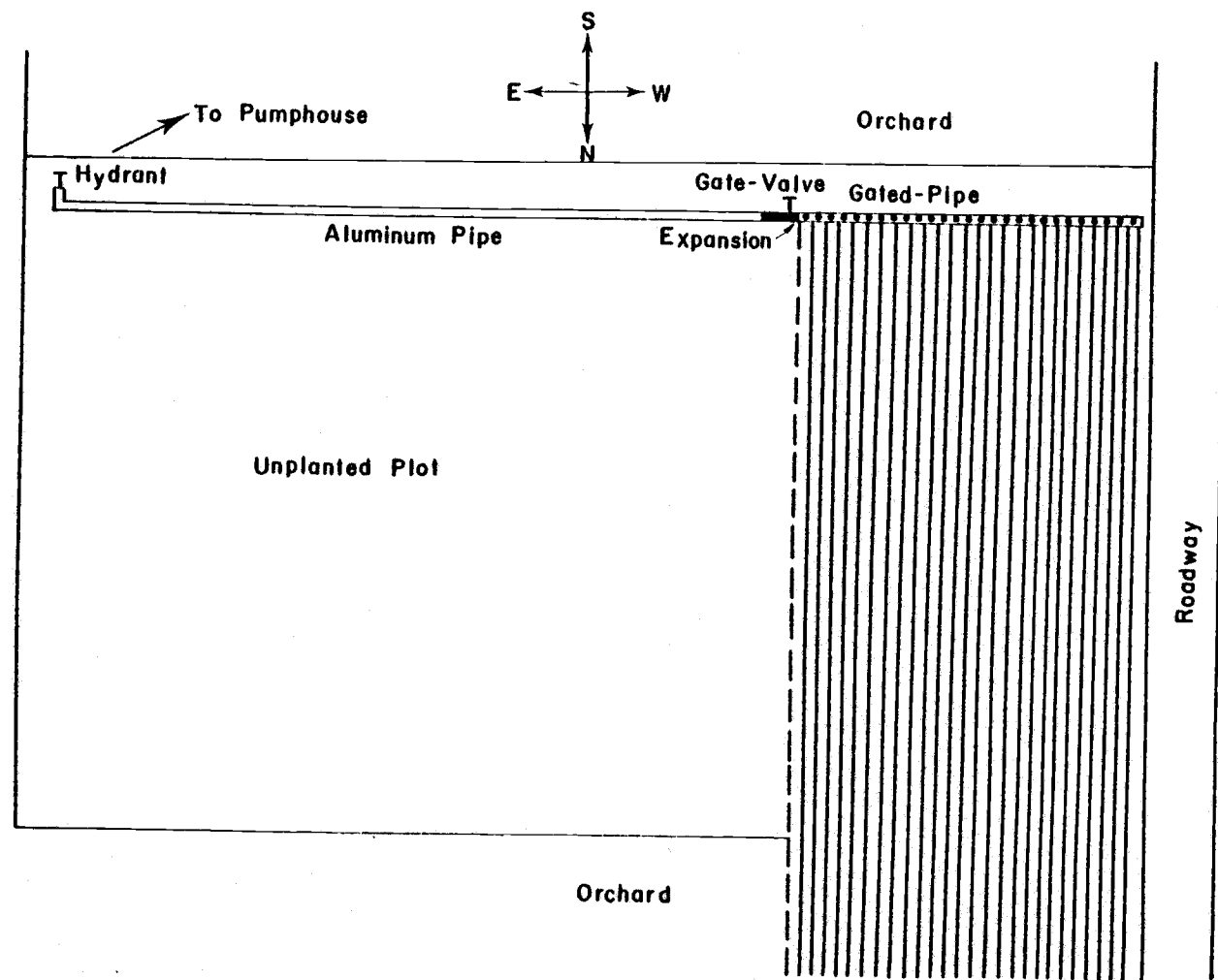
Figure 8. Gated-pipe system layout

the aluminum pipe to the larger diameter gated-pipe system (see Figure 8).

As the distance to the pump was quite far from the field site, once the pump was in operation the system discharge was controlled by a screw-valve on the hydrant. A gate valve located at the gated-pipe entrance provided additional flow regulation.

To roughly calibrate the relative pressure within the system and thus aid to some degree the flow regulation process, two clear plastic L-shaped tubes, one-quarter inch (0.63 cm) in diameter were inserted into the gated-pipe to measure the pressure head at the inlet and the far end of the pipe. The horizontal piece of the L-tube was inserted into the pipe on the side opposite the ports, penetrating a distance of one-half the pipe diameter. The vertical piece of the L-tube extended a distance of 36 in (91.4 cm) above the center of the gated-pipe.

Design

. Furrow System

Because the focus of the experimental study was on the advance time differences between surge and continuous flow treatments, it was not necessary to carry out the irrigation beyond the advance phase. However, a general furrow system design was formulated for a complete irrigation based on assumed continuous inflow. The design procedures follow the Soil Conservation Service design

method for an open-ended gradient furrow system (USDA, 1983).

The site at the time of the experiment had been recently cultivated and had not been irrigated for over 100 days. It was assumed that the soil moisture had been sufficiently depleted throughout the root zone and that an irrigation applied to a depth of 5 in (13 cm) would increase the soil moisture to near field capacity. The average intake rate of the soil was estimated by the Soil Conservation Service to be about 0.8 in/hr (2.0 cm/hr) and this value was used for the design soil intake family.

The other parameters required for the design include the field slope, taken as 1.0%; the field length, 570 ft (174 m); the furrow spacing, 30 in (76 cm); and the furrow inflow, 7 gpm (0.44 l/s). The complete design procedure and equations are presented in Appendix A.

. Flow Calibration Device

The device used in calibrating the rate of flow from the ports was suggested by Jack Gasten of the USDA-ARS Snake River Conservation Research Center, Kimberly, Idaho. The device was a thin-walled, tin, cylindrical can, 7 in (18 cm) in height and 6 in (15 cm) in diameter. A section of the can was cut out 2.5 in (6.4 cm) below the top, extending one-half the circumference around the can. A one and one-eighth inch (2.9 cm) diameter hole was
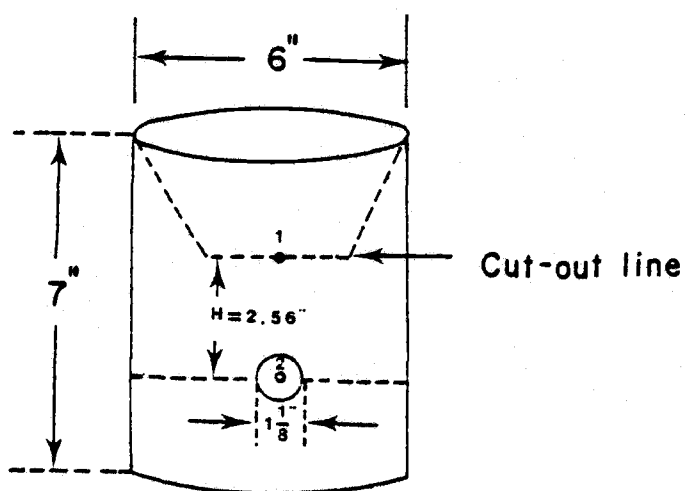
Figure 9. Flow calibration can dimensions.

drilled into the can wall with the hole centered 2.56 in (6.5 cm) below the cutout line (Figure 9).

A stream flowing into the can which could maintain a constant water level at the cut-out line, while flowing freely from the hole, would then be known to have a pre-determined discharge rate. The calibration procedure for the port discharge required that the can be held level at a position which allowed the stream to flow directly into the can, while at the same time adjusting the gate opening until the water level remained constant at the cut-out level.

The design of the device is based on the principles applied in determining the rate of flow from a reservoir through an orifice (Streeter and Wylie, 1979, pp. 342 - 346). The head on the orifice is assumed to be held constant and is measured from point 1 on the free surface to point 2 at the center of the orifice (see Figure 9). The energy equation between points 1 and 2 can be written as:

$$\frac{V_1^2}{2g} + \frac{p_1}{\gamma} + z_1 = \frac{V_2^2}{2g} + \frac{p_2}{\gamma} + z_2 + h_f \qquad (1)$$

where:

$\frac{V_1^2}{2g}$ and $\frac{V_2^2}{2g}$ are the velocity heads at points 1 and 2

$\dfrac{p_1}{\gamma}$ and $\dfrac{p_2}{\gamma}$ are the pressure heads at points 1 and 2

z_1 and z_2 are the elevation heads at points 1 and 2

and h_f is the head loss between points 1 and 2

With point 2 as elevation datum, the velocity head at point 1 negligible and taken as zero, and both p_1 and p_2 at atmospheric pressure, the energy equation becomes:

$$H = \frac{V_2{}^2}{2g} + h_f \qquad (2)$$

where H is the total head on the orifice center, equal to z_1.

Equation 2 is conveniently expressed by the orifice formula (Christiansen, 1942) in terms of discharge:

$$Q = 448.8 \, C_d \, A \, (2gH)^{\frac{1}{2}} \qquad (3)$$

where:

Q, gpm

A, ft^2

H, ft

g, 32.2 ft/s^2

C_d, dimensionless discharge coefficient between 0 and 1.0

The discharge coefficient C_d, is the ratio of the actual discharge to the theoretical discharge and accounts for the energy loss due to friction between points 1 and 2.

Since the discharge coefficient is not known in advance
it must be estimated.

Similar metering devices were calibrated by the
USDA-ARS in Idaho for discharge rates between 4 and 17 gpm
(0.25 and 1.0 l/s) using hole diameters between 0.75 and
1.625 in (1.9 and 4.1 cm). The observed coefficient of
discharge ranged from 0.59 to 0.67. A calibration was
not made for a 7 gpm (0.44 l/s) discharge rate which was
the desired rate for the furrow advance experiment.
Consequently, the hole diameter (1.125 in) and correspond-
ing discharge coefficient (0.61) for an 8 gpm (0.48 l/s)
discharge rate as calibrated by the USDA-ARS were used
as the design parameters for calibrating a 7 gpm (0.44 l/s)
metering device.

Using a value of 0.61 for the coefficient of dis-
charge and a given hole diameter of 1.125 in (2.9 cm),
the head required above the center of the hole for a
discharge rate of 7 gpm (0.44 l/s) was found by rewriting
equation 3:

$$H = (\frac{Q}{448.8 \ C_d \ A})^2 \ \frac{1}{2g}$$

$$= \{\frac{7}{448.8(0.61)(\pi/4)(1.125/12)^2}\}^2 \ \frac{1}{2(32.2)}$$

$$= 0.213 \ ft$$

$$= 2.56 \ in \ (6.5 \ cm)$$

It was found when the discharge was measured by the time required to fill a two gallon (7.5 l) bucket, that the device calibrated the stream flow at 6.8 gpm (0.43 l/s). Thus, the discharge coefficient may have been closer to 0.59. However, for the advance time comparisons the important element was that the discharge rate to one furrow was the same as the next. Since the discharge rate calibrated by the device did not deviate very much, the furrow inflow rate will be referred to as 7 gpm (0.44 l/s).

Procedures

In Experiment B only 15 furrows were used in the advance trials. Of the 15, seven were treated with a continuous flow application. The remaining eight were divided into two surge flow treatments with four furrows in each treatment. To avoid any variation in discharge rate among the furrow inflows each test furrow was paired side by side with a furrow used only while calibrating inflows.

Previous work had demonstrated that a significant pressure drop occurred along the gated-pipe system. Because of the hydrant's proximity to the test site, water entered the system from the east, the lowest point in elevation across the field width. Consequently, due to the rising pipe elevation, and to a lesser extent friction head loss within the system, pressure gradually

decreased from the port nearest the inlet to the end of the system.

The pressure differences among the discharging ports along the system had to be compensated for in order to provide an equal discharge to the furrows. Generally, this was accomplished by decreasing the area opening for ports closer to the system entrance and increasing the area for ports farther down the line. However, with the initial activation of the pump, a considerable amount of time passed in pressurizing and regulating the flow to the system. Once the approximate experimental flow condition was achieved, additional time was required to "fine tune" the stream sizes of each opened port. During this process water was necessarily discharging to the field. To compensate, flow was diverted to the adjacent calibration furrow which accomodated the excess water during the flow regulation process. After establishing an equal discharge from all the ports, the streams were then directed into the designated test furrows. In this manner the procedure ensured that each test furrow essentially received the exact volume of water intended during the experimental period.

Since total discharge into the system was constant over the duration of the experiment it was necessary to operate the system with the same number of ports opened at all times. Consequently, the four ports for each of the two surge treatments were simultaneously alternated on and

off so that at any given time only 11 ports (7 continuous and 4 surge) were discharging. Accordingly, this required that the cycle time for the two surge treatments be of equal durations.

Experiment A had involved two, 60 minute cycle time surge applications with both treatments at a cycle ratio of 1:2 and a furrow inflow rate of approximately 7 gpm (0.44 l/s). In conducting this experiment it had been observed that the 30 minute surge typically required only about 10 to 13 minutes to completely recede from the surface following the inflow cutoff to the furrows. Also, for some of the furrows tested it was found that the 30 minute on-time duration was long enough to advance water the length of the field after a relatively few surge cycles.

In Experiment B the two surge treatments were operated for different cycle times but using the same 7 gpm (0.44 l/s) furrow inflow rate as in Experiment A. One surge treatment again received water for 30 minute intervals. However because it was anticipated that the recession time would be about the same as before, it was desirable to shorten the off-period to 15 minutes, giving the treatment a 2:3 cycle ratio in a cycle time of 45 minutes.

To counterbalance the cyclic pattern for the 2:3 cycle ratio treatment, the other treatment had an on-time of 15 minutes and an off-time of 30 minutes over the

45 minute cycle time duration. It was suspected that this treatment, having a cycle ratio of 1:3, might not be able to produce an advance across the entire field length because of the shorter 15 minute on-time. However, the treatment was of interest because it received only 1/3 the volume of water applied in the continuous flow treatment.

Figure 10 shows the type of treatment which the 15 test furrows received during the experiment. With the pair nearest the system inlet designated as furrow 1, the 15 pairs were numbered 1 through 15 across the field width. Continuous flow was applied to furrows 1 through 4 and 13 through 15. The 1:3 cycle ratio surge treatment was applied to furrows 5 through 8, while the 2:3 cycle ratio treatment was applied to furrows 9 through 12.

The gated-pipe system was positioned to provide one port centered between each of the 15 furrow pairs, and only these 15 ports delivered water to the furrows. All other ports remained closed throughout the experiment.

Arranging the treatments in the manner indicated in Figure 10 provided an effective pattern operational control of the gated-pipe system. Earlier work had shown that during operation the opening or closing of gates near the two ends of the system significantly altered the discharge from those ports producing continuous streams to test furrows, making it necessary to readjust these ports at every surge cycle. However, streamsize changes were not noticeable when gates were opened and closed towards the
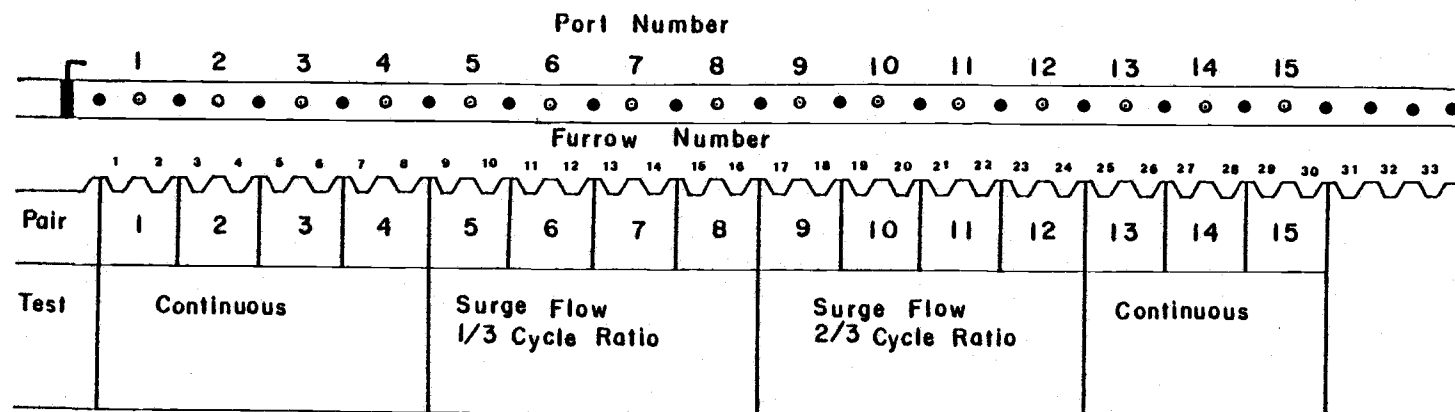
Figure 10. Furrow arrangement showing the type of treatment applied to each furrow pair and the corresponding port of each furrow pair.

center of the system. Therefore, to reduce the flow regulation complexities during the experimental testing, all continuous streams were located on the two ends of the system and surge treatments were located at the center of the system. At the same time, this arrangement allowed the continuous flow treatment to be distributed over the test site at two separate areas, which would help to offset significant variations in soil factors.

Of the 33 furrows formed in the test site area, 30 were used for testing purposes with 15 of these used for actual advance testing. Originally 32 furrows were intended to be used with the one remaining furrow stationed at the very end of the pipe-system acting as a relief furrow to "bleed" water if necessary to reduce flow across the system. However, one week before the experiment, while flushing out the pipe-system (which had been unused for some time) a large volume of water was inadvertently allowed to enter the last three furrows (31, 32, 33) and advance to the end of the field. As a result, the three furrows had to be eliminated from the advance trials because they were no longer considered non-irrigated.

Advance Time Measurements

Experiment B was performed on September 27, 1983 beginning at approximately 8:30 a.m. Two graduate research assistants carried out the experimental operations. One person was responsible for pump operation and for

recording advance time data. The other was in charge of flow regulation to the furrows and alternating the surge flow treatments.

During the experiment, the initial surge application was the 2:3 cycle ratio surge treatment, which coincided with the beginning of the continuous flow treatment. The initial surge of the 1:3 cycle ratio treatment began 33 minutes later. For all test furrows the time was recorded at which water applied at an instantaneous discharge rate of 7 gpm (0.44 l/s) advanced to stations along the furrows located at 100 ft (30.5 m) increments down the field length.

Before the experiment began, a small head ditch was formed for each furrow pair so that water could be diverted to either furrow by damming the entrance to the other with soil. The bottom level of the head ditch, with respect to the port elevation, was made low enough so that the metering can could be held level, and that water could flow freely from the device. In addition it was necessary to block all possible entrances to which water could flow other than the furrow itself, such as behind the gated-pipe system or over furrow crowns.

The experiment began with all entrances to the 15 actual test furrows blocked so that, initially, only calibration furrows would receive water from the pipe system. Since the 2:3 cycle ratio surge treatment would begin at the same time as the continuous flow treatment, the ports which provided flow to furrows 1 through 4 and

9 through 15 were opened just prior to pumping. The ports for the 1:3 cycle ratio treatment, those providing flow to furrows 5 through 8, were closed at this time.

At 9:00 a.m. pumping began with the valves at the hydrant and gated-pipe entrance completely opened. The control valve at the pump was steadily opened to a pressure near 25 psi (1.76 kg/cm^2) which pressurized the system and provided a discharge from the opened ports. The pressure head reading at the pipe system inlet was over 2 ft (0.61 m). The streams when measured with the calibrated can were found to be much larger than desired so that it was necessary to reduce the total discharge into the system. This was accomplished by partial closure of the screw-valve at the hydrant. Another check of the stream-sizes revealed that the discharge to the system, though reduced, still produced stream discharges greater than 7 gpm (0.44 l/s).

By closing the gate-valve at the system entrance to a one-half opening, the total discharge needed was obtained. The pressure head at the system inlet was now approximately 5 in (12.7 cm), while at the end of the system the tube indicated a head of slightly under 2 in (5 cm).

Streams from the ports were once again checked and the gates were readjusted until each stream discharged at the 7 gpm (0.44 l/s) rate. With this accomplished, the setting of the area opening for the ports accomodating furrows 9 through 12 was marked, thus enabling a quick

flow calibration at those ports in the subsequent surge cycles.

At 9:17 a.m. furrow advance time trials began as water was turned into the 11 furrows and blocked out of the calibration furrows. With the first surge of the 2:3 cycle ratio treatment complete after 30 minutes, ports to furrows 9 through 12 were closed and ports to furrows 5 through 8 were opened. As water flowed to the adjacent calibration furrows, the newly opened ports were adjusted and calibrated in the same manner as before. After each port was set to the 7 gpm (0.44 l/s) discharge rate, the port openings were individually marked. This was followed by the first surge for the 1:3 cycle ratio treatment.

This procedure continued through two complete cycles of each surge treatment during which it was found that the 7 gpm (0.44 l/s) rate was established almost immediately at each new on/off cycle. The calibration furrows were then no longer needed. It was only necessary to close the four gates for one surge treatment and open the ports to the marked setting for the other surge treatment. However, with each new surge cycle all ports were checked to ensure that they maintained the 7 gpm (0.44 l/s) discharge rate.

The experiment ran until both surge treatments had completed 11 cycles. The final surge for the 2:3 cycle ratio treatment concluded 15 minutes prior to the end of the continuous treatment while the 1:3 cycle ratio treatment concluded at the same time as the continuous treat-

ment. At the end of the last surge, water was cutoff to the system at the gate-valve. Following the shutdown of the system, water continued to flow in the furrows for another 10 to 13 minutes. Afterwhich, all test furrow advances not reaching the end of the field were noted and their final field distances were recorded.

IV. EXPERIMENTAL RESULTS

Experiment B

The results of the furrow advance-time trials of Experiment B (irrigation of a newly furrowed, fallow field) are summarized in Table 1. The times entered are the observed total elapsed times in minutes for the advance in each furrow to reach the indicated distances after water was initially applied to the furrows.

Since water advanced very slowly in the furrows and because the experiment could not be continued at night, water reached the 570 ft (173.8 m) field length in only one-third of the furrows within the time period allowed. For those which did not, the final distance of advance is shown in Table 1 at the final time representing the end of the irrigation for the particular treatment. For the surge treatments the final time indicated is the total elapsed time, including off times, through the last on-time period; and for the continuous treatment the total elapsed time through inflow cutoff. In all treatments an additional 10-minutes is added to the final time because the final distance measurements were made after the 10-minute recession period.

Within the experimental time period all furrow flows advanced at least 400 ft (122.0 m). For each treatment the average advance-time and the variability of advance-time, as measured by the standard deviation, have been

Table 1. Experiment B: Total Elapsed Time (Minutes) Since Irrigation Began for Furrow Advance to Reach Indicated Distance, with Mean and Standard Deviation (SD) at 100-400 ft for Each Treatment.

DISTANCE, FEET		100	200	300	400	410	420	450	460	485	495	500	540	570
TREATMENT	FURROW													
	1	15	105	219	412		513							
	2	13	45	165	490	513								
	3	13	27	220	353			513						
CONTINUOUS	4	14	89	319	513									
	13	13	59	182	305			513						
	14	12	29	93	188						513			
	15	17	49	92	175							412	513	
	MEAN	13.9	57.6	184.3	346.6									
	SD	1.7	29.5	79.4	132.7									
	5	10	58	154	209							388		480
SURGE	6	11	58	109	201							346		477
1:3 CYCLE	7	17	111	236	337						481			
RATIO	8	11	63	160	292					481				
	MEAN	12.3	72.5	164.8	259.8									
	SD	3.2	25.8	52.7	65.9									
	9	13	62	154	210							373		484
SURGE	10	17	110	255	341			498						
2:3 CYCLE	11	12	81	158	204							344		475
RATIO	12	12	57	115	181							306		365
	MEAN	13.5	77.5	170.5	234.0									
	SD	2.4	24.0	59.6	72.4									

included in Table 1 at distances of 100, 200, 300, and 400 ft (30.5, 61.0, 91.5, and 122.0 m).

Generally through a distance of 300 ft (91.5 m) the average advance-time and variability are not distinctly different among the three treatments. However, beyond this distance the decline in furrow advance rate is much more pronounced in the continuous treatment. In advancing from 300 to 400 ft (91.5 to 122.0 m) the continuous treatment required on the average 67 minutes more than the 1:3 cycle ratio treatment and 99 minutes more the the 2:3 cycle ratio treatment.

The decline in advance rate in the continuous treatment is accompanied by a wide variation in the time for the furrows to advance to 400 ft (122.0 m). The variability of advance-time in both surge treatments at 400 ft (122.0 m) is substantially less, with standard deviations about 50% of that for continuous.

The advantage of surge flow is perhaps most apparent in the furrow advance performance beyond 400 ft (122.0 m). During essentially the same time period, none of the seven continuously irrigated furrows had an advance reach the end of the field, while the distance was completed in five of the eight furrows treated by surge flow (see Figure 11). Furthermore, it was observed that in six of the seven continuous flow furrows advance virtually stopped between 400-500 ft (122.0-152.4 m). On the other hand, only one furrow (furrow 10) of the eight treated by surge flow
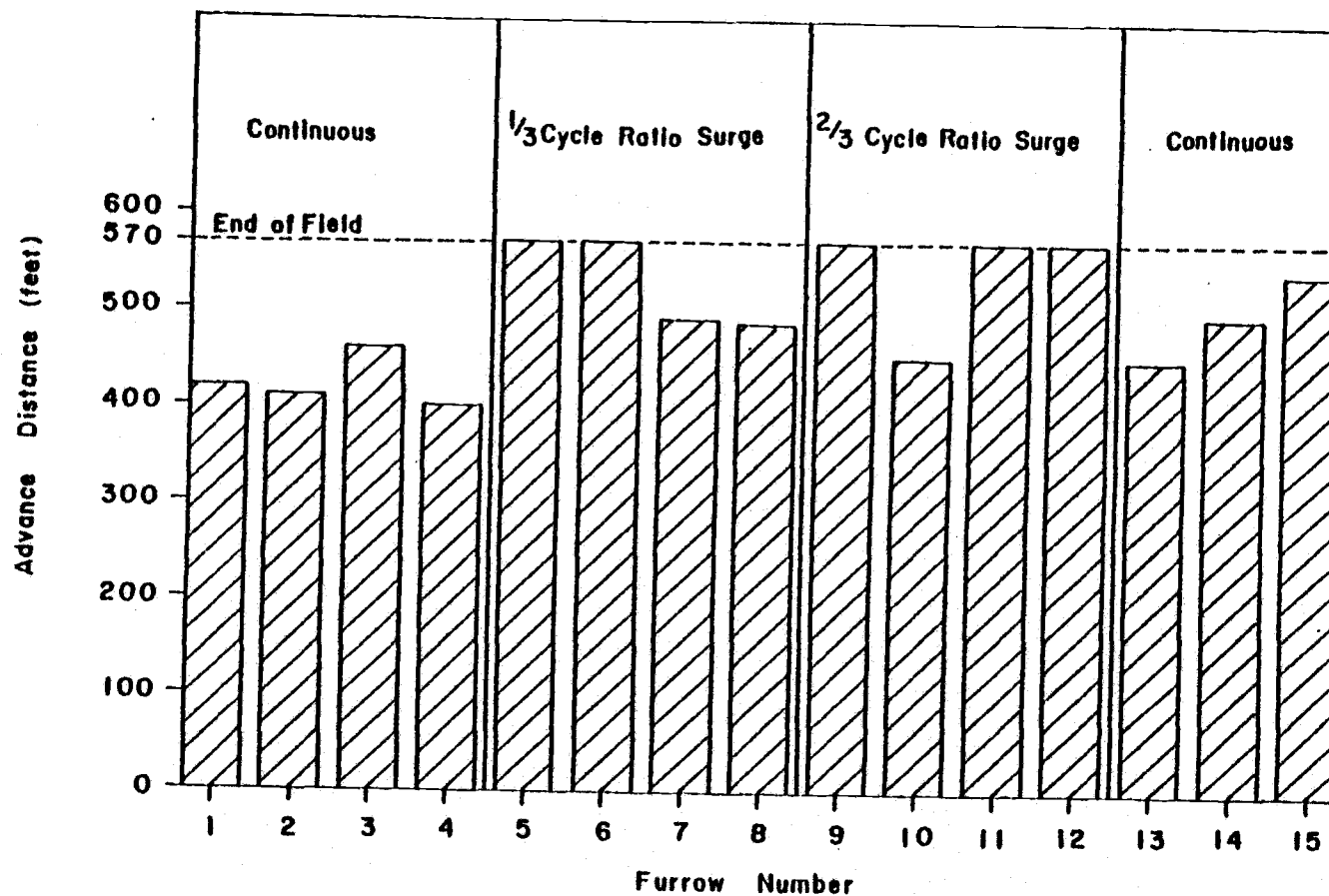
Figure 11. Experiment B: Final Advance Distance at End of Irrigation for Furrows of Continuous, 1/3 Cycle Ratio Surge and 2/3 Cycle Ratio Surge Flow Treatment.

exhibited a similar decline in advance rate.

For each treatment a power curve relating time and distance was fit by linear regression using the data of Table 1. The three power curves are presented in Figures 12, 13 and 14 corresponding to the continuous, 2:3 cycle ratio surge and 1:3 cycle ratio surge treatment, respectively. The three regression curves are presented together in Figure 15 and effectively illustrate the variation in advance among the treatments.

Through the first 200 ft (61.0 m) of furrow length, advance is quite rapid in each treatment although slightly faster in the continuous treatment. Interestingly, the advance of two furrows within the continuous treatment traveled the 200 ft (61.0 m) distance in less than 30-minutes (see Figure 12). By comparison, none of the four furrows in the 2:3 cycle ratio surge treatment had an advance reach 200 ft (61.0 m) during the first surge application.

As the distance increased beyond 200 ft (61.0 m) the advance rate declined more rapidly in the continuous treatment. The advance to 500 ft (152.4 m) in the 1:3 cycle ratio surge treatment occurred 105 minutes before the continuous treatment. The same advance distance is achieved by the 2:3 cycle ratio treatment 150 minutes sooner than the continuous treatment. The general trend of the advance curves indicates that a greater time differential would occur between continuous and surge
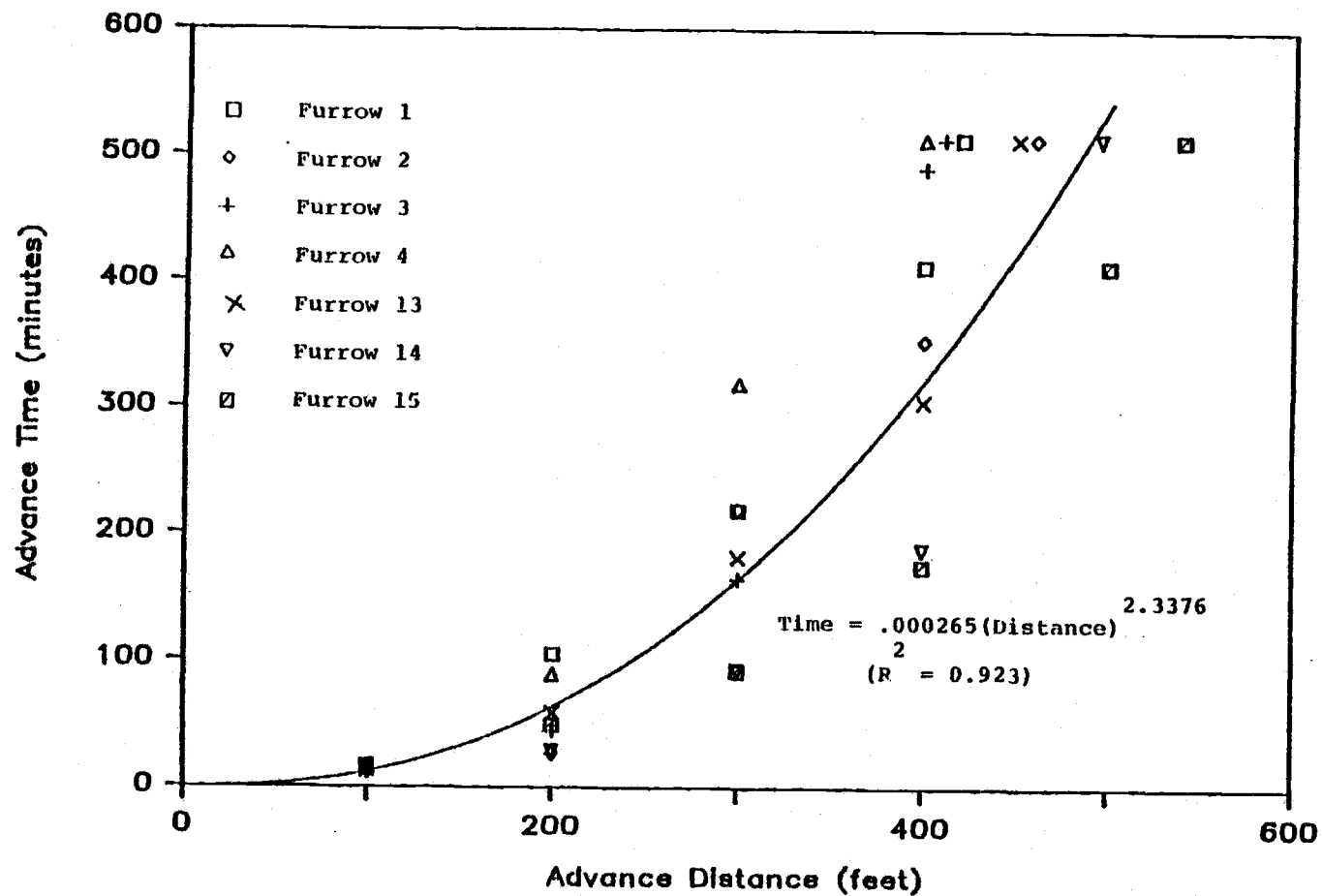
Figure 12.   Experiment B: Advance-Time Observations and Plotted Power Curve for Furrows under Continuous Flow.
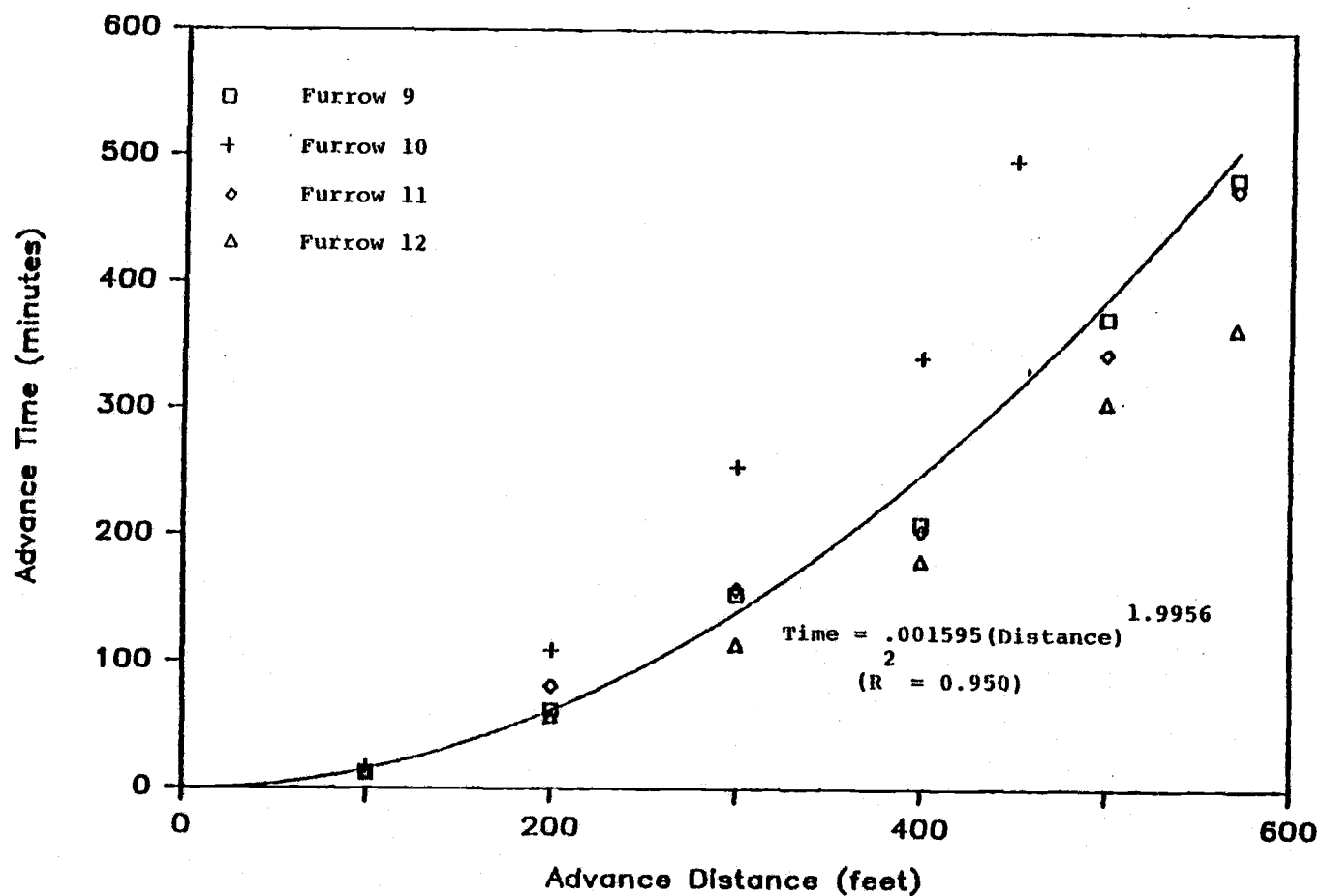
Figure 13. Experiment B: Advance-Time Observations and Plotted Power Curve for Furrows under 2:3 Cycle Ratio Surge Flow.

Figure 14.   Experiment B: Advance-Time Observations and Plotted
             Power Curve for Furrows under 1:3 Cycle Ratio Surge
             Flow.

Figure 15. Experiment B: Advance Power Curves for Continuous
Flow and Two Variable Cycle Ratio Surge Flow
Treatments.

treatments at the end of the furrow run.

The advance curve relationship of Figure 15 is quite similar to the advance characteristics found by Bishop and Walker (1981). In that study advance curves were derived from a test in which furrows treated by continuous and surge flow (1:2 cycle ratio) at a discharge rate of 5 gpm (0.3 1/s) were compared on a silt loam field of 1% slope (see Figure 4). In both experiments the advance-times of the treatments did not differ much over the first 250 ft (76.2 m) of furrow length. Beyond this distance, however, furrow advance was accelerated in furrows treated by surge flow.

Because the amount of water required to complete the advance phase has a significant bearing on the efficiency of an irrigation system, it is important to compare the total water applied during the advance phase. Since the actual inflow time is indicative of the volume applied, the observed elapsed times were converted to cumulative on-times for the furrows in the two surge treatments.

During the experiment, on and off-times for both surge treatments were recorded, along with the total elapsed time for an advance to reach the downfield distances. The cumulative on-time at each distance was found by first determining the number of complete surge cycles that had occurred previous to the current surge in which the advance reached the particular distance. This was accomplished by dividing the 45 minute cycle-time into the

observed total elapsed time in advancing to the distance. The integer portion of this division is the number of surge cycles which had occurred before the current surge.

For an advance reaching an observed distance the cumulative on-time was derived by first multiplying the particular treatment on-time (either 15 or 30 minutes) by the prior number of surge cycles. The resulting product was then added with the difference between the observed total elapsed time and the product of cycle time and prior surge cycles.

In equation form this can be written as:

$$\text{Cumulative on-time} = N \cdot OTR + (OT - N \cdot 45) \quad\quad (4)$$

where:

OT = observed total elapsed time, minutes

OTR = treatment on-time, minutes

N = number of previous surge cycles (the integer portion of OT divided by the 45 minute cycle time)

In some instances the value of the term $(OT - N \cdot 45)$ was greater than the treatment on-time meaning that the advance distance was obtained during the recession phase of the current surge cycle. If this was the case, the value for $(OT - N \cdot 45)$ was taken as the treatment on-time.

Table 2 presents the advance distances with the corresponding cumulative on-time in minutes. The time-distance summary for the continuous flow furrows is the same as in Table 1, except that the final time at each furrow does not include the 10-minute recession period

Table 2. Experiment B: Cumulative On-Time (Minutes) for Furrow Advance to Reach Indicated Distance, with Mean and Standard Deviation (SD) at 100-400 ft for Each Treatment.

DISTANCE, FEET		100	200	300	400	410	420	450	460	485	495	500	540	570
TREATMENT	FURROW													
	1	15	105	219	412		503							
	2	13	45	165	490	503								
	3	13	27	220	353				503					
CONTINUOUS	4	14	89	319	513									
	13	13	59	182	305			503						
	14	12	29	93	188						503			
	15	17	49	92	175							412	503	
	MEAN	13.9	57.6	184.3	346.6									
	SD	1.7	29.5	79.4	132.7									
	5	10	28	60	75							135		165
SURGE	6	11	28	45	75							120		165
1:3 CYCLE	7	17	45	90	120						165			
RATIO	8	11	30	60	105					165				
	MEAN	12.3	32.8	63.8	93.8									
	SD	3.2	8.2	18.9	22.5									
	9	13	47	109	150							253		330
SURGE	10	17	80	180	236		330							
2:3 CYCLE	11	12	60	113	144							239		325
RATIO	12	12	42	85	120							210		245
	MEAN	13.5	57.3	121.8	162.5									
	SD	2.4	17.0	40.8	50.7									

following inflow cutoff.

In order to compare advance performance as a function of amount of water applied, the cumulative on-times at each distance were multiplied by the 7 gpm (0.44 l/s) discharge rate and then divided by a conversion factor, 7.48 gal/ft^3, to obtain volume in cubic feet. Table 3 presents the volume of water applied in cubic feet at the indicated distances for each furrow. A power curve relating volume to advance distance for each treatment was fit by linear regression using the volume-distance data of Table 3. The three curves are presented in Figures 16, 17 and 18 corresponding to the continuous, 2:3 cycle ratio, and 1:3 cycle ratio treatments, respectively. The three curves are shown together in Figure 19 to illustrate the variation among the treatments. As the downfield distance increases, furrow advance under surge flow is achieved with significantly less water than required by the continuous flow treatment. In advancing 500 ft (152.4 m) a continuous flow furrow required a volume application of about 505 ft^3 (14.3 m^3). By contrast the same distance was traveled in a furrow advancing under a 2:3 cycle ratio surge treatment with a volume application of only 245 ft^3 (6.9 m^3), a 49% reduction. More impressive is furrow advance under a 1:3 cycle ratio surge which required only 26% of the water applied to continuous and 53% of that required by the 2:3 cycle ratio surge at 500 ft (152.4 m).

As mentioned previously, the degree of advance unifor-

Table 3. Experiment B: Volume of Water Applied (Ft^3) for Furrow Advance to Reach Indicated Distance.

DISTANCE, FEET	100	200	300	400	410	420	450	460	485	495	500	540	570
TREATMENT FURROW													
CONTINUOUS 1	14.0	98.3	204.9	385.6		470.7							
2	12.2	42.1	154.4	458.6	470.7								
3	12.2	25.3	205.9	330.3				470.7					
4	13.1	83.3	298.5	470.7									
13	12.2	55.2	170.3	285.4			470.7						
14	11.2	27.1	87.0	175.9						470.7			
15	15.9	45.9	86.1	163.8							385.6	470.7	
SURGE 1:3 CYCLE RATIO 5	9.4	26.2	56.1	70.2							126.4		154.4
6	10.3	26.2	42.1	70.2							112.3		154.4
7	15.9	42.1	84.2	112.3						154.4			154.4
8	10.3	28.1	56.1	98.3					154.4				
SURGE 2:3 CYCLE RATIO 9	12.2	44.0	102.0	140.4							236.8		308.8
10	15.9	74.9	168.4	220.9			308.8						
11	11.2	56.1	105.7	134.8							223.7		304.1
12	11.2	39.3	79.5	112.3							196.5		229.3
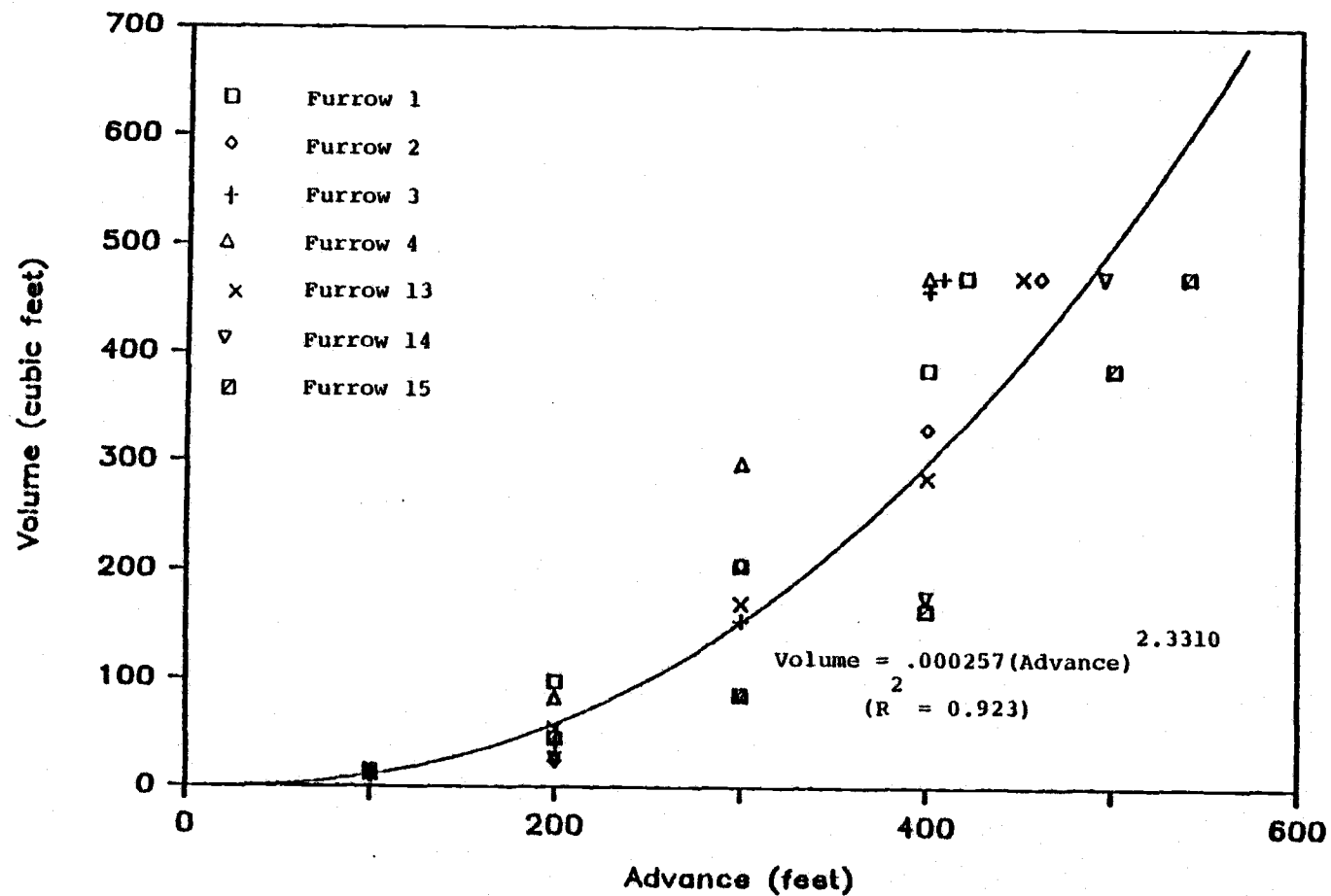
Figure 16. Experiment B: Volume-Advance Data and Fitted Power
Curve for Furrows under Continuous Flow.
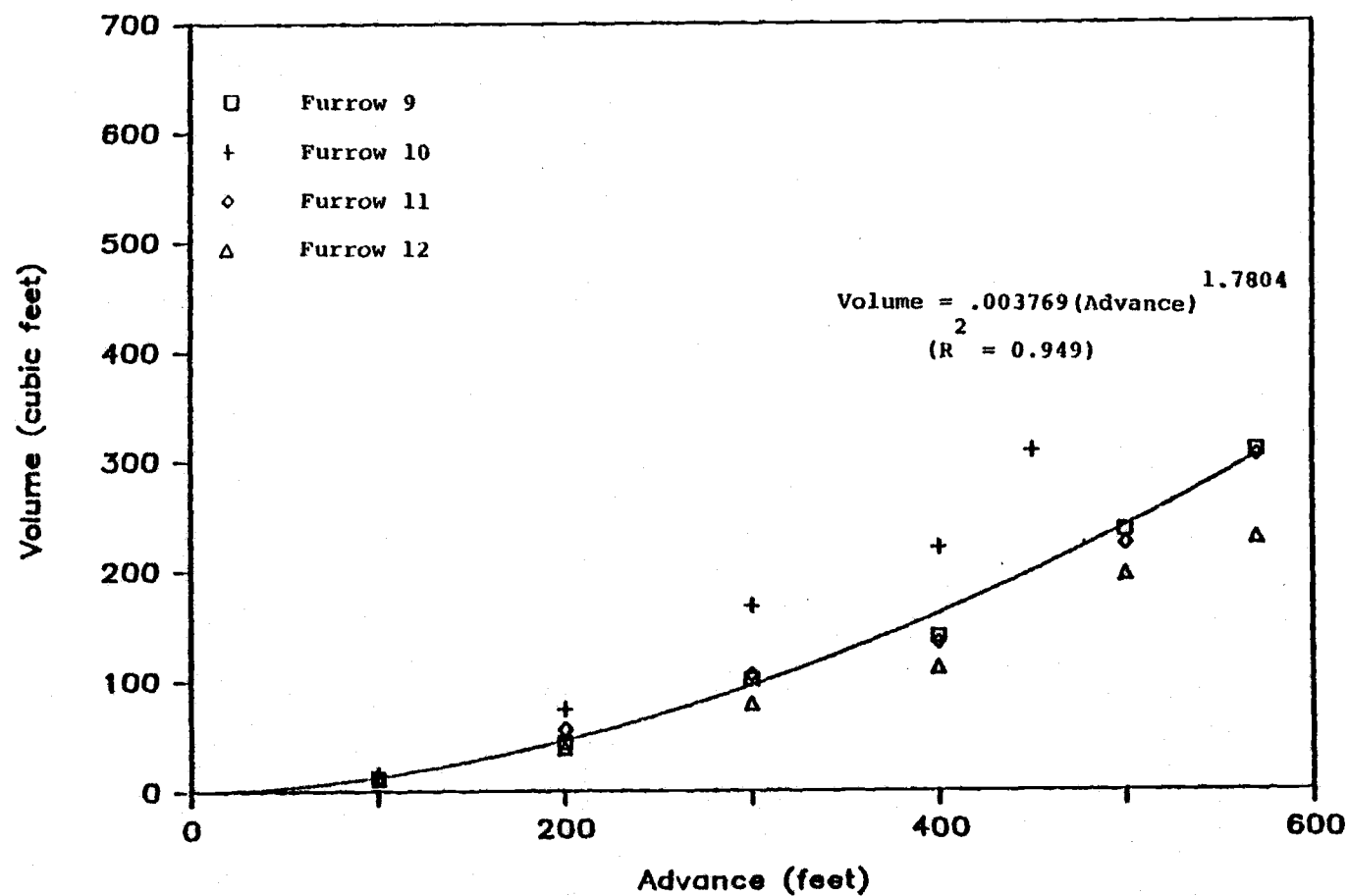
Figure 17. Experiment B: Volume-Advance Data and Fitted Power Curve for Furrows under 2:3 Cycle Ratio Surge Flow.
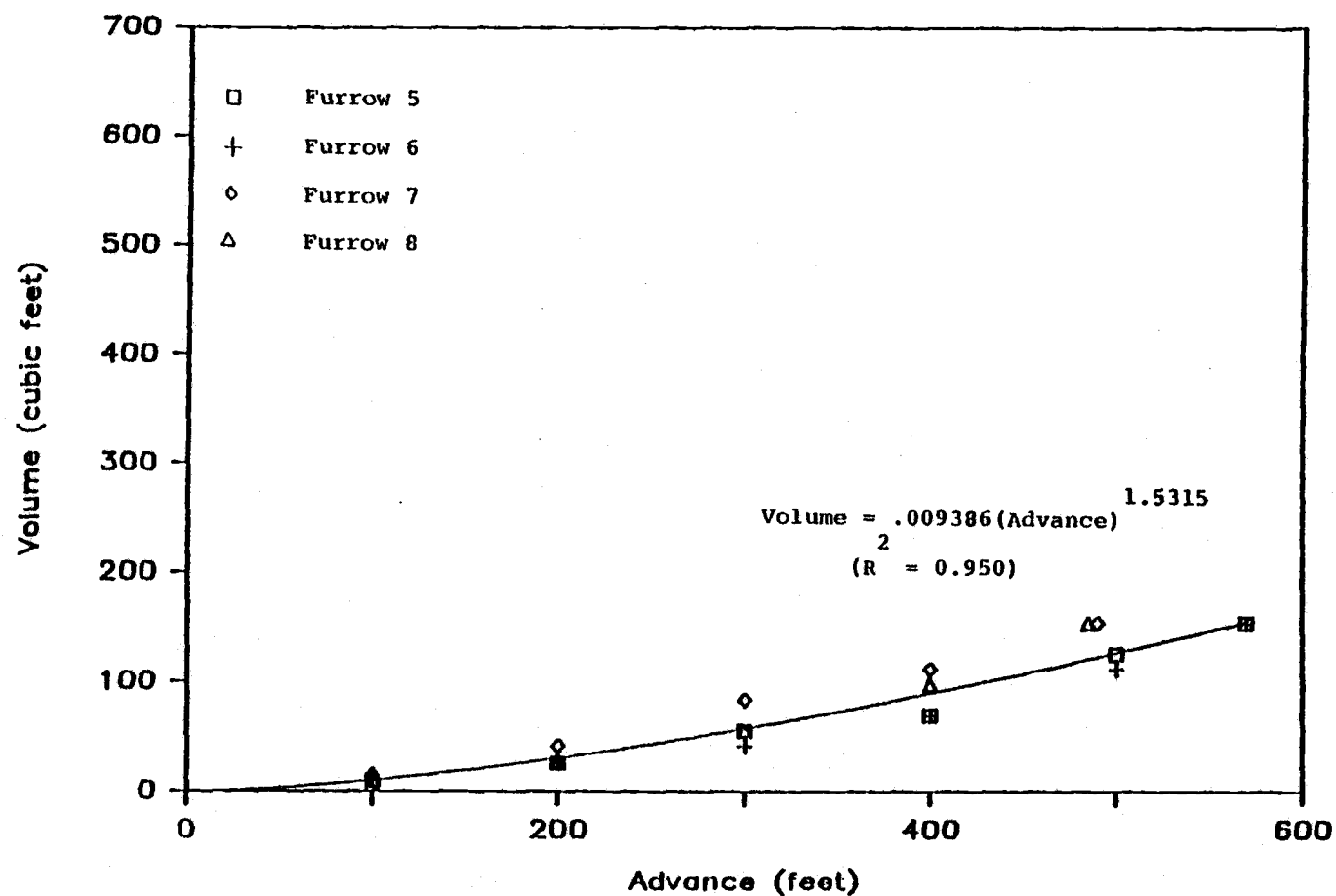
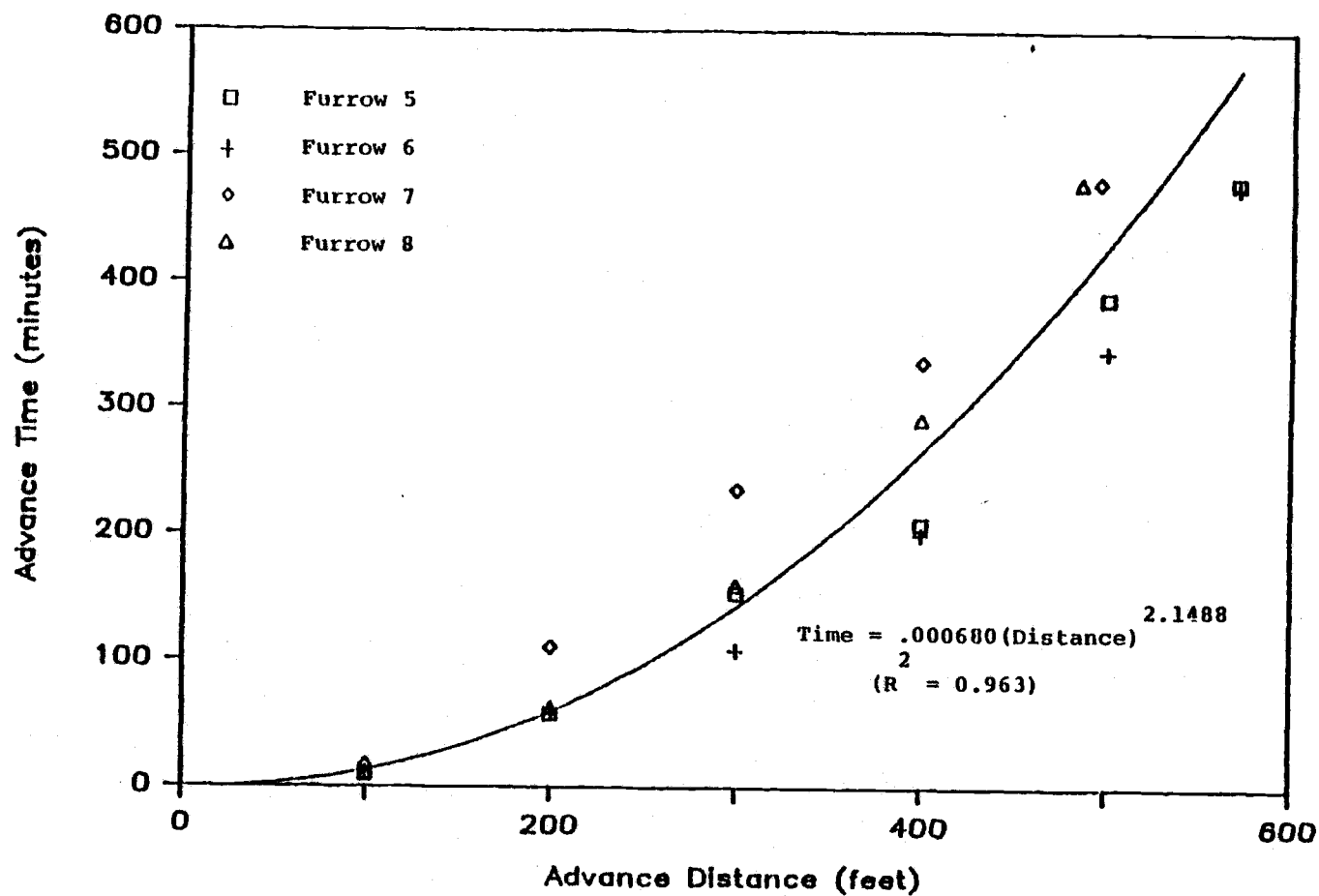Figure 18.   Experiment B: Volume-Advance Data and Fitted Power
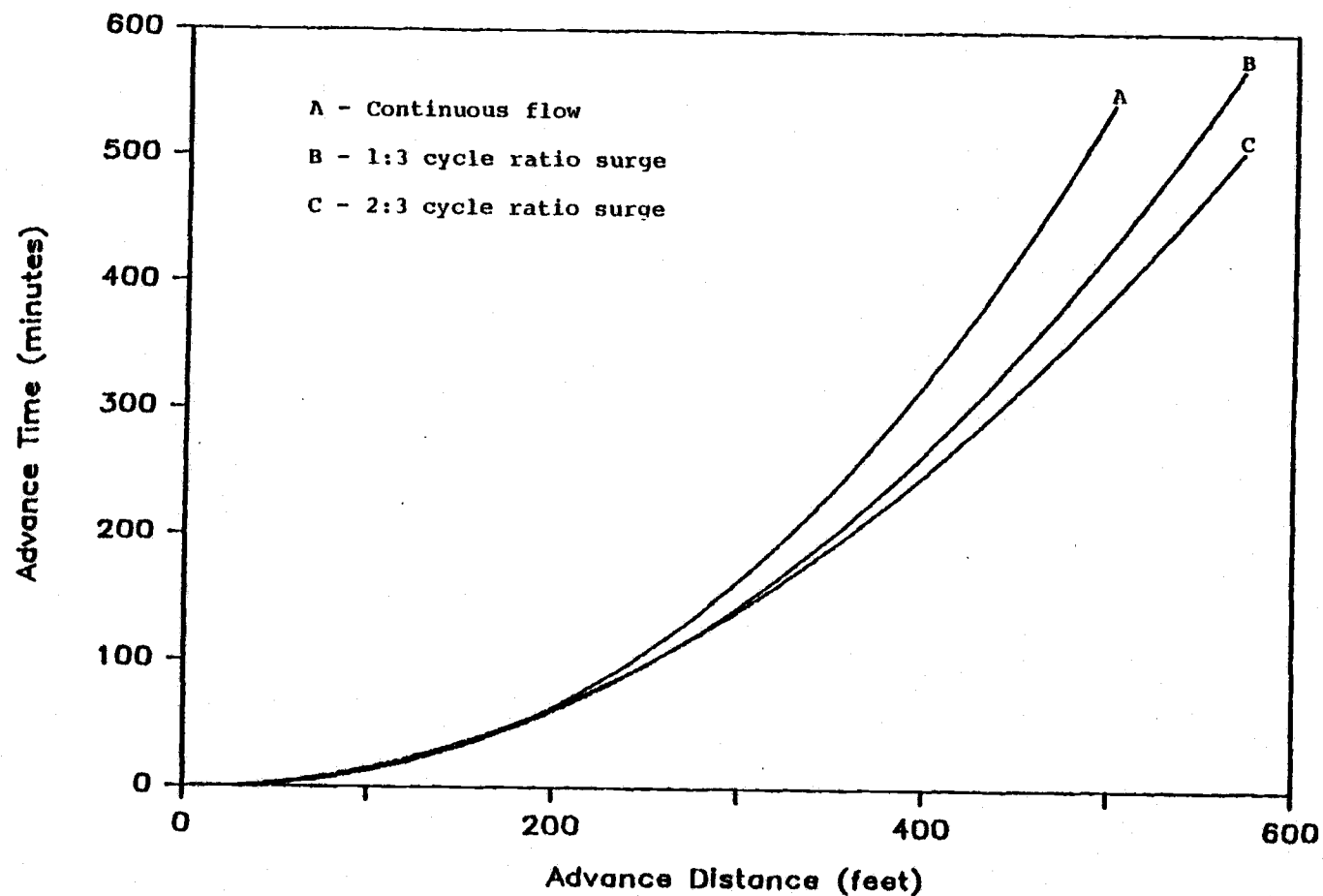Curve for Furrows under 1:3 Cycle Ratio Surge Flow.
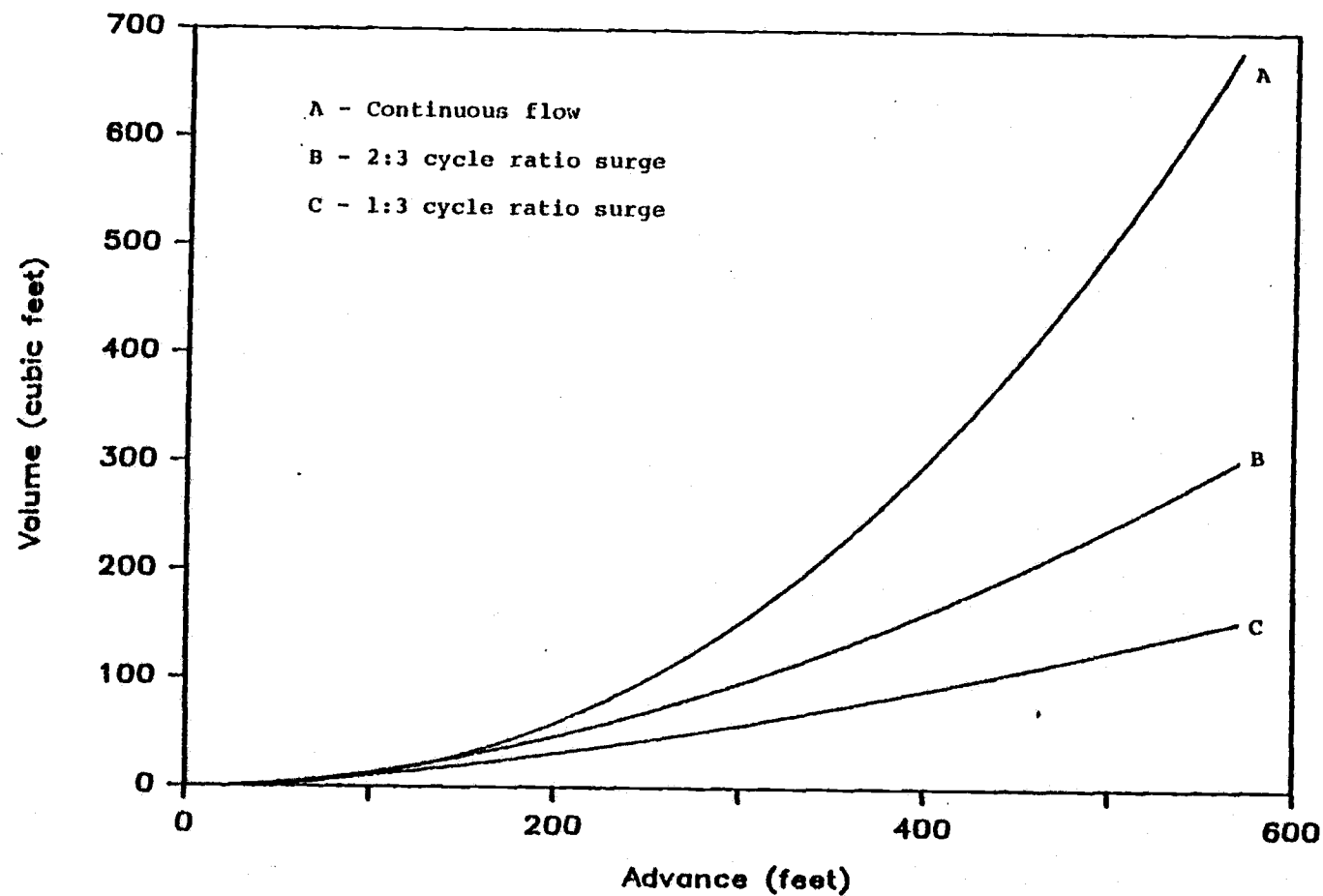
Figure 19. Experiment B: Volume-Advance Curves for Continuous
and Two Variable Cycle Ratio Surge Flow Treatments.

mity in the surge flow treatments is much more apparent.
The trend is demonstrated to a greater extent with the
advance times converted to actual inflow time as presented
in Table 2, which also includes the mean and standard
deviations for each treatment at distances of 100 - 400 ft
(30.5 - 122.0 m). At all distances beyond 100 ft (30.5 m),
the average inflow time and standard deviation are lower
for the two surge treatments. At the 400 ft (122.0 m)
distance the standard deviation in the 1:3 cycle ratio
treatment is only 17% that of the continuous flow. At
the same distance the variation in time for the 2:3 cycle
ratio treatment is nearly twice that of the 1:3 cycle
ratio treatment, but only 38% of the value for the contin-
uous treatment.

Experiment A

In Experiment A (furrows cut in a pre-existing barley
field) furrow advance rates were much slower than those
observed in Experiment B. Although the furrow length was
70 ft (21.3 m) shorter in Experiment A, the duration of the
irrigation lasted over one hour longer than the time period
for Experiment B. Nevertheless, only seven of the 28
furrows tested advanced water the 500 ft (152.4 m) furrow
length. However, of these seven, six were from the group
treated by surge flow.

The results of the advance-time trials of Experiment A
are summarized in Table 4 which shows the observed elapsed

Table 4. Experiment A: Total Elapsed Time (Minutes) Since Irrigation Began for Furrow Advance to Reach Indicated Distance, with Mean and Standard Deviation (SD) at 125 and 265 ft for Each Treatment.

TREATMENT	FURROW	125	265	300	325	350	375	400	420	440	450	460	475	480	490	500
CONTINUOUS	1	125	355				580									
	2	120	300												580	
	3	115	375										580			
	4	135	445		580											
	5	145	450		580											
	6	85	280									580				
	7	85	380					580								
	8	75	210													420
	9	95	390					580								
	10	135	365		580											
	11	95	315					580								
	12	55	200										580			
	13	135	235													580
	14	135	465							580						
	MEAN	109.6	340.4													
	SD	27.8	86.9													
SURGE 1:2 CYCLE RATIO	15	75	190													390
	16	205	435			580										
	17	130	270									580				
	18	135	315													
	19	145	270											580		390
	20	80	330							580						
	21	85	275								580					
	22	150	420					580								
	23	90	200													390
	24	75	255													555
	25	125	385	580												
	26	75	195													
	27	80	245													390
	28	145	450	580												555
	MEAN	113.9	302.5													
	SD	39.8	89.4													

time for furrow advance at distances of 125, 265 and 500 ft
(38.1, 80.8 and 152.4 m). As in Table 1, the final advance
distance and time for those furrows not completing the
entire furrow length are included with the time correspon-
ding to the duration of the irrigation plus 10 minutes for
recession. Table 4 also includes the average advance-time
and standard deviation of both treatments at 125 and 265 ft
(38.1 and 80.8 m).

Over the first 125 ft (38.1 m) of furrow length the
continuous and surge flow treatments do not differ very
much in either average advance-time or variability. Beyond
this distance the indication is that the advance rate is
generally faster in the surge flow treatment. However,
while the advance in six furrows treated by surge flow
reached the end of the furrow run, the final advance was
400 ft (122.0 m) or less in four furrows. By comparison,
one furrow within the continuous group had an advance
reach the end of the run, while six did not advance beyond
400 ft (122.0 m).

As pointed out in the previous chapter, several
difficulties existed at the time of Experiment A which
might have contributed to the rather large advance-time
variation observed in both treatments. Contrary to the
findings in Experiment B, uniformity of advance does
not appear to be improved by the surge flow treatment.
Nevertheless, there is an indication that surge flow
increased the furrow advance rate.

Power curves relating time as a function of distance were derived from the time-distance data in Table 4 and are presented separately for the continuous and surge flow treatment in Figures 20 and 21, respectively. With the two curves presented together as in Figure 22, there is a noticeable increase in the advance rate of the surge flow beyond 250 ft (76.2 m).

The relationship between the two curves is quite similar to the advance curve relationships derived in Experiment B between the continuous and cycled treatments. Despite the slower advance rates in Experiment A, both experiments demonstrated a more rapid advance in the surge flow treatments beyond 250 ft (76.2 m).

As in Experiment B the observed advance-times for furrows in the surge treatment were converted to cumulative inflow on-times. These are presented in Table 5 at the corresponding distances along with the continuous flow time-distances observations. The continuous flow time-distance summary is the same as in Table 4, except that the final time does not include the 10-minute recession period in those furrows failing to complete the advance. Power curves fit from the data of Table 5 were derived for both treatments and are shown together in Figure 23.

The variation in the two curves of Figure 23 follows the volume-distance trend of Experiment B between continuous and cycled flows (see Figure 19). In both cases the indication is that surge flow reduced total water require-
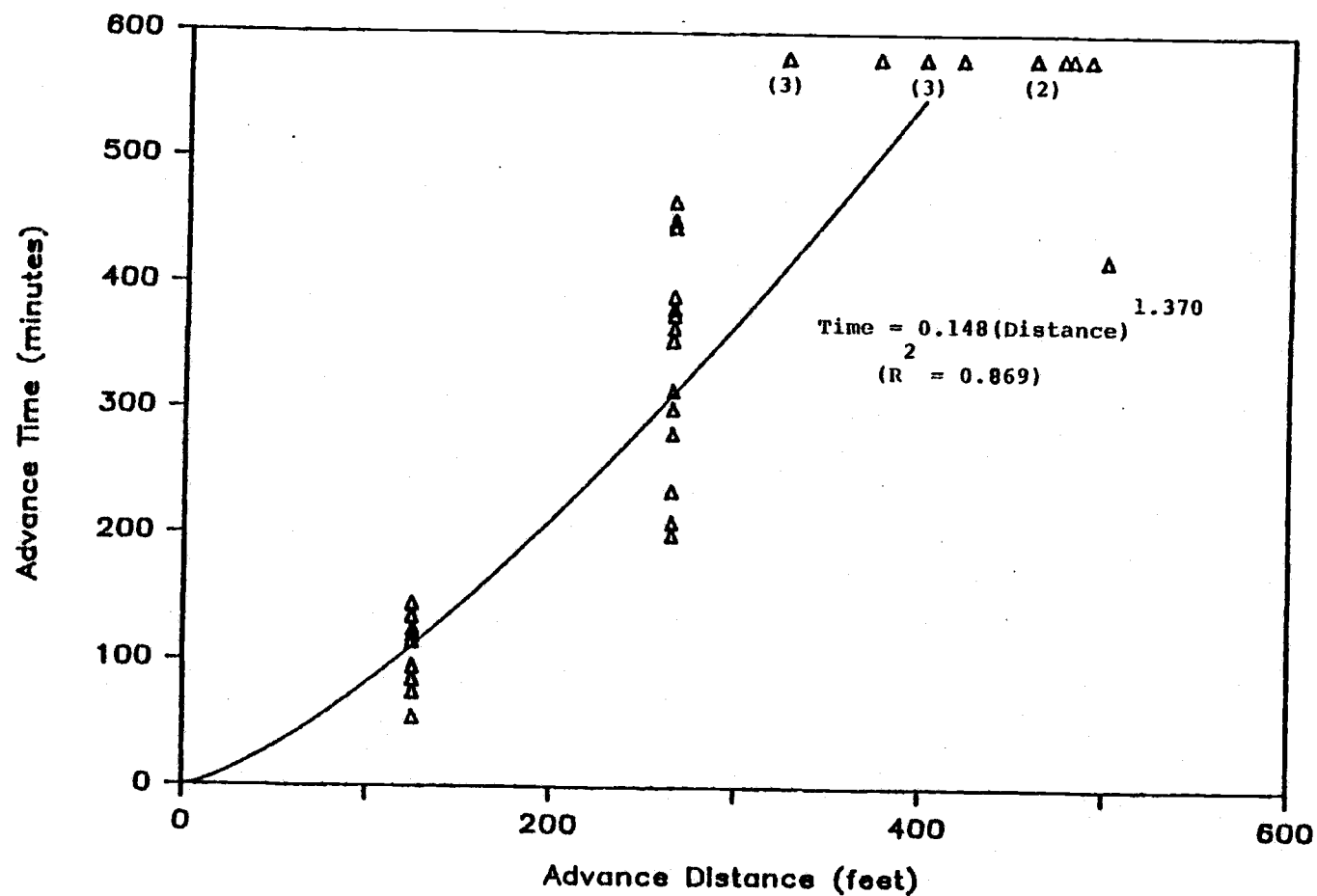
Figure 20. Experiment A: Observed Time of Advance and Plotted Advance Curve for 14 Furrows under Continuous Flow.

The plotted equation:

$$\text{Time} = 0.148(\text{Distance})^{1.370}$$
$$(R^2 = 0.869)$$
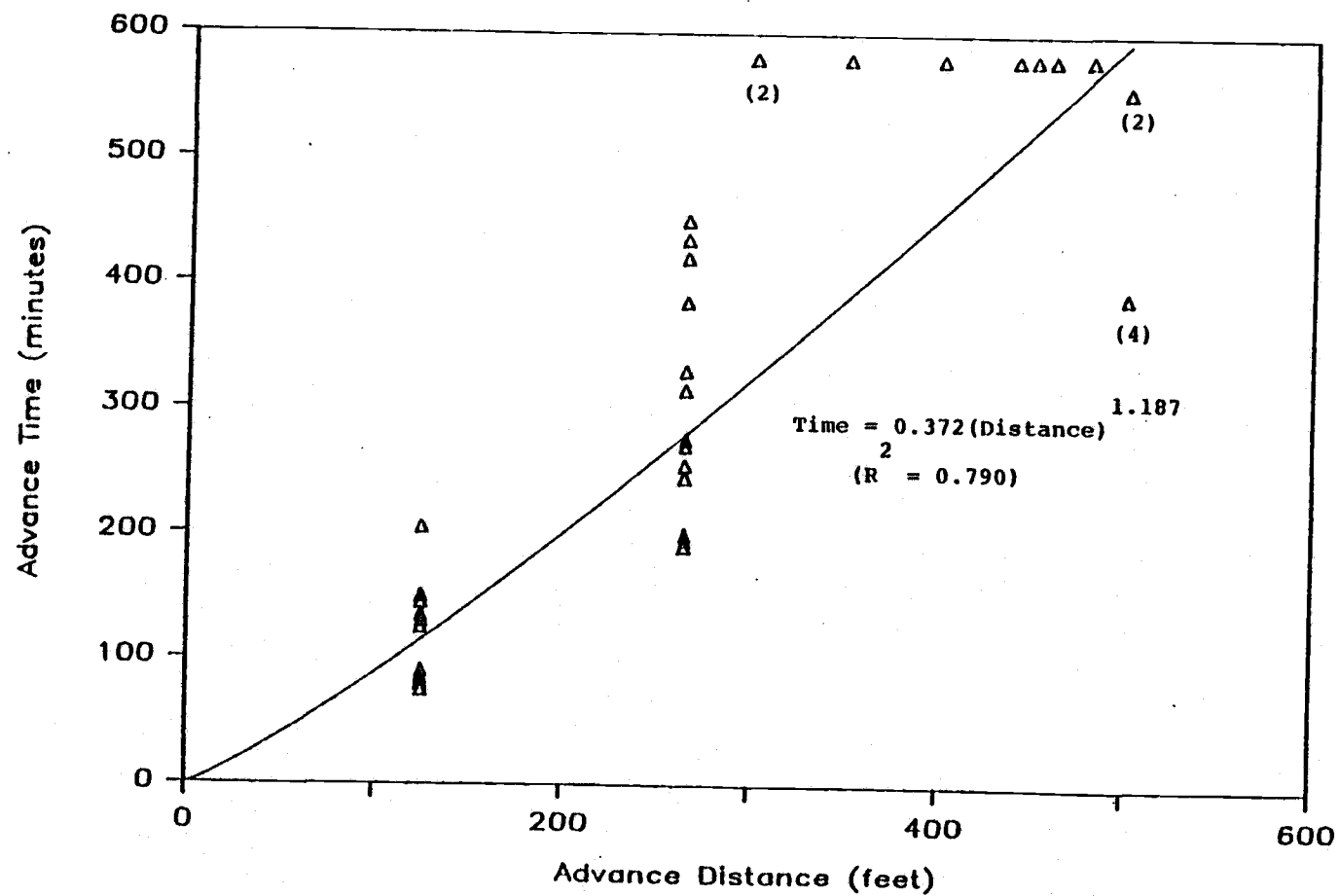
Figure 21. Experiment A: Observed Time of Advance and Plotted Advance Curve for 14 Furrows under 1:2 Cycle Ratio Surge Flow.
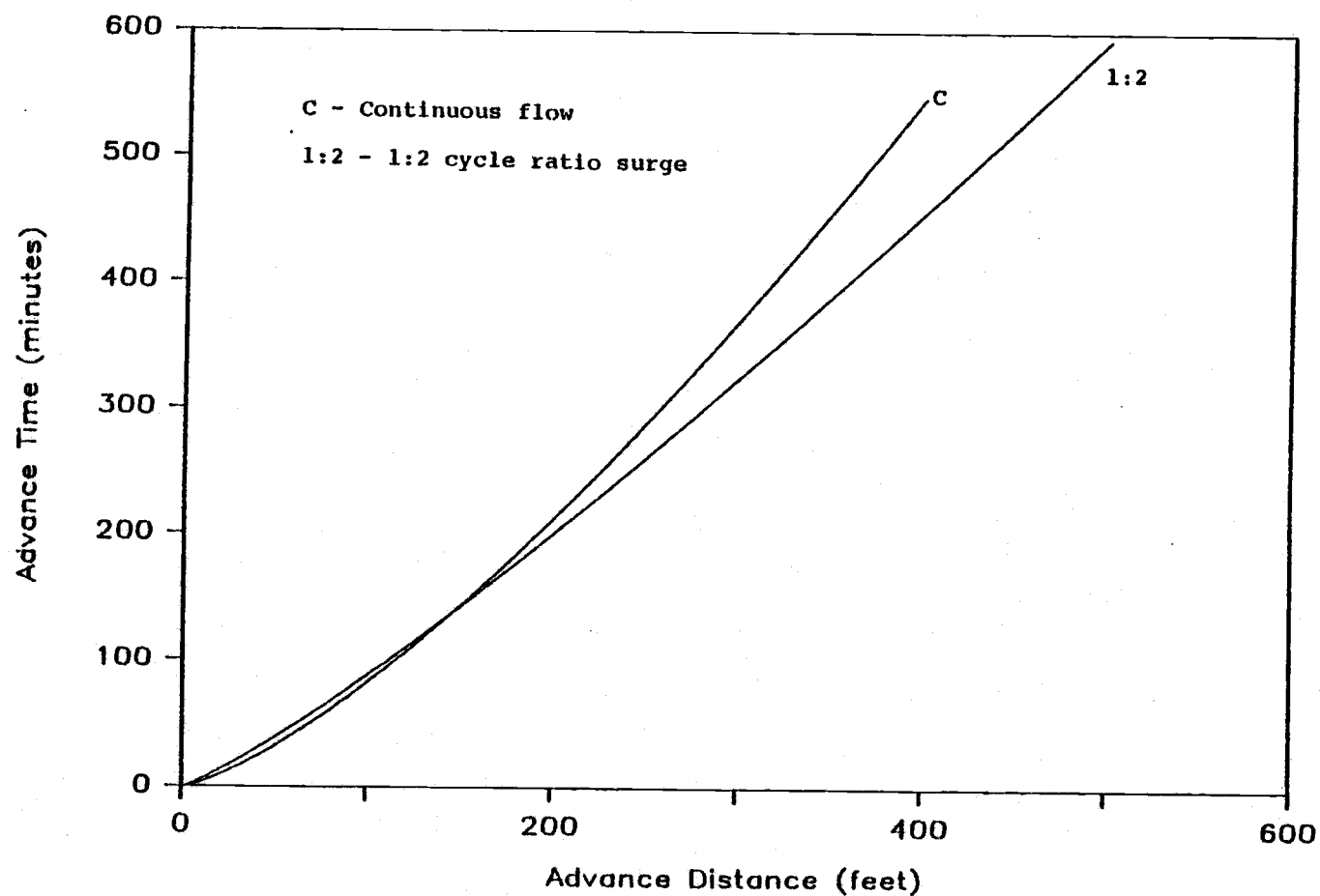
Figure 22. Experiment A: Advance Curves for Continuous and 1:2 Cycle Ratio Surge Flow.

Table 5. Experiment A: Cumulative On-Time (Minutes) for Furrow Advance to Reach Indicated Distance, with Mean and Standard Deviation (SD) at 125 and 265 ft for Each Treatment.

TREATMENT	FURROW	125	265	300	325	350	375	400	420	440	450	460	475	480	490	500
CONTINUOUS	1	125	355			570										
	2	120	300											570		
	3	115	375										570			
	4	135	445		570											
	5	145	450		570											
	6	85	280									570				
	7	85	380				570									
	8	75	210													420
	9	95	390				570									
	10	135	365		570											
	11	95	315				570									
	12	55	200									570				
	13	135	235												570	
	14	135	465					570								
	MEAN	109.6	340.4													
	SD	27.8	86.9													
SURGE 1:2 CYCLE RATIO	15	45	100													210
	16	115	225			300										
	17	70	150									300				
	18	75	165													210
	19	85	150										300			
	20	50	180							300						
	21	55	150								300					
	22	90	210					300								
	23	60	110													210
	24	45	135													285
	25	69	205	300												
	26	45	105													210
	27	50	120													285
	28	85	240	300												
	MEAN	67.1	160.4													
	SD	21.1	45.7													

78

Figure 23. Experiment A: Advance Curves based on Cumulative Inflow On-time for Continuous and 1:2 Cycle Ratio Surge Flow.

ments by a significant amount in advancing 200 ft (61.0 m) and beyond. Because of the slower advance rates of Experiment A the volume reduction is apparent even at 100 ft (30.5 m) where the surge treatment requires approximately 64% of the volume required by the continuous treatment. Beyond 200 ft (61.0 m) however, the continuous and surge flow curves in Figure 23 generally demonstrate a similar trend as the continuous and 2:3 cycle ratio treatment of Experiment B.

V.   KINEMATIC WAVE MODEL

Introduction

In support of experimental field studies, a variety
of mathematical computer simulation models of furrow irri-
gation have been developed to predict the performance of
continuous flow advance and recession.

Attempts to simulate the surge flow regime have been
limited to date. However, a kinematic wave model which
incorporates surge flow has been developed by Walker and
Lee (1981) and appears to offer an effective simulation
approach. Since then, the characterization of infiltration
under cycled flow has been more extensively researched
(Walker, Malano, and Replogle, 1982). As a result, the
Walker-Lee model has been modified to describe the surge
flow infiltration process with the same infiltration
function used for continuous advance. However, the func-
tion parameters that are used are different when flow is
over a previously wet furrow section, as is the case for
cycled surges.

The kinematic wave model development presented in this
chapter generally follows the methodology outlined by
Walker and Lee (1981), but includes the modified infiltra-
tion function mentioned above for surge flow. The hand-
ling of accumulated infiltration in previously wet sec-
tions, which will be described later in the chapter, is
approached in a different manner than in Walker and Lee's

model.

Developmental Background

Surface flow of irrigation water can be described mathematically by the Saint-Venant equations. For unsteady, gradually varied, one-dimensional flow in open channels, the complete hydrodynamic partial differential equations consist of an equation of mass conservation:

$$\frac{\partial Q}{\partial x} + \frac{\partial A}{\partial t} + \frac{\partial Z}{\partial t} = 0 \tag{5}$$

and an equation of energy conservation:

$$\frac{\partial V}{g \partial t} + \frac{V \partial V}{g \partial x} + \frac{\partial y}{\partial x} = S_o - S_f + (\frac{\partial Z}{\partial t})\frac{V}{2gA} \tag{6}$$

In equations 5 and 6, A = cross-sectional area of flow (L^2); Q = discharge across a section (L^3/T); x = horizontal distance along channel (L); y = depth of flow (L); t = time (T); V = Q/A = average flow velocity (L/T); Z = lateral outflow (infiltration volume per unit length of channel, L^3/L); g = gravitational constant L^2/T); S_o = channel bottom slope (L/L); S_f = channel friction slope (L/L) (Jensen, et al., 1980, p 455).

The complete hydrodynamic models have demonstrated a high degree of accuracy in describing the irrigation process of gravity systems. However, the numerical solution of the Saint-Venant equations with all terms retained is quite complex and relatively expensive to

execute (Strelkoff and Katapodes, 1977). Consequently, several simpler models capable of producing good results have been developed which are generally easier to program and less costly to run. Among these simplified models is the zero-inertia approximation model which involves the numerical solution of equations 5 and 6 with the three acceleration (inertial) terms deleted from the energy equation. The justification for deleting the acceleration terms is that the water velocities in surface irrigation are quite low and, therefore, can be neglected (Strelkoff and Katapodes, 1977). When the acceleration terms are deleted, equation 6 becomes:

$$\frac{\partial y}{\partial x} = S_o - S_f \tag{7}$$

Elliot, et al. (1982) developed a zero-inertia model describing the advance phase of continuous flow furrow irrigation. An important feature of this model was a reduction in the number of dependent variables, accomplished by mathematically relating the flow depth, y, and the cross-sectional area of flow, A, in the following power function:

$$y = \sigma_1 A^{\sigma 2} \tag{8}$$

and by relating hydraulic radius, R, and area in the function:

$$A^2 R^{4/3} = \rho_1 A^{\rho 2} \tag{9}$$

in which σ_1, σ_2, ρ_1, and ρ_2 are geometrical data fitting parameters derived by linear regression.

The friction slope which is defined by the Manning equation as:

$$S_f = \frac{Q^2 n^2}{A^2 R^{4/3}}$$

(10)

could then be redefined by substituting equation 9 into equation 10. The result is:

$$S_f = \frac{Q^2 n^2}{\rho_1 A^{\rho_2}}$$

(11)

where n = Manning's coefficient of roughness.

Additional assumptions made in the zero-inertia analysis were that the geometry parameters (σ_1, σ_2, ρ_1 and ρ_2), bottom slope, S_o, Manning's n, and the soil intake characteristics are constant over the entire furrow length (Elliot, et al., 1982).

Kinematic Wave Model Development

The kinematic wave analysis incorporates a deformable control volume representation of the conservation of mass equation, an approach used by both Strelkoff and Katapodes (1977) and Elliot, et al. (1982) in their respective zero-inertia models. Initially developed by Lighthill and Whitham (1955) to model flood movement in rivers, the kinematic wave model was extended to furrow advance

applications by incorporating the furrow geometry function of equation 9 (Walker and Lee, 1981). The following discussion deals with four aspects of the kinematic wave model; the advance phase, infiltration, the recession phase, and the surge flow modifications.

. Advance Phase

The development of the kinematic wave model follows the approach outlined by Walker and Lee (1981) in which only equation 5, the mass conservation equation, is evaluated and the energy equation (equation 7) is replaced by the assumption that the surface flow profile is uniform, resulting in a unique depth-discharge relationship. Inherent to this assumption is that the bottom slope, S_o, is sufficiently steep, thus making the depth gradient $(\frac{\partial y}{\partial x})$ of equation 7 much smaller than either of the two right hand terms. This implies that S_o is essentially equal to S_f everywhere, and therefore flow is at uniform depth.

With the assumption of uniform flow, S_f can be replaced with S_o in equation 10 (Manning's equation), and the equation can be rewritten relating depth and discharge as follows:

$$Q = \frac{A \, R^{2/3} \, (S_o)^{\frac{1}{2}}}{n} \tag{12}$$

in which A and R are functions of depth, and S_o and n are constant as also assumed in the zero-inertia model.

If equation 11 is employed, it is possible to describe the flow rate, Q, as a function of cross-sectional flow area, A, alone. That is, equation 12 may be re-written as:

$$Q = \alpha A^{m+1} \tag{13}$$

where:

$$\alpha = (\rho_1 S_o)^{\frac{1}{2}}/n \tag{14}$$

and

$$m+1 = \frac{\rho_2}{2} \tag{15}$$

in which α and $m+1$ are known constants.

Program computations occur at a succession of specified time steps during which a numerical solution is sought for the incremental advance at the end of each time step. Except during the first time interval, the solution depends upon the solution in the preceding time step and on the known discharge at the furrow inlet.

At any time during advance, the volume of water which has entered the furrow either infiltrates into the soil or is stored on the soil surface. This volume of water is represented by a group of moving, deforming control volume cells which are introduced one at a time at the furrow inlet at the beginning of each new time interval.

Figure 24 illustrates how the control volume cells move relative to one another through time and space. At the end of the first time interval, δt_1, the first cell (which was introduced at time t_o) extends over the first
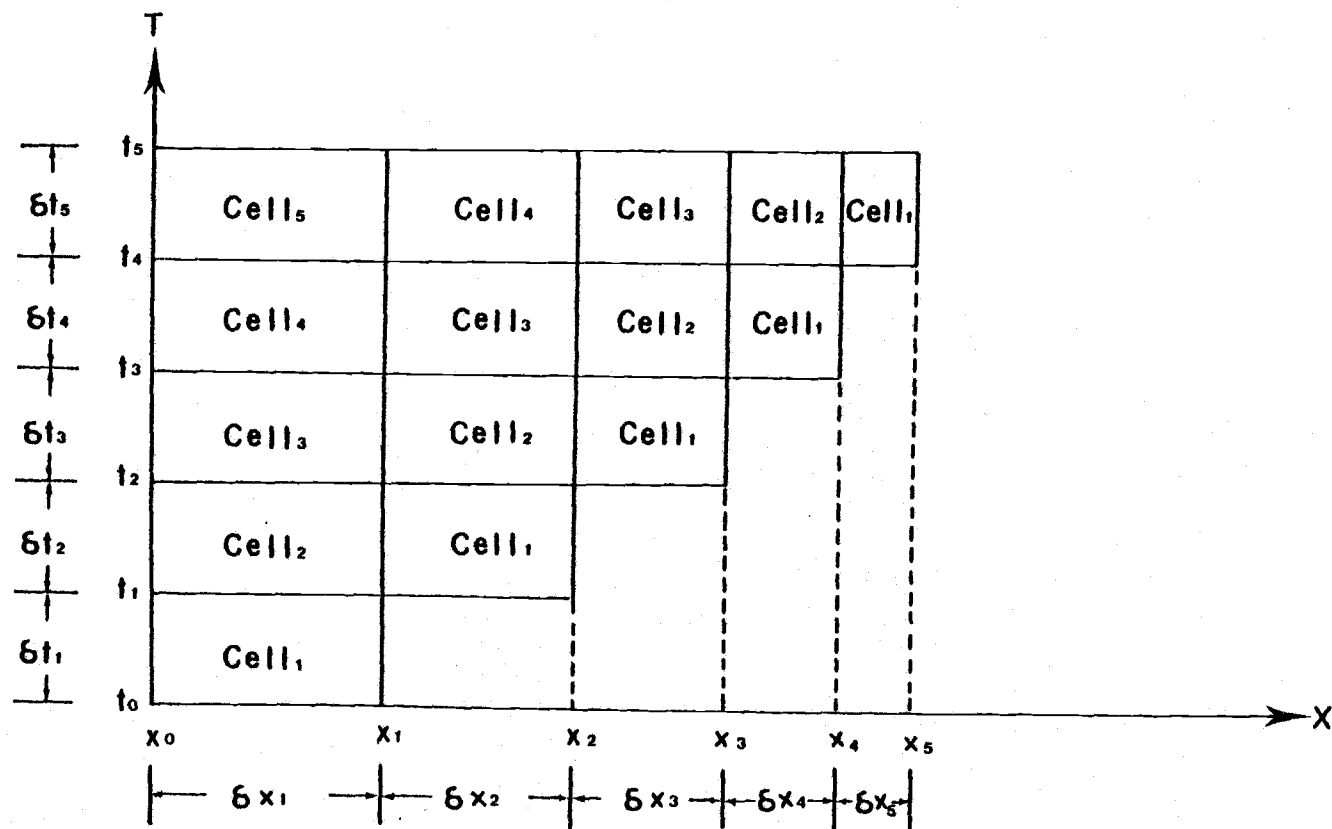
Figure 24. Movement of control volume cells relative to one another in the x and t directions during advance.

incremental advance distance, δx_1, bounded between x_o and x_1. At time t_1 the second cell is introduced. At the end of δt_2, the second cell extends over the first incremental advance distance, δx_1, while the first cell, having been "pushed" downstream, extends over the second incremental distance, δx_2, bounded by x_1 and x_2. With the introduction of each new cell, all previously introduced cells move downstream an incremental advance distance during each time interval (Figure 24 illustrates this process through five time intervals).

As the control volume cells move in time, the properties at the control volume boundaries change. To illustrate this, $cell_3$ of Figure 24 is depicted at two successive times, t_4 and t_5, in Figure 25. At t_4 the left boundary of $cell_3$ is at x_1. The discharge rate at this boundary is Q_J, while the cross-sectional area of surface flow is A_J and the infiltrated volume per unit length is Z_J. At the right boundary, x_2, the properties are Q_M, A_M and Z_M.

During the time interval, δt_5, the left and right boundaries of the cell move a downstream distance δx_2 and δx_3, respectively. At the end of the time interval (i.e., at t_5), the discharge rates at the left and right boundaries are now Q_L and Q_R, respectively, while the flow area and infiltration are A_L and Z_L at the left boundary and A_R and Z_R at the right boundary. The use of the subscripts J, M, L, R clarifies which cell boundary is under
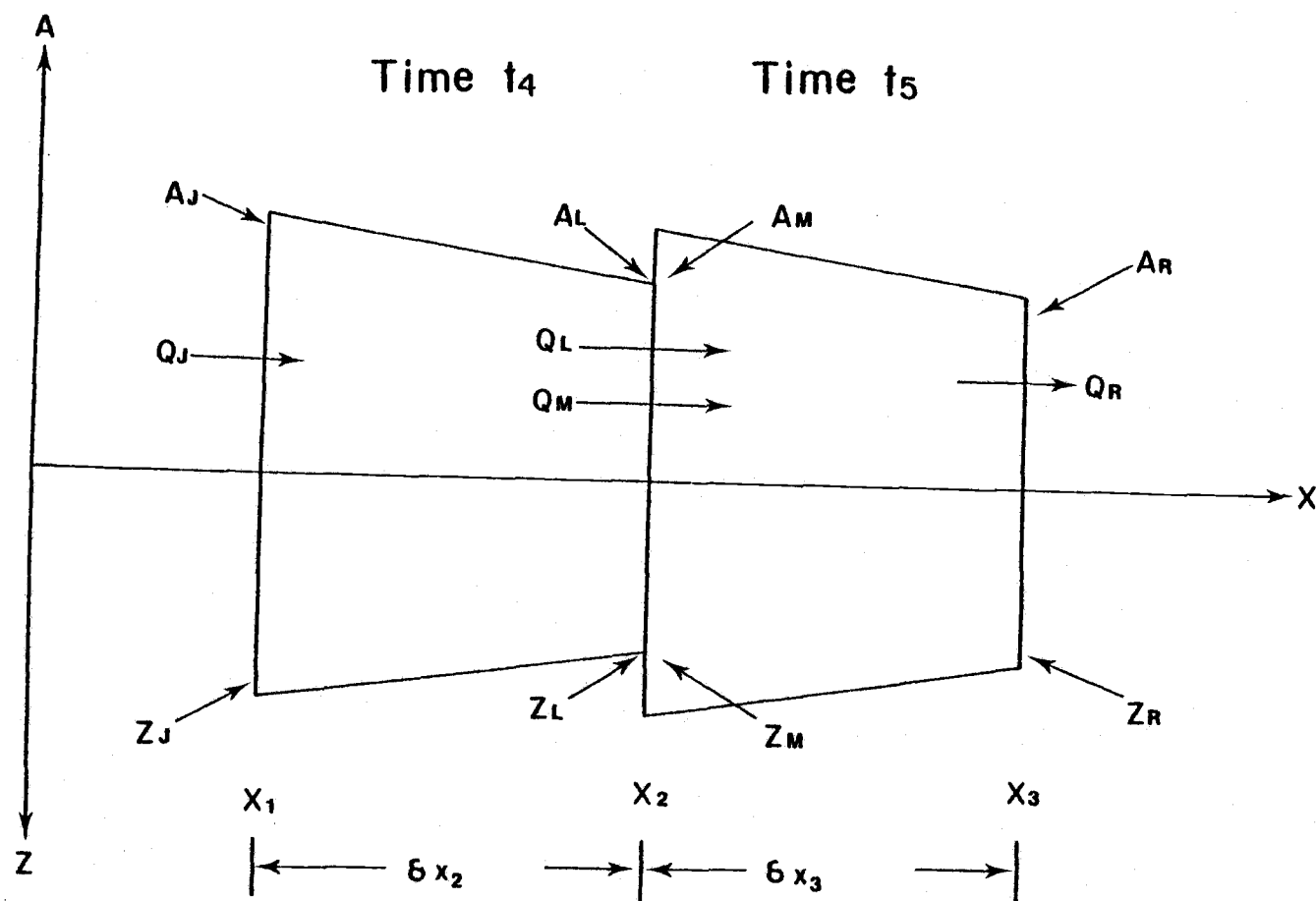
Figure 25. A deformable control volume cell at two succeeding times (after Strelkoff and Katapodes, 1977).

consideration and whether the beginning or end of the time interval is being referenced.

To advance the numerical solution from time t_{i-1} to t_i, the conservation of mass equation (equation 5) is numerically integrated sequentially over each control volume cell during the time interval. In order to facilitate the numerical solution of equation 5 over a cell of finite size in the x-t plane, the cells during advance are taken in the oblique form rather than the rectangular form as they appear in Figure 24 (Strelkoff and Katapodes, 1977).

Reference is again made to $cell_3$ which is now shown as the shaded trapezoidal shaped cell in the x-t computational grid of Figure 26. The cell boundaries MJLR correspond to the boundaries depicted for $cell_3$ at times t_4 and t_5 in Figure 25. It should be clear that the number of cells, N, on any given time line, t_i, in the x-t grid is equal to i.

In the following discussion the number of a cell will not be referenced as it was previously. In the present context, the number of a given cell, k, will correspond to the incremental advance distance, δx_k, over which it is bounded at any particular time line.

The conservation of mass equation states that the net inflow into the control volume equals the change in the volume of water stored during any time interval, δt. The numerical integration of the mass conservation equation over a cell volume during δt is accomplished by
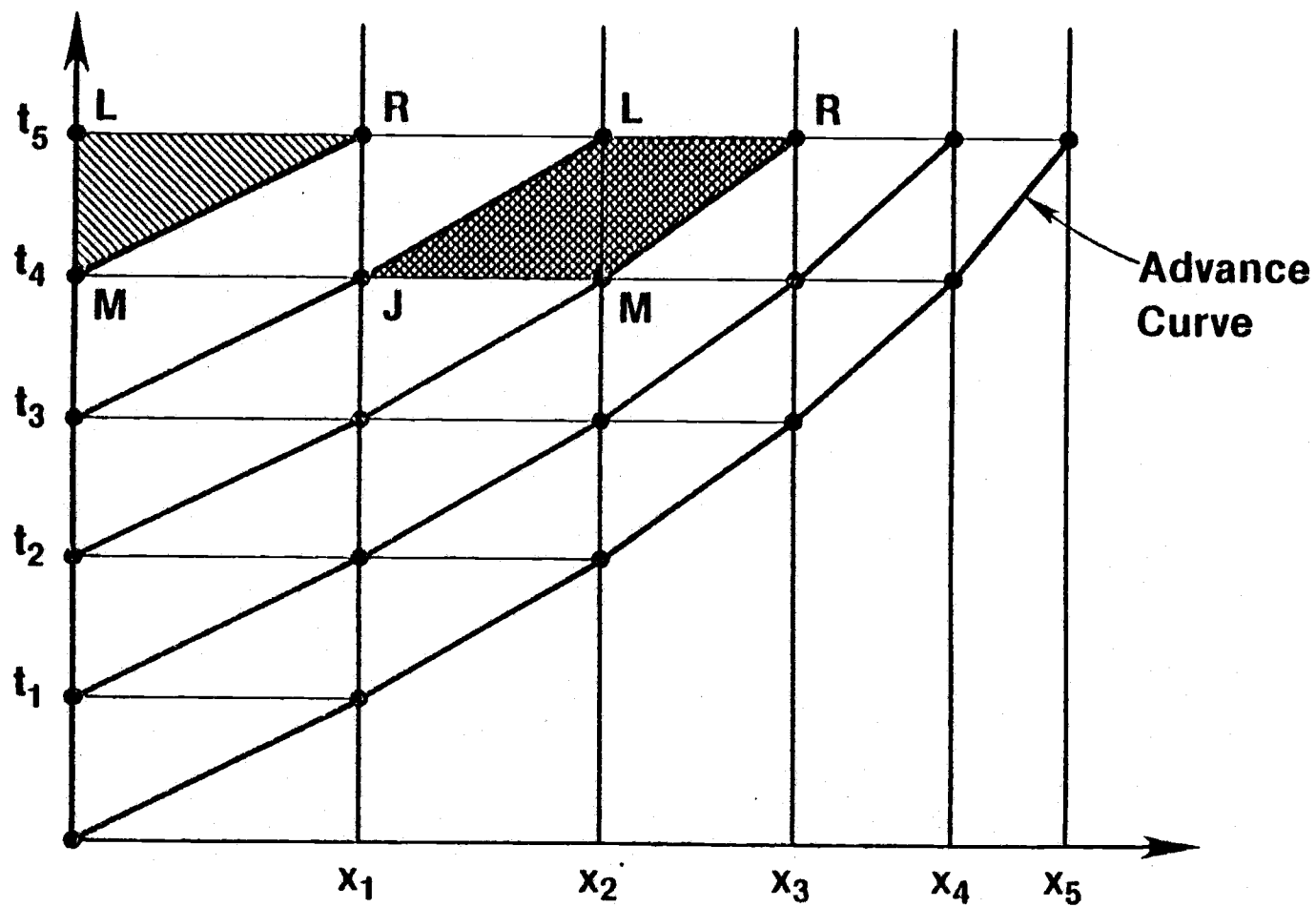
Figure 26. A deformable control volume x-t computational grid.

replacing the derivitives in the differential equation with
finite difference quotients. The derivation of the kinema-
tic wave equations are equivalent to the expressions
developed by Elliot, et al. (1982).

As shown in Figure 25, the cross-sectional boundaries
of the deforming cell volume cut across both surface and
infiltrated water defining surface and subsurface profile
regions. Integration of the mass conservation equation
over a time period δt for any interior cell, k, (where
$1 < k < N$) can be expressed approximately as:

$$\{(A_L + Z_L)\phi + (A_R + Z_R)(1-\phi)\}\delta x_k -$$

$$\{(A_J + Z_J)\phi + (A_M + Z_M)(1-\phi)\}\delta x_{k-1} = \tag{16}$$

$$\delta t\{\theta((Q_L - (A_L + Z_L)\delta x_{k-1}/\delta t) - (Q_R - (A_R + Z_R)\delta x_{k-1}/\delta t))$$

$$+(1-\theta)((Q_J - (A_J + Z_J)\delta x_{k-1}/\delta t) - (Q_M - (A_M + Z_M)\delta x_k/\delta t))\}$$

in which the integrands of the mass conservation equation
have been expressed by weighted numerical averages of their
values at each node. The variables ϕ and θ in equation 16
are the weighting factors used for spacewise and timewise
integration, respectively, and both have values in the
vicinity of 0.5 (Strelkoff and Katapodes, 1977).

For the first cell, k = 1, the left and right bound-
aries of the cell are collapsed together at the beginning
of the time interval. The right boundary moves a distance
δx_1 by the end of the interval, while the left boundary
remains fixed, which gives rise to the triangular shaped
cell shown shaded in Figure 26. For this cell, equation 16

simplifies to:

$$\{(A_L + Z_L)\phi + (A_R + Z_R)(1-\phi)\delta x_1 = \tag{17}$$
$$\delta t\{\theta(Q_L - Q_R - (A_R + Z_R)\delta x_1/\delta t) + (1-\theta)((A_M + Z_M)\delta x_1/\delta t)\}$$

In equation 17, Q_L is known from the specified inflow rate and A_M and Z_M are known from solution at the preceding time step leaving only Q_R, A_R and Z_R as dependent variables. A_L is calculated directly from the given inflow rate and furrow geometry, while Z_L is calculated by the Kostiakov relation described later. A key assumption made concerning infiltration is that in any particular cell, Z_R equals Z_M and Z_L equals Z_J. With this assumption and the use of equation 13, equation 17 can be expressed in terms of one dependent variable, A_R. Thus, equation 17 may be written as:

$$A_R^{m+1} + C_1 \cdot A_R - C_2 = 0 \tag{18}$$

where:

$$C_1 = \frac{(1-\phi-\theta)}{\alpha\theta} \delta x_1/\delta t \tag{19}$$

and

$$C_2 = -\frac{(1-\phi-\theta)}{\alpha\theta} Z_R \delta x_1/\delta t + A_L^{m+1} - \frac{(A_L + Z_L)\phi\delta x_1/\delta t}{\alpha\theta}$$

$$+ \frac{(A_M + Z_M)}{\alpha\theta}(1-\theta)\delta x_1/\delta t \tag{20}$$

Equation 18 can be solved explicitly for A_R using a "second order" method, such as the Newton-Rhapson procedure (Walker

and Lee, 1981).

Equation 16, the mass conservation equation for all interior cells, also reduces to equation 18. However in this case C_2 becomes:

$$C_2 = -\frac{(1-\phi-\theta)}{\alpha\theta} Z_R \delta x_k/\delta t + A_L{}^{m+1} + \frac{(1-\theta)}{\theta} A_J{}^{m+1}$$

$$-\frac{(1-\theta)}{\theta} A_M{}^{m+1} - \frac{(A_L+Z_L)}{\alpha\theta} (\phi\delta x_k/\delta t + \theta\delta x_{k-1}/\delta t)$$

$$+\frac{(A_J+Z_J)}{\alpha\theta} (\phi\delta x_{k-1}/\delta t - (1-\theta)\delta x_{k-1}/\delta t) +$$

$$\frac{(A_M+Z_M)}{\alpha\theta} ((1-\phi)\delta x_{k-1}/\delta t + (1-\theta)\delta x_k/\delta t) \qquad (21)$$

For cells $1<k<N$ on a given time line, A_L is found from the preceding cell calculation of A_R, and A_M and A_J are known from the preceding time step. The infiltration values, Z_J and Z_M, are computed at the corresponding infiltration time thereby defining Z_L and Z_R, respectively.

An incremental advance distance, δx_N is computed at the end of each time step, and in so doing establishes the δx_k distance boundaries over which succeeding cells move as the solution proceeds in time. During the first time step δt_1, flow advances an incremental distance, δx_1. In this instance, variables A_R, A_J, A_M, and Z_R, Z_J, Z_M are zero, thereby reducing equations 18 through 20 to:

$$-A_L{}^{m+1} + \frac{\phi}{\alpha\theta} (A_L+Z_L)\frac{\delta x_1}{\delta t} = 0 \qquad (22)$$

Since A_L can be determined from the specified inflow rate and Z_L is assumed related to δt in the Kostiakov function, the unknown incremental advance can be approximated as:

$$\delta x_1 = \frac{\theta Q_L \delta t}{\phi (A_L + Z_L)} \qquad (23)$$

where:

Q_L is the specified inflow rate

A_L is found using the relationship of equation 13

Z_L is found from the Kostiakov infiltration function

$\theta = 0.65$

$\phi \quad 0.65$

During subsequent time steps δt_i (where i>1), flow advances an incremental distance δx_N (where N=i). As in the previous case, values at the boundaries MJR are zero and equations 18 through 20 again reduce to equation 22. Thus, the unknown incremental advance δx_N is approximated as:

$$\delta x_N \approx \frac{\theta \alpha A_L^{m+1} \delta}{\phi (A_L + Z_L)} \qquad (24)$$

where:

A_L is found from the preceding cell calculation of A_R

Z_L is found from the Kostiakov infiltration function

$\theta = 0.65$

$\phi = 0.65$

The values of time and space weighting factors θ and

ϕ used in equations 23 and 24 are defined differently than in the interior cell equations. In earlier models a different value for ϕ in the form of surface and subsurface weighting or "shape" factors has been used in equations 23 and 24 for both A_L and Z_L (Strelkoff and Katapodes, 1977; Elliot, et al., 1981; Walker and Lee, 1981). However, in these models the shape factor applied to A_L assumes a uniform flow velocity behind the advancing tip. This is simply not observed in short advance increments, as applied in equations 23 and 24. Also, the subsurface shape factor applied to Z_L assumes that the contribution to the total infiltrated volume from the basic intake term (see equation 26) of the Kostiakov function is negligible, which for many soils is not the case (Walker and Humpherys, 1983).

Consequently, Walker and Humpherys (1983) have suggested replacing the shape factor assumptions and retain equations 23 and 24 in their present turns. In their kinematic wave furrow irrigation model, Walker and Humpherys (1983) have successfully used a value of 0.65 for both θ and ϕ.

. Infiltration

The Kostiakov infiltration function is commonly used in surface irrigation applications. The modified form of the Kostiakov function describes the soil infiltration rate as:

$$\frac{\partial Z}{\partial t} = aKt^{a-1} + f_o \qquad (25)$$

where $\partial Z/\partial t$ is the infiltration rate ($L^3/T/L$); t is the intake opportunity time (T); f_o is basic intake rate of the soil ($L^3/L/T$); K is an empirical constant ($L^3/T^a/L$); and a is an empirical exponent (dimensionless). When integrated over time, equation 25 yields the volume of water per unit length infiltrating the soil through time t. For this model, the infiltration, Z, is approximated by the integrated form of the Kostiakov function:

$$Z = Kt^a + f_o t \qquad (26)$$

where Z is in units L^3/L, and K, a, and f_o are as indicated above.

The values of the Kostiakov parameters (K, a, and f_o) must be experimentally determined at the particular site under consideration in the model. In the advance simulations presented by Elliot, et al. (1981), the parameters were derived from advance and inflow-outflow data at the sites studied. Thus, the model predictions of advance did not provide an independent simulation of actual field conditions. More recently, Walker, Malano, and Replogle (1982) have developed a flowing infiltrometer used in determining the infiltration parameters prior to an irrigation for both continuous and surge flow regimes.

. Recession

The recession phase begins when inflow is cutoff at
the upper end of the field. Cell computations follow the
same steps as in the advance phase (i.e., the cells pro-
ceed downstream over a given time line), however, during
recession cells are no longer introduced. At cutoff the
existing cell volumes shrink beginning with the uppermost
cell (k=1) first. The flow area gradually declines at
each point further along the furrow length, eventually
approaching zero. The field of computation is bounded
at the upstream end by the first cell, k, downstream from
the cell where the flow area falls below a prescribed
amount (generally 0 to 10% of the flow area at the furrow
inlet during the advance phase)(Walker and Lee, 1981).
The volume of surface water remaining in a cell having
a computed flow area less than the prescribed area is
added to the accumulated infiltrated volume per length
at the corresponding field station, δx_k (the assumption
being that the advance velocity is essentially zero at
this time, and the remaining water will ultimately
infiltrate uniformly over this section)(Strelkoff and
Katapodes, 1977).

Computations continue until the flow area for all
cells fall below the prescribed area at which time the
recession phase is considered over and the final advance
distance is obtained. The ultimate distribution of
infiltrated water can then be computed over each δx_k

section. The prescribed flow area minimum amount used in the model is 5% of the inlet flow area during the advance phase as recommended by both Walker and Humpherys (1983) and Strelkoff and Katapodes (1977).

. Surge Flow Modifications

The incorporation of surge flow into the kinematic model requires two key changes in the program. First, since surge flow alters the intake characteristics of the soil, different parameters are used in the Kostiakov function to describe infiltration in previously wet sections. If the computational cell corresponds to a previously wet section the infiltration function becomes:

$$Z = K't^{a'} + f_o't \qquad (27)$$

where K', a', f_o' are the Kostiakov parameters which have the same dimensions as K, a, and f_o described in equation 25.

Inherent in the assumption that soil intake is uniform throughout the field is the additional assumption that infiltration in unwetted sections will exhibit the same characteristics whether the irrigation is continuous or cycled. Thus, during the initial surge, or when a surge advances beyond a previously wet section, the infiltration function used is equation 26. In the later case, the intake opportunity time, t, is initialized to zero at the time the tip cell (k=N) crosses the wet-dry interface. Infiltration in subsequent cells reaching

the interface during a surge cycle is evaluated with equation 26 at the corresponding intake opportunity time.

The second modification is in the evaluation of the accumulated infiltration for previously wetted sections. In the case of continuous advance, the distance increments, δx, established in the x-t plane are maintained throughout the simulated irrigation. Infiltration is simply summed for each δx as time goes on. With surge flow, the incremental distances advanced are different for each surge. In that case, values of the infiltrated volume over the δx increments established during a prior surge are interpolated to estimate infiltration in each of the increments formed during the present surge. The interpolated values are than added to the accumulated infiltration over the currently established δx increments.

Comparison of Model With Experiment

The kinematic-wave model computer program listing, program flow chart, and definition of program symbols are presented in Appendix B.

Two computer runs were made to compare the predicted advance curves derived from the model output with the advance curves derived for the continuous and 1:3 cycle ratio surge flow treatments of Experiment B. For the two computer runs, field data from Experiment B were used to evaluate the model input parameters concerned with the physical aspects of the irrigation. Since the dimensional

units of the model are in Standard International (SI) units, all program input was converted to this unit system where necessary.

. Model Input Parameters

The assumed values of furrow inflow rate, Q, bottom slope, S_o, Manning's roughness coefficient, n, time increment, δt, space and time weighting factors, ϕ and θ, and the furrow geometry parameters (ρ_1, ρ_2) were the same for the continuous and surge flow computer runs. The value of Q was 7 gpm (0.000442 m^3/s) and S_o was 0.01 ft/ft (0.01 m/m). Although the true value of n is difficult to determine, the value of 0.04 which was used is recommended for furrow irrigation by the USDA Soil Conservation Service. The values of δt, ϕ, and θ were 1 minute, 0.5, and 0.6, respectively.[2] These values have been used by Strelkoff and Katapodes (1977) and Elliot, et al. (1982).

Furrow geometry measurements were made at several locations along the furrows prior to Experiment B. The furrow channel shape was best approximated as a trapezoid having a one inch (2.5 cm) base width, b, and a side slope of 1:1. By computing the cross-sectional area, A, and hydraulic radius, R, for a trapezoid with b=1 and slope = 1, while varying flow depth, y, from one to three

---

[2] In the case of an advancing tip cell, both ϕ and θ were set equal to 0.65.

inches (2.5 to 7.5 cm), the relationships between y and A, and $A^2R^{4/3}$ and A could be determined. Least squares regression was used to derive the following furrow geometry parameters of equations 8 and 9:

$\sigma_1 = 0.666$

$\sigma_2 = 0.603$

$\rho_1 = 0.267$

$\rho_2 = 2.657$

The Kostiakov infiltration function parameters used in the computer run of continuous and surge flow were calibrated using the field advance measurements of Experiment B for each treatment, respectively. Although it is difficult to assess the values of the infiltration parameters by field advance measurements alone, they can be reasonably approximated by employing the conservation of mass equation to account for all water (stored on the surface or infiltrated) that has entered the furrow over a given time and length (Christiansen, et al., 1966).

In the Kostiakov infiltration function, where

$$Z_o = Kt^a + f_o t \qquad (28)$$

infiltration Z_o (m^3/m) is assumed to be a function of infiltration time, t, alone. Since a value for Z_o can be calculated with the conservation of mass equation at several different known advance times, it is possible to fit a power curve relating Z_o as a function of t, providing f_o is known or estimated before hand. The coefficients derived for the power curve yield the estimated values of

a and K.

The basic intake rate recommended[3] for the Central Point series in continuous flow applications was 0.4 in/hr which when converted to the units used in the model becomes 0.000169 m^3/min/m. This value was used for the value of f_o during simulated continuous or dry advance, as well as in determining the values of K and a under these conditions. Information regarding the basic intake rate under cycled flow conditions is not currently available for the specific soil series. However, research by Walker, Malano, and Replogle (1982) indicates that in sandy loams, cycled flow commonly reduces the basic intake rate by about 50% of the value under continuous flow irrigation during a first irrigation. Therefore, for flow over previously wetted furrow sections, a discretionary value of 0.00008 m^3/min/m was used for f_o'.

Strelkoff and Katapodes (1977) presented a simplified technique for modeling advance as a function of time. The theoretical basis is a modified form of the conservation of mass equation which assumes that the surface stream and infiltrated-water profiles are known and that they follow a monomial power law of some constant degree. It is also assumed that flow is at normal depth at the upper end of the furrow segment for the given inflowing discharge. The normal flow area, A_o, can be calculated from equation 12.

---

[3] Personal communication--Ed Weber, SCS District Manager in Medford, Oregon.

With these assumptions, conservation of mass during advance can be expressed as:

$$60 \cdot Qt = \{A_o(\frac{1}{1+\beta}) + Z_o(t)(\frac{1}{1+a})\}x \qquad (29)$$

where Q = discharge rate, m^3/s

A_o = normal flow area at upper end of furrow segment, m^2

$Z_o(t)$ = volume infiltrated per length at the upper end of furrow segment where intake opportunity time equals irrigation time, m^3/m

x = length of advance, m

t = infiltration time at advance length (x), min

$\frac{1}{1+\beta}$ = surface stream shape factor, dimensionless

$\frac{1}{1+a}$ = infiltrated-water shape factor, dimensionless

The shape factor for the surface stream represents the ratio of stream volume at time t to the volume $A_o \cdot x$. The infiltrated-water shape factor represents the ratio of the infiltrated-water volume at time t to the volume $Z_o(t) \cdot x$. It can be shown (Elliot, et al., 1982) that:

$$\beta = \frac{1}{\sigma_2 + \rho_2 - 1} \qquad (30)$$

and a is the exponent in the Kostiakov function (equation 28). Therefore, in this model:

$$\beta = \frac{1}{.603 + 2.657 - 1} = 0.442$$

With the assumption of a monomial power law of degree β for the surface profile, the value of the flow area at any point along the advance can be approximated by:

$$A(s) = A_o(x-s)^\beta \qquad (31)$$

in which s = distance down the furrow, m

$\qquad$ A(s) = the flow area at s, m^2

In solving the infiltrated volume per unit length of advance at a given time, the term $Z_o(t)/1+a$ in equation 29 must be solved as a single quantity since both $Z_o(t)$ and a are unknown. Rearranging and setting $\dfrac{Z_o(t)}{1+a} = y$, equation 29 becomes:

$$y = \frac{60 \cdot Qt}{x} - \frac{A_o}{1+\beta} \qquad (32)$$

For continuous flow, $Z_o(t)/1+a$ was computed at the observed advance and corresponding average times of 100, 200, and 300 ft (30.5, 61.0, and 91.5 m). Dividing both sides of equation 28 by 1+a:

$$\frac{Z_o(t)}{1+a} = \frac{Kt^a + f_o t}{1+a} \qquad (33)$$

which can be rewritten as:

$$y(1+a) - f_o t = Kt^a \qquad (34)$$

Using the constant value given for f_o and an estimated value for a, a power function relating the left hand side of equation 34 to t was fit until the exponent of the

power function yielded the same value as the estimated value of a.

After rearranging the terms in equation 34, the Kostiakov infiltration function for either continuous flow or the first advance in surge flow is again expressed in the form of equation 28:

$$Z_o(t) = Kt^a + f_o t$$

The calibrated parameters found in the analysis were:

$K = 0.00357 \ m^3/m/min^a$

$a = 0.485$

with

$f_o = 0.000169 \ m^3/m/min$

Parameters a' and K' for the 1:3 ratio cycled flow over previously wetted sections were estimated in a similar manner as in the continuous flow condition. However, in this case the infiltration was evaluated only over the first 100 ft (30.5 m) of furrow length which was entirely wetted by the first surge. Infiltration time, t, for the cycled flow condition was then zero at the instant the second surge began, 15 minutes at the instant the third surge began, 30 minutes when the fourth surge began, and 45 minutes when the fifth surge began corresponding to the 15 minute on-time duration for each surge.

The infiltration quantity, $Z_o/1+a'$, was computed over the 100 ft (30.5 m) length beginning with the second

surge and repeated for surges 3, 4 and 5. Each computed

value of $Z_o/1+a'$ was then added to the previous values

to give an accumulated quantity of $Z_o/1+a'$ at times of

15, 30, 45 and 60 minutes. A power function relating

$(Z_o/1+a'-f_o't)$ to t was fit in the same procedure des-

cribed in the continuous flow analysis to determine the

parameters a' and K'.

For each of surges 2 through 5 the average advance

length, x, at the cumulative time through inflow cutoff

was found from the 1:3 cycle ratio surge flow advance

curve in Figure 13. This enabled the computation of the

flow area, A(100), at s = 100 ft (30.5 m) by equation 31.

Using equation 12 the runoff rate, Q(100), at the time

of inflow cutoff is related to A(100) as:

$$Q(100) = \alpha A(100)^{m+1}$$

Assuming that essentially all the surface water

remaining between zero and 100 ft (30.5 m) at the time of

cutoff infiltrates over this distance, $Z_o/1+a'$ can be

solved with the mass conservation equation rewritten as:

$$\left(\frac{Z_o}{1+a'}\right) = \frac{(Qin - Q(100)60t}{x} \tag{35}$$

where x = 100 ft (30.5 m)

t = 15 minutes

Qin = inflow rate at furrow head, m^3/s

Q(100) = runoff rate at x, m^3/s

and Z_o and a' are as defined in equation 27.

For 1:3 ratio cycled flow over previously wetted
furrow sections the calibrated parameters found were:

$K' = 0.00175 \text{ m}^3/\text{m/min}^a$

$a' = .1003$

with

$f_o' = 0.00008 \text{ m}^3/\text{m/min}$

. Results

The computer simulation of advance and infiltration
for the continuous and 1:3 cycle ratio surge flow are
presented in Appendix C and Appendix D. The program
output shows the input values, including the time at
which inflow is cutoff, and the maximum time allowed for
the computer run. The advance trajectory from one minute
through recession is shown for the advance in meters at
the end of each time step. The indicated cumulative
infiltration in cubic meters per meter corresponds to the
total volume of water which infiltrated by the end of
recession over the incremental distance (i.e., the furrow
segment between the advance length at one time step and
the advance length at the previous time step). The time
at which all water disappears from the surface is indicated
as 'recession complete'.

Also presented in the program output is a volume
balance comparison showing the total volume infiltrated at
the end of the recession with the total volume of inflow.
The total infiltrated volume is derived by the summation

of the infiltrated volumes at each incremental distance.
The total volume of inflow is simply the product of the
inflow rate and inflow time in seconds.

For continuous flow the model was programmed to
simulate advance for an inflow time period of 180 minutes.
A prior model run for continuous flow with an inflow time
of 200 minutes showed that after 160 minutes the advance
rate was extremely slow, decreasing to less than 6 inches
(15 cm) per minute. In fact, the simulated advance ceased
at 183 minutes after advancing a distance of 256.6 ft
(78.24 m). However, the model does not adequately handle
advance and infiltration computations in situations where
recession occurs at the tip cell prior to inflow cutoff
(i.e., when the computed flow area in the tip cell falls
below 5% of the furrow inlet flow area prior to inflow
cutoff). Consequently, for comparison purposes the model
was run for an inflow time of 180 minutes so that infil-
tration and volume balance computations could occur before
the recession of the advancing tip ended the simulation.

An advance curve relating time and advance distance
for continuous flow, fit by linear regression (R^2 =
0.9939), is presented in Figure 27 for the simulated 180
minute irrigation. Time and distance data were taken from
the program output from 15 through 175 minutes at 15 minute
intervals. Also shown in the same figure is the advance
curve for the experimental continuous flow treatment
presented earlier in Figure 12.
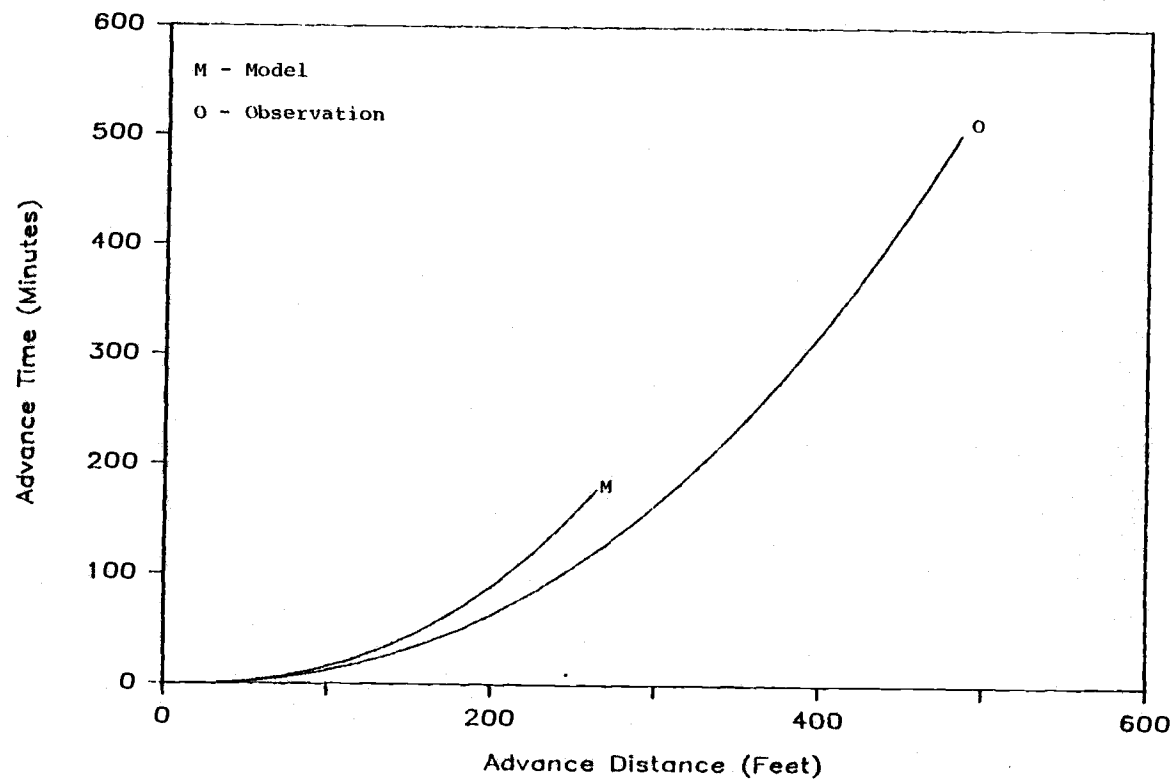
Figure 27.   Plotted power curves of predicted and observed advance
for continuous flow.

Figure 27 illustrates the discrepancy between predicted and observed advance times for continuous flow. Essentially, the model predicts that advance would stop after a 180 minute inflow time at a furrow distance of 256 ft (78 m). Consequently, the model prediction of continuous flow advance underestimated the advance observed in the experiment where all furrows tested advanced at least 400 ft (122 m). Nevertheless, it should be emphasized that the infiltration parameters (which in this case were not experimentally evaluated) have a tremendous bearing on the advance model results.

The model prediction of advance under a 1:3 cycle ratio surge flow is generally consistent with the observed field advance under this treatment. However, even in this case the simulated advance was unable to reach the distances attained by the actual 15 minute on-time surge flows. As indicated in Appendix D the simulated advance of the eighth surge advanced no farther than the 395 ft (120.5 m) distance attained by the seventh surge, indicating a relationship between the maximum simulated advance length and the input flow rate, on-time, and infiltration parameters.

Still, the advance trend of the model predicts fairly well the actual advance characteristics through the first seven surge cycles. An advance curve for the simulated irrigation relating the cumulative elapsed time with the advance distance was fit by linear regression ($R^2 = 0.991$)

with data from the model output. Time and distance points were taken at the end of each surge from surge 1 through 8. The fitted curve is presented in Figure 28 along with the corresponding advance curve derived from the field advance measurements of the 1:3 cycle ratio surge flow (also presented earlier in Figure 13).

The relationship between the two curves shows that the simulated advance slightly underestimates the observed advance of the experiment through a 400 ft (122 m) furrow length distance. However, as previously mentioned the simulated advance does not proceed beyond this distance while the advance in the furrows experimentally tested reached at least 485 ft (147.8 m).

If it is assumed that the programmed infiltration parameters overestimated the actual infiltration rates of the field experiment, the physical representation of the advance by the two simulated runs appears to be reasonable. In either simulation the advance trend did not deviate significantly from the observed trend of advance in the corresponding experimental case. In both simulated model runs advance was quite rapid over the first 100 - 125 ft (30.5 - 38.1 m) segment of furrow length, declining gradually beyond this point. The two field treatments advanced in a similar manner although the advance rates were significantly greater than those of the simulation.

The relationship between the two simulated treatments demonstrates an advantage for the surge flow treatment
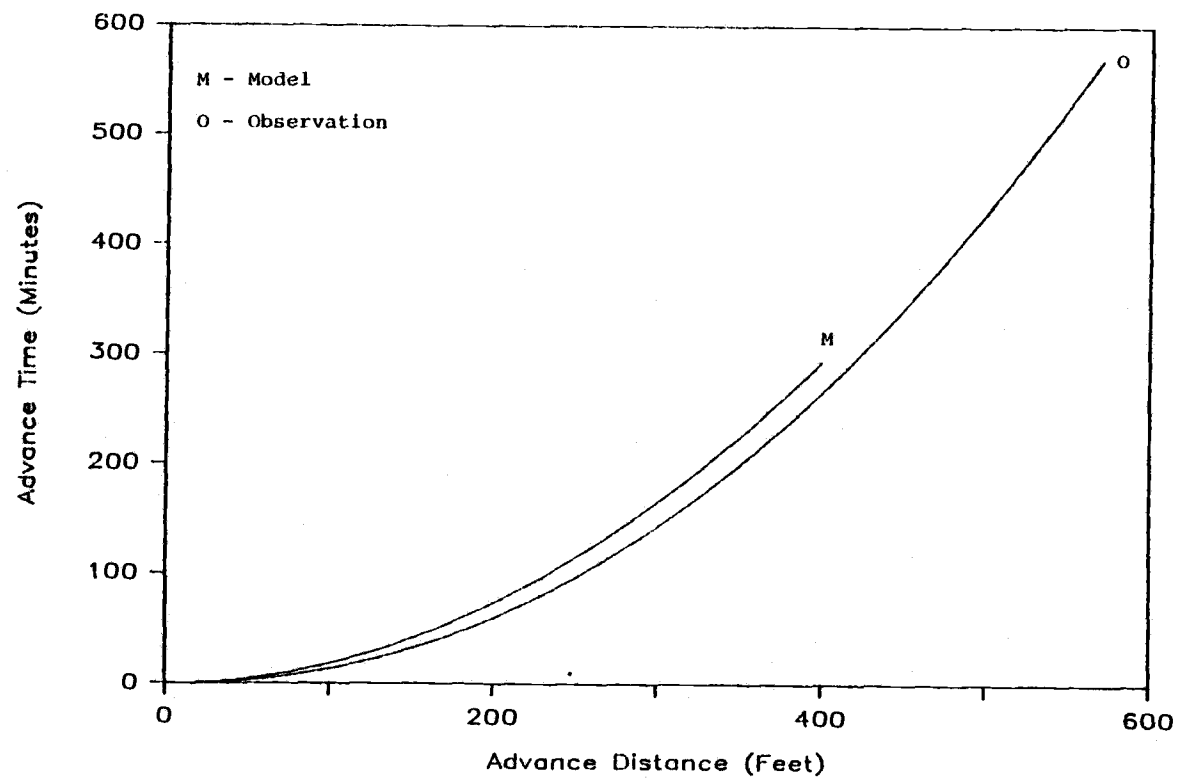
Figure 28.   Plotted power curves of predicted and observed
advance for 1:3 cycle ratio surge flow.

similar to that seen in the field experiments. This can be illustrated by presenting the advance curves of the two simulated treatments based on inflow on-time as shown in Figure 29. In general the relationship between the two simulated treatment curves of Figure 29 is quite similar to the experimentally found volume-distance curve relationship between the continuous and 1:3 cycle ratio surge flow treatments found in Figure 19. For advance distances of 150 ft (45.7 m) and 250 ft (76.2 m) the simulated surge flow used 58% and 37% of the volume of water required by the simulated continuous flow treatment. At these same two distances Figure 19 indicates that the 1:3 cycle ratio surge flow used 66% and 44% of the volume of water required by continuous flow. In both simulation and experiment the percent volume reduction of surge flow to continuous flow decreased by about 21% in advancing from 150 ft (45.7 m) to 250 ft (76.2 m). Although it is difficult to determine with great accuracy the distribution profile after an irrigation, it has been shown that surge flow can significantly improve the distribution uniformity over that of continuous flow. An important feature of the simulated advance model is in the description of the distribution of infiltrated water over the advance length.

In the two model runs program output indicates that infiltration is more uniform throughout the furrow in the case of surge flow. At the end of eight surge flow cycles, infiltration in m^3/m is 1.2, 1.5, 1.5 and 1.7 times greater
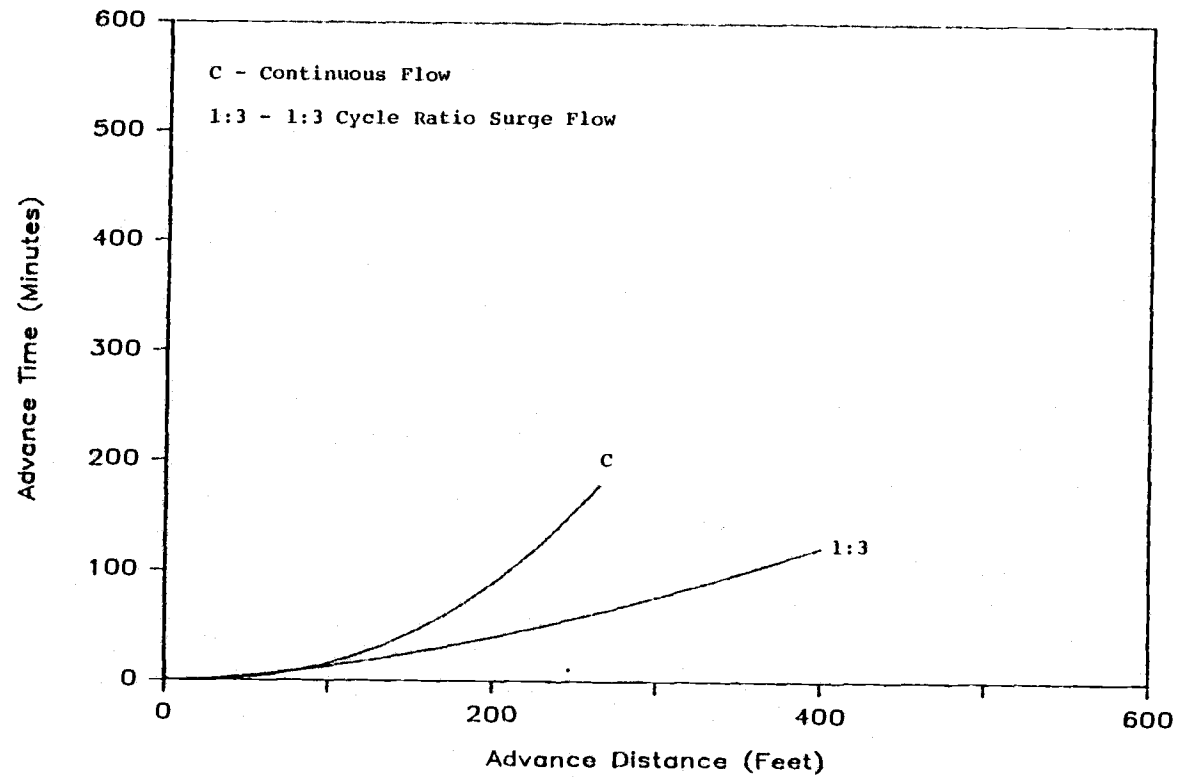
Figure 29.   Plotted power curves of predicted continuous and
             1:3 cycle ratio surge flow based on inflow on-times.

at the upper end of the furrow than at furrow length distances of 150, 200, 225, 250 ft (45.7, 61.0, 68.6 and 76.2 m), respectively. By comparison, after 180 minutes of continuous flow infiltration is 1.2, 1.5, 2.0 and 4.6 times greater at the upper end than at the same furrow length distances. Thus, over the first 200 ft (61.0 m) of furrow, uniformity is about equal for the two flow regimes. Beyond this distance the infiltration from continuous flow is much more variable.

VI. SUMMARY AND CONCLUSIONS

Two field experiments were conducted in southern Oregon to compare and evaluate furrow advance rates under surge flow and continuous flow irrigation. Both experiments were carried out at the same site on a moderately sloping sandy loam field. In support of the field studies, a kinematic wave model was developed and programmed to simulate both surge flow and continuous flow furrow advance.

The results of the two field experiments were consistent with the findings of other surge flow researchers. In the second experiment, advance was considerably faster in furrows irrigated by surge flow than in furrows irrigated by continuous flow. During the same irrigation time period, and using the same instantaneous application rate, none of the seven continuously irrigated furrows had an advance reach the end of the field, while the distance was completed in five of the eight furrows treated by surge flow. A comparison of the advance variation within treatments showed that the advance rate differences were substantially less under surge flow than under continuous flow. Both cycled flow treatments required significantly less water to advance than did the continuous flow treatment. The reduction was most pronounced in the 1:3 cycle ratio treatment which used only 26% of the water required by the continuous treatment

in advancing 500 ft (152.4 m).

In the first experiment, surge flow advance was also faster than continuous flow advance, although the uniformity of advance was not improved under surge flow as it was in the second experiment. However, several difficulties occurred during the first experiment which might have contributed to the rather large advance-time variation observed in both treatments. Nevertheless, the surge flow treatment required considerably less water than the continuous flow treatment in advancing downfield.

The observed continuous and surge flow advance from the second experiment and the model predictions of advance were fairly consistent. However it should be noted that the model infiltration function parameters were calibrated from the field data rather than experimentally determined. The model underestimated advance in both cases. This was particularly evident in the case of continuous flow where the model predicted the advance to stop at a furrow distance of about 256 ft (78 m). In the experiment, the observed continuous flow advance essentially stopped at a distance between 400-500 ft (122-152.4 m).

In the case of surge flow the model predicted the advance to stop at a furrow distance of 400 ft (122 m), about 130 ft (39.6 m) less than the observed average distance attained at the end of the irrigation for this treatment. However, through a distance of 400 ft (122 m)

the advance curve predicted by the model only slightly underestimated the advance curve derived from the experiment.

Conclusions

Specific problems associated with the operations and field conditions during the first experiment might have affected the advance performance, and thus, the results of that experiment. However, the results of the first experiment generally favored surge flow, and demonstrated similar differences in advance rates between continuous and surge flow irrigation as were observed later in the second experiment.

The results of the second experiment were consistent with the findings of other surge flow research; that is, surge flow irrigation provided a substantial increase in advance rates and a significant reduction in the volume of water needed for the advance phase. In addition, the advance uniformity between furrows irrigated by surge flow was greatly improved. For these reasons, surge flow irrigation could improve surface irrigation application uniformities and efficiencies considerably.

The development of simulation models to predict the surge flow irrigation process can lead to an improvement in the design and performance of surge systems, without having to rely on extensive field experimentation.

However, research on the infiltration process under surge flow has been limited to date. More intensive research in this area will probably be necessary if models are to be able to successfully predict the surge flow process.

The kinematic wave model presented in this thesis underestimated advance in the two model runs tested against the observed field advance. Nevertheless, the model was able to simulate the advance phase reasonably well. It should be remembered, however, that the infiltration function parameters were derived from field advance observations rather than experimentally determined.

BIBLIOGRAPHY

Bishop, A.A. 1980. Surge Flow - A Revolution in Surface Irrigation. Utah Science 41(2):60-63

Bishop, A.A. and W.R. Walker. 1981. Surge Flow Update. Utah Science 42(4):126-129.

Bishop, A.A., W.R. Walker, N.L. Allen, and G.J. Poole. 1981. Furrow Advance Rates Under Surge Flow Systems. Journal of the Irrigation and Drainage Division, ASCE 107 (IR3):257-264.

Bondurant, J.A. and A.S. Humpherys. 1962. Surface Irrigation Through Automatic Control. Agricultural Engineering 43(1):20-21.

Bondurant, J.A. 1969. Design of Recirculating Irrigation Systems. Transactions of the ASAE 12(1):195-198.

Chen, C.L. 1970. Surface Irrigation Using Kinematic Wave Method. Journal of the Irrigation and Drainage Division, ASCE 96(IR1):39-46.

Christiansen, J.E. 1942. Irrigation by Sprinkling. California Agricultural Experiment Station Bulletin 670, p. 52.

Christiansen, J.E., A.A. Bishop, F.W. Kiefer, and Yu-S, Fok. 1966. Evaluation of Intake Rates Constants as Related to Advance of Water in Surface Irrigation. Transactions of the ASAE 9(5):671-674.

Coolidge, P.S., W.R. Walker, and A.A. Bishop. 1982. Advance and Runoff - Surge Flow Irrigation. Journal of the Irrigation and Drainage Division, ASCE 108(IRI): 35-41.

Elliot, R.L., W.R. Walker, and G.V. Skogerboe. 1982. Zero-Inertia Modeling of Furrow Irrigation Advance. Journal of the Irrigation and Drainage Division, ASCE 108(IR3):179-195.

Fischbach, P.E. 1970. An Automated Surface Irrigation Valve. ASAE Paper No. 70-742, American Society of Agricultural Engineers.

Garton, J.E., R.P. Beasley, and A.D. Barefoot. 1964. Automation of Cut-Back Furrow Irrigation. Agricultural Engineering 45(6):328-329.

Gasten, J. 1983. USDA-ARS Engineer. Snake River Conservation Research Center, Kimberly, Idaho. Personal communication.

Humpherys, A.S. 1975. Automatic Valves for Surface Irrigation Pipelines. _Journal of the Irrigation and Drainage Division_, ASCE 101(IR2):95-109.

Jensen, M.E. (ed). 1980. _Design and Operation of Farm Irrigation Systems_. ASAE, St. Joseph, Michigan.

Kemper, W.D., B.J. Ruffing, and J.A. Bondurant. 1982. Furrow Intake Rates and Water Management. _Transactions of the ASAE_ 25(2):333-343.

Lewis, M.R. and W.E. Milne. 1938. Analysis of Border Irrigation. _Agricultural Engineering_ 19(6):267-272.

Lighthill, M.J. and R.B. Whitham. 1955. On Kinematic Waves: I. Flood Movement in Long Rivers. _Proceedings of the Royal Society of London_ A(229):201-316.

Nicolaescu, I. and E.G. Kruse. 1971. Automatic Cutback Furrow Irrigation System Design. _Journal of the Irrigation and Drainage Division_, ASCE 97(IR3):343-353.

Ross, E. 1983. USDA-SCS Engineer. Portland, Oregon. Personal communication.

Streeter, V.L. and E.B. Wylie. 1979. _Fluid Mechanics_. New York: McGraw-Hill, Inc.

Strelkoff, T. 1969. One-Dimensional Equations of Open-Channel Flow. _Journal of the Hydraulics Division_, ASCE 95(HY3):861-876.

Strelkoff, T. 1970. Numerical Solution of Saint-Venant Equations. Journal of the Hydraulics Division, ASCE 96(HY1):223-252.

Strelkoff, T. and N.D. Katapodes. 1977. Border-Irrigation Hydraulics with Zero Inertia. _Journal of the Irrigation and Drainage Division_, ASCE 102(IR3):325-342.

Stringham, G.E. 1975. Design of Irrigation Runoff Recovery Systems. _Journal of the Irrigation and Drainage Division_, ASCE 101(IR3):209-219.

Stringham, G.E. and J.M. Keller. 1979. Surge Flow for Automatic Irrigation. Presented at the National ASCE Irrigation and Drainage Division Specialty Conference, Albuquerque, New Mexico, July.

USDA, Soil Conservation Service. 1974. Soil Survey - Central Point Series, Jackson County, Oregon.

USDA, Soil Conservation Service. 1979. Soil Survey - Central Point Series, Jackson County, Oregon.

USDA, Soil Conservation Service. 1983. Furrow Irrigation. National Engineering Handbook 15(5):1-73.

Walker, W.R. and T.S. Lee. 1981. Kinematic-Wave Approximations of Surge Flow Furrow Advance. ASAE Paper No. 81-2544, American Society of Agricultural Engineers.

Walker, W.R., H. Malano, and J.A. Replogle. 1982. Reduction in Infiltration Rates Due to Intermittent Wetting. ASAE Paper No. 82-2029, American Society of Agricultural Engineers.

Walker, W.R. (Chairman) and Ad Hoc Committee. 1982. Surge Flow Irrigation. Surge Flow Regional Research Project Paper.

Walker, W.R. and A.S. Humpherys. 1983. Kinematic Wave Furrow Irrigation Model. Journal of the Irrigation and Drainage Division, ASCE 109(4):377-392.

Weber, E. USDA-SCS District Manager, Medford, Oregon. Personal communication.

Zur, B. 1976. The Pulsed Irrigation Principle of Controlled Soil Wetting. Soil Science 122(5):282-291.

APPENDICES

APPENDIX A

CONTINUOUS FLOW GRADIENT FURROW DESIGN

The SCS design equations describe the relationship between furrow length (L), inflow time (Ti), inflow rate (Q), deep percolation (DP), surface runoff (RO), and application efficiency (AE) for the selected design values of application depth (Fn), soil intake family (If), furrow spacing (W), and field slope (S). The design method includes empirical equations which are used for describing advance time (Tt), intake opportunity time (To), gross application depth (Fg), and furrow wetted-perimeter (P). The values for the Manning retardance coefficient (n), taken as 0.04 for furrows, and the recession time (Tr), taken as zero for graded open-ended furrows, are general recommendations suggested for use in the design (USDA, 1983).

Table 6. Furrow-Intake Family and Advance Coefficients.

I_f	a	b	c	d
0.05	0.0210	0.6180	23.5040	5.2567×10^{-4}
.10	.0244	.6610	23.7975	6.0449×10^{-4}
.15	.0276	.6834	24.0908	6.8331×10^{-4}
.20	.0306	.6988	24.3841	7.6213×10^{-4}
.25	.0336	.7107	24.6773	8.4045×10^{-4}
.30	.0364	.7204	24.9706	9.1977×10^{-4}
.35	.0392	.7285	25.2639	9.9859×10^{-4}
.40	.0419	.7356	25.5511	1.0774×10^{-3}
.45	.0445	.7419	25.8504	1.1562×10^{-3}
.50	.0471	.7475	26.1436	1.2350×10^{-3}
.60	.0520	.7572	26.7302	1.3427×10^{-3}
.70	.0568	.7656	27.3167	1.5503×10^{-3}
.80	.0614	.7728	27.9032	1.7080×10^{-3}
.90	.0659	.7792	28.4898	1.8656×10^{-3}
1.00	.0703	.785	29.0763	2.0232×10^{-3}
1.50	.0899	.799	32.0090	2.8114×10^{-3}
2.00	.1084	.808	34.9416	3.5996×10^{-3}

Summary of Graded Furrow Equations

a & b = intake coefficients based on intake family as given in Table 6

c & d = advance coefficients based on intake family as given in Table 6

Adjusted Wetted Perimeter, P

$$P(ft) = 0.2686(Qn/S^{\frac{1}{2}})^{0.4247} + 0.7462 \qquad (A-1)$$

where Q is in gpm

and S is ft/ft

Advance Time, Tt

$$Tt(min) = \frac{X}{c} e^{(dX/QS^{\frac{1}{2}})} \qquad (A-2)$$

where X is furrow length to point X, feet

Intake Opportunity Time, To

$$To(min) = Ti - Tt + Tr \qquad (A-3)$$

where Ti is the inflow time, min

and Tr is assumed to be zero

The subscript, n, is used rather than o to describe the net opportunity time required for a cumulative intake, Fn.

Average Opportunity Time For Furrow Length(L), To-L

$$To\text{-}L(min) = Ti - \left\{ \frac{1}{cL(\frac{d}{QS^{\frac{1}{2}}})^2} (\frac{dL}{QS^{\frac{1}{2}}} - 1)e^{(dL/QS^{\frac{1}{2}})+1} \right\} \qquad (A-4)$$

where the subtracted value is the average

advance time(min) determined by the integra-

tion of equation A-2 between the limits of
zero and L, and divided by L.

Gross Application Depth, Fg

$$Fg(in) = \frac{1.6041QTi}{WL} \tag{A-5}$$

where W is in ft

Cumulative Intake At Design Point, Fn

$$Fn(in) = (aTn^b + 0.275)P/W \tag{A-6}$$

where Tn is in minutes

Average Cumulative Intake For Furrow Length(L), Fo-L

$$Fo-L = \{a(To-L)^b + 0.275\}P/W \tag{A-7}$$

Runoff Depth, RO

$$RO(in) = Fg - Fo-L \tag{A-8}$$

Deep Percolation, DP, and Application Efficiency, AE,
at L

$$DP(in) = Fg - RO - Fn \tag{A-9}$$

$$AE(\%) = 100\ Fn/Fg \tag{A-10}$$

Design of Graded Furrow

Information available:

Intake family: If = 0.8

Design Application Depth: Fn = 5.0 in

Length: L = 570 ft

Slope: S = 0.01 ft/ft

Spacing: W = 2.5 ft

Roughness Coefficient: n = 0.04

Inflow Rate: Q = 7 gpm

Procedure:

(1) Find intake and advance coefficients for the 0.8 intake family from Table A-1.

a=0.0614 b=0.7728 c=27.9032 d=1.7080x10^{-3}

(2) Compute the advance time for the 570-ft furrow, using equation A-2.

$$Tt = \frac{570}{27.9032} \; e \; \{\frac{(1.7080x10^{-3})(570)}{7(0.01)^{\frac{1}{2}}}\}$$

Tt = 82 min

(3) Calculate the wetted perimeter from equation A-1

$$P = 0.2686 \, (\frac{7x0.04}{0.01^{\frac{1}{2}}})^{0.4247} + 0.7462$$

P = 1.16 ft

(4) Calculate net opportunity time(Tn) required for design application(Fn) of 5.0 in using eq. A-6

$$Fn = (aTn^{b} + 0.275)P/W$$

$$Tn = \{\frac{(Fn \times W/P) - 0.275}{a}\}^{1/b}$$

$$Tn = \{\frac{(5 \times 2.5/1.16) - 0.275}{0.0614}\}^{1/.7728}$$

Tn = 774 min

(5) Determine the application time, Ti:

Ti = Tt + Tn = 82 + 774 = 856 min

(6) Calculate the average opportunity time (To-L) for
     the 570 ft length, using equation A-4.

Let $H = dL/QS^{\frac{1}{2}}$

$$= (1.708 \times 10^{-3})(570)/7(0.01)^{\frac{1}{2}}$$

$$= 1.3908$$

$$To\text{-}L = 856 - \frac{(H-1)e^{H+1}}{27.9032 \times 570(1.708 \times 10^{-3}/7 \times .01^{\frac{1}{2}})^2}$$

$$= 856 - 45$$

To-L = 811 min

(7) Calculate the gross application by equation A-5.

$$Fg = \frac{1.6041(7)(856)}{(2.5)(570)}$$

Fg = 6.75 in

(8) Compute the average intake for the entire furrow
     length, equation A-7.

$$Fo\text{-}L = (0.0614(811)^{.7728} + 0.275)\frac{1.16}{2.5}$$

Fo-L = 5.17 in

(9) Calculate the surface runoff, equation A-8.

RO = 6.75 - 5.17

RO = 1.58 in

(10) Calculate the deep percolation, equation A-9.

DP = 6.75 - 1.58 - 5.0

DP = 0.17 in

(11) Calculate the application efficiency, A-10.

AE = 100 × 5.0/6.75 = 74%

(12)   Summary of the results

If = 0.8

W = 2.5 ft

S = 0.01 ft/ft

Q = 7 gpm

L = 570 ft

Tt = 82 min

Ti = 856 min

RO = 1.58 in

DP = 0.17 in

AE = 74%

APPENDIX B

MODEL LISTING, FLOWCHART, AND SYMBOLS

```
      PROGRAM FURROW(INPUT,OUTPUT,TAPE5=INPUT,TAPE6=OUTPUT)
C****************    MAY 1983    ***************************
C        KINEMATIC-WAVE FURROW IRRIGATION MODEL FOR CONTINOUS
C                  AND SURGE FLOW
C
C                    BY DOUGLAS HUNSAKER
C************************************************************
      DIMENSION AJ(400),AR(400),AL(400),AM(400),AEX(400),ZRL(400)
      DIMENSION ZJ(400),ZR(400),ZL(400),ZM(400),ZEX(400),DX(400),Z(400)
      DIMENSION ARJ(400),DH(400),AAA(400),ZZZ(400),DK(400),ZS(400)
      DIMENSION DS(400),ZSUR(400),ATOT(400)
C***
C***                  INPUT DATA
C
      READ(5,*)NF,NSURGE
      READ(5,*)Q,SK,A,FO,F,D,L
      READ(5,*)KT,SO,FN,ETA,PHI
      IF(NF.EQ.2)READ(5,*)R1,R2,A1
C***            PRINT VALUES OF INPUT DATA
C
      PRINT 21
   21 FORMAT(//)
      PRINT*,'FURROW INFLOW IN M**3/SEC= ',Q
      PRINT*,'FIELD SLOPE IN M/M        = ',SO
      PRINT*,'MANNINGS N                = ',FN
      PRINT*,'CONTINOUS FLOW INFILTRATION PARAMETERS'
      PRINT*,'                      K= ',SK
      PRINT*,'                      A= ',A
      PRINT*,'                     FO= ',FO
      PRINT*,'SPATIAL AVERAGING FACTOR = ',PHI
      PRINT*,'TEMPORAL "       "      "    = ',ETA
C
      PRINT*,'DELTA TIME IN MINUTES    = 1.0'
      PRINT*,'MAXIMUM TIME OF RUN,MIN  = ',L
      PRINT*,'TIME OF CUTOFF IN MINUTES= ',KT
      PRINT*,'FURROW GEOMETRY PARAMETERS'
      PRINT*,'                     RHO1= ',D
      PRINT*,'                     RHO2= ',F
      IF(NF.EQ.1)GO TO 15
      PRINT*,'SURGE FLOW INFILTRATION PARAMETERS'
      PRINT*,'                      K= ',R1
      PRINT*,'                      A= ',A1
      PRINT*,'                     FO= ',R2
C
C***COMPUTE EQUATION CONSTANTS***********
   15 P=F/2.
      C=SQRT(D*SO)/FN
      CON=(1.0-PHI-ETA)/(C*ETA)
      AET=C*ETA
C******INITIALIZE AO,ZO,AND FIRST INCREMENT DX/DT*************
      AO=(Q/C)**(1./P)
      ZO=SK+FO
      DL=0.0
      ICOUNT=1
      AH=0.05*AO
      CUMZ=0.0
      AR(1)=AO
      DO 20 I=1,L
      ZRL(I)=0.0
      ARJ(I)=0.0
```

```fortran
      Z(I)=0.0
      ATOT(I)=50.
 20   CONTINUE
      DX(1)=Q/(AO+ZO)
C****BEGIN SIMULATION,EACH I=1 MINUTE,J DEFINES CELL NUMBER*****
      DO 100 I=1,L
      IF(ATOT(1).LE.AH)AR(1)=0.0
      IF(ATOT(1).LE.AH)AM(1)=0.0
      IF(ATOT(1).LE.AH)GO TO 30
      AL(1)=AO
      AM(1)=AO
      IF(I.GT.KT)AL(1)=0.05*AO
      IF(I.GT.KT+1)AM(1)=0.05*AO
      IF(I .EQ. 1)GO TO 70
 30   ZL(1)=SK*FLOAT(I)**A+FO*FLOAT(I)
      ZM(1)=SK*FLOAT(I-1)**A+FO*FLOAT(I-1)
 31   ZR(1)=ZM(1)
      ZEX(I)=ZR(1)
      IF(ATOT(1).LE.AH)GO TO 43
 40   C1=CON*DX(1)
      C2=-(CON*ZR(1)*DX(1))+AL(1)**P-((AL(1)+ZL(1))*PHI*DX(1))/AET+
     $((AM(1)+ZM(1))*(1.-ETA)*DX(1))/AET
      TR=AO*.95
      AR(1)=RHAP(TR,C1,C2,P)
 45   ATOT(1)=(AL(1)+AM(1))/2.
      IF(ATOT(1).LE.AH)ZRL(1)=ZR(1)
      IF(ATOT(1).LE.AH)ARJ(1)=ATOT(1)
      IF(ATOT(1).LE.AH)AL(1)=0.0
      IF(I .EQ. 2)AEX(1)=AR(1)
      IF(I .EQ. 2)GO TO 60
 43   N=I-1
      K=I-1
C*****COMPUTE INTERIOR CELLS FLOW PROFILE**********
 41   DO 50 J=2,N
      ZM(J)=ZEX(K)
      K=K-1
      ZR(J)=ZM(J)
      ZL(J)=ZR(J-1)
      ZJ(J)=ZL(J)
      IF(ATOT(J).LE.AH)AM(J)=0.0
      IF(ATOT(J).LE.AH)GO TO 48
      AL(J)=AR(J-1)
      AJ(J)=AM(J-1)
      AM(J)=AEX(J-1)
      IF(ATOT(J).LE.AH)GO TO 48
      C1=CON*DX(J)
      C2=-(CON*ZR(J)*DX(J))+AL(J)**P+((1.-ETA)/ETA)*AJ(J)**P-
     $((1.-ETA)/ETA)*AM(J)**P-((AL(J)+ZL(J))/AET)*(PHI*DX(J)+
     $ETA*DX(J-1))+((AJ(J)+ZJ(J))/AET)*(PHI*DX(J-1)-(1.-ETA)*DX(J-1))
     $+((AM(J)+ZM(J))/AET)*((1.-PHI)*DX(J-1)+(1.-ETA)*DX(J))
      TR=AO*.95
 49   AR(J)=RHAP(TR,C1,C2,P)
      ATOT(J)=(AJ(J)+AL(J))/2.
      IF(ATOT(J).LE.AH)ZRL(J)=ZR(J)
      IF(ATOT(J).LE.AH)ARJ(J)=ATOT(J)
      IF(ATOT(J).LE.AH)ICOUNT=ICOUNT+1
      IF(ATOT(J).LE.AH)AL(J)=0.0
      IF(ATOT(J).LE.AH)AJ(J)=0.0
      IF(ATOT(J).LE.AH.AND.ICOUNT.EQ.N)GO TO 101
 48   AEX(J-1)=AL(J)
```

```
      IF(J .EQ. N)AEX(J)=AR(J)
   50 CONTINUE
C******COMPUTE TIP CELL BOUNDARIES AND NEW INCREMENTAL ADVANCE*
   60 J=I
      ZL(J)=ZR(J-1)
      ZJ(J)=ZL(J)
      AL(J)=AR(J-1)
      AJ(J)=AM(J-1)
      IF(AL(J).LE.AH)DX(I)=.000001
      IF(AL(J).LE.AH)GO TO 70
   65 DX(I)=C*AL(J)**P/(AL(J)+ZL(J))
   70 DL=DL+DX(I)*60.
      DH(I)=DL
      IF(DX(I).NE..000001)GO TO 100
      DO 13 JX=1,N
      IF(ATOT(JX).LE.AH)GO TO 13
      ARJ(JX)=ATOT(JX)
      ZRL(JX)=ZR(JX)
   13 CONTINUE
      GO TO 101
  100 CONTINUE
  101 CONTINUE
      DO 110 IK=1,N
      Z(IK)=ZRL(IK)+ARJ(IK)
  110 CONTINUE
      IF(NF.EQ.1)WRITE(6,113)
  113 FORMAT(//,5X,'CONTINOUS FLOW ADVANCE-RECESSION TRAJECTORY')
      IF(NF.EQ.2)WRITE(6,114)
  114 FORMAT(//,5X,'ADVANCE-RECESSION TRAJECTORY FOR SURGE 1 ')
      WRITE(6,90)
      DO 115 M=1,N
      WRITE(6,95)M,DH(M),Z(M)
  115 CONTINUE
      WRITE(6,99)I
      DO 135 M=1,N
      CUMZ=CUMZ+Z(M)*DX(M)*60.
  135 CONTINUE
   90 FORMAT(/,10X,'TIME,MINUTES',10X,'ADVANCE,METERS',10X,
     $'CUM. INFILTRATION,M**3/M')
   95 FORMAT(15X,I3,18X,F8.2,18X,F8.5)
   99 FORMAT(/,5X,'RECESSION COMPLETE AT T= ',I3,' MINUTES')
      TINFLO=Q*60.0*FLOAT(KT)
      WRITE(6,131)
  131 FORMAT(//,' VOLUME BALANCE')
      WRITE(6,132)TINFLO
  132 FORMAT(9X,'TOTAL INFLOW= ',F7.2,' M**3')
      WRITE(6,133)CUMZ
  133 FORMAT(9X,'TOTAL INFILT= ',F7.2,' M**3')
      IF(NF.EQ.1)GO TO 940
      DO 299 IJK=1,NSURGE-1
C*
C*    INITIALIZE PARAMETERS FOR SURGE FLOW ********
C*
      DO 220 I=1,L
      ZZZ(I)=0.0
      ZS(I)=0.0
      AJ(I)=0.0
      AL(I)=0.0
      AM(I)=0.0
      AR(I)=0.0
```

```
      ZR(I)=0.0
      ZM(I)=0.0
      ZL(I)=0.0
      ZJ(I)=0.0
      AEX(I)=0.0
      ZEX(I)=0.0
      AAA(I)=0.0
      ATOT(I)=50.
C**********
  220 CONTINUE
C*********
      ZO=R1+R2
      ICOUNT=1
      DLS=0.0
      JJJ=0
      LL=150
      KB=0
      CUMZ=0.0
      AR(1)=A0
C*
C****   FIRST INCREMENTAL ADVANCE ****
C*
      DK(1)=Q/(A0+ZO)
C*
C**     BEGIN SIMULATION OF SURGE ****
      DO 300 I=1,L
      IF(ATOT(1).LE.AH)AR(1)=0.0
      IF(ATOT(1).LE.AH)AM(1)=0.0
      IF(ATOT(1).LE.AH)GO TO 330
      AL(1)=A0
      AM(1)=A0
      IF(I.GT.KT)AL(1)=AH
      IF(I.GT.KT+1)AM(1)=AH
      IF(I.EQ.1)GO TO 570
  330 ZL(1)=R1*FLOAT(I)**A1+R2*FLOAT(I)
      ZM(1)=R1*FLOAT(I-1)**A1+R2*FLOAT(I-1)
      ZR(1)=ZM(1)
      ZEX(I)=ZR(1)
      IF(ATOT(1).LE.AH)GO TO 343
  340 C1=CON*DK(1)
      C2=-(CON*ZR(1)*DK(1))+AL(1)**P-((AL(1)+ZL(1))*PHI*DK(1))/AET+
     $((AM(1)+ZM(1))*(1.-ETA)*DK(1))/AET
      TR=A0*.95
      AR(1)=RHAP(TR,C1,C2,P)
      ATOT(1)=(AL(1)+AM(1))/2.
      IF(ATOT(1).LE.AH)ZZZ(1)=ZR(1)
      IF(ATOT(1).LE.AH)AAA(1)=ATOT(1)
      IF(ATOT(1).LE.AH)AL(1)=0.0
  345 IF(I.EQ.2)AEX(1)=AR(1)
      IF(I.EQ.2)GO TO 500
  343 NS=I-1
      K=I-1
      DO 350 J=2,NS
      ZM(J)=ZEX(K)
      ZL(J)=ZR(J-1)
      ZJ(J)=ZL(J)
      ZR(J)=ZM(J)
      K=K-1
      IF(ATOT(J).LE.AH)AR(J)=0.0
      IF(ATOT(J).LE.AH)AM(J)=0.0
```

```
      IF(ATOT(J).LE.AH)GO TO 333
      AL(J)=AR(J-1)
      AJ(J)=AM(J-1)
      AM(J)=AEX(J-1)
  333 IF(DS(I-1).LT.DH(N))GO TO 347
      IF(DS(I-1).GE.DH(N).AND.JJJ.NE.0)GO TO 346
      IF(I-1.EQ.J)LL=I
      IF(I-1.EQ.J)JJJ=1
  346 IF(J.LT.LL)GO TO 347
      KB=I-J
      ZL(J)=SK*FLOAT(KB)**A+FO*FLOAT(KB)
      ZJ(J)=ZL(J)
      IF(KB.EQ.1)GO TO 347
      ZM(J)=SK*FLOAT(KB-1)**A+FO*FLOAT(KB-1)
      ZR(J)=ZM(J)
  347 IF(ATOT(J).LE.AH)GO TO 348
      C1=CON*DK(J)
      C2=-(CON*ZR(J)*DK(J))+AL(J)**P+((1.-ETA)/ETA)*AJ(J)**P-
     $((1.-ETA)/ETA)*AM(J)**P-((AL(J)+ZL(J))/AET)*(PHI*DK(J)+
     $ETA*DK(J-1))+((AJ(J)+ZJ(J))/AET)*(PHI*DK(J-1)-(1.-ETA)*DK(J-1))
     $+((AM(J)+ZM(J))/AET)*((1.-PHI)*DK(J-1)+(1.-ETA)*DK(J))
      TR=A0*.95
      AR(J)=RHAP(TR,C1,C2,P)
      ATOT(J)=(AJ(J)+AL(J))/2.
      IF(ATOT(J).GT.AH)GO TO 348
      ZZZ(J)=ZR(J)
      AAA(J)=ATOT(J)
      AL(J)=0.0
      AJ(J)=0.0
      ICOUNT=ICOUNT+1
      IF(ICOUNT.EQ.NS)GO TO 601
  348 AEX(J-1)=AL(J)
      IF(J.EQ.NS)AEX(J)=AR(J)
  350 CONTINUE
  500 J=I
      ZL(J)=ZR(J-1)
      ZJ(J)=ZL(J)
      AL(J)=AR(J-1)
      AJ(J)=AM(J-1)
      IF(AL(J).LE.AH)DK(I)=0.0000001
      IF(AL(J).LE.AH)GO TO 570
      DK(I)=C*AL(J)**P/(AL(J)+ZL(J))
  570 DLS=DLS+DK(I)*60.
      DS(I)=DLS
      IF(DK(I).NE..0000001)GO TO 300
  312 DO 313 JX=1,NS
      IF(ATOT(JX).LE.AH)GO TO 313
      AAA(JX)=ATOT(JX)
      ZZZ(JX)=ZR(JX)
  313 CONTINUE
      GO TO 601
  300 CONTINUE
C*****
C*******    CUMULATIVE INFILTRATION COMPUTATION
C*
  601 LN=I
      KK=0
      DO 700 I=1,NS
      IF(KK.NE.2)GO TO 603
      J=J+1
```

```
         KK=0
   603 ZLM=0.0
       IF(I.GT.1)GO TO 802
       DO 720 J=1,N
       IF(DS(I).GT.DH(1))GO TO 609
       ZS(I)=Z(1)
       KK=2
       IN=2
       GO TO 700
   609 IF(DS(I).GT.DH(J))GO TO 710
           DO 760 K=1,J-1
           ZLM=ZLM+Z(K)
   760     CONTINUE
       XYZ=(DS(I)-DH(J-1))/(DH(J)-DH(J-1))
       ZS(I)=(ZLM+Z(J)*XYZ+Z(J-1)*(1.-XYZ))/FLOAT(J)
       IN=J
       GO TO 700
   710 IF(J.NE.N)GO TO 720
           DO 770 K=1,N
           ZLM=ZLM+Z(K)
   770     CONTINUE
       ZS(I)=ZLM/FLOAT(N)
       GO TO 900
   720 CONTINUE
   802 XYH=(DS(I-1)-DH(J-1))/(DH(J)-DH(J-1))
       HHH=(1.-XYH)*Z(J)+XYH*Z(J-1)
       DO 820 J=IN,N
       IF(DS(I).LE.DH(IN))ZS(I)=HHH
       IF(DS(I).LE.DH(IN))IN=IN+1
       IF(DS(I).LE.DH(IN-1))KK=2
       IF(DS(I).LE.DH(IN-1))GO TO 700
       IF(DS(I).GT.DH(J))GO TO 810
       DO 860 K=IN,J-1
       ZLM=ZLM+Z(K)
   860 CONTINUE
       XYZ=(DS(I)-DH(J-1))/(DH(J)-DH(J-1))
       ZS(I)=(ZLM+Z(J)*XYZ+Z(J-1)*(1.-XYZ)+HHH)/FLOAT((J+2)-IN)
       IN=J
       GO TO 700
   810 IF(J.NE.N)GO TO 820
       DO 870 K=IN,N
       ZLM=(ZLM+Z(K)+HHH)/FLOAT((N+2)-IN)
   870 CONTINUE
       ZS(I)=ZLM
       GO TO 900
   820 CONTINUE
   700 CONTINUE
   900 CONTINUE
       DO 1000 M=1,NS
       ZSUR(M)=ZS(M)+ZZZ(M)+AAA(M)
  1000 CONTINUE
       IHH=IJK+1
       WRITE(6,1003)IHH
  1003 FORMAT(//,5X,'ADVANCE-RECESSION TRAJECTORY FOR SURGE ',I3)
       PRINT*,CUMZ
       DO 1005 M=1,NS
       CUMZ=CUMZ+ZSUR(M)*DK(M)*60.
  1005 CONTINUE
       TINFLO=Q*60.0*FLOAT(KT)*FLOAT(IHH)
   605 WRITE(6,90)
```

```
      DO 630 M=1,NS
      WRITE(6,95)M,DS(M),ZSUR(M)
630   CONTINUE
      WRITE(6,99)LN
      WRITE(6,131)
      WRITE(6,132)TINFLO
      WRITE(6,133)CUMZ
      IF(IJK.EQ.NSURGE-1)GO TO 940
      DO 901 I=1,NS
      DH(I)=DS(I)
      Z(I)=ZSUR(I)
901   CONTINUE
      N=NS
299   CONTINUE
940   STOP
      END
      FUNCTION RHAP(X,Q1,Q2,P1)
      DO 200 K=1,50
      IF(X.LE.0.0)X=0.0
      H=X**P1+Q1*X-Q2
      H1=P1*(X**(P1-1.))+Q1
      R=-H/H1
      Y=X*.0001
      IF(ABS(R).LE.Y)GO TO 150
      IF(K.EQ.50)GO TO 150
      X=X+R
      GO TO 200
150   RHAP=X
      RETURN
200   CONTINUE
      RETURN
      END
```

Program Flowchart

Start → Read Input: Q, S_O, KT, NF, etc. → Print Input → Compute all Equation Constants: α, m+1, etc. → Initialize: A_O, Z_O, etc.

Is I.GT.KT? — Yes → / No ↓

I=I+1 ← Compute First Incremental Advance DX(1) ← Begin Advance Phase I=Time=1

Compute Flow Profile at Time=I, For All Cells J=1,I → Update all Values of A and Z For All Cells J=1,I → Compute Incremental Advance DX(I)

Begin Recession Phase, $A_L(1)=.05A_O$

Compute Flow Profile For Time=I For All Cells. Update & Compute DX(I). ← $A_M(1)=.05A_O$ ← Yes — Is I-KT=2? — No

I=I+1

Is ATOT(J) .LE..05 A_O? — No → All ATOT(J) Checked? — Yes → Is $A_L(I)$ .LE..05A_O? — No →

All ATOT(J) .LE..05 A_O? — No / Yes

Move Cell Boundary Up By 1

Add All Remaining ATOT(J) To Z(J)

Update All Values For Surge Flow

Compute Total Inflow & Cumulative Infiltration → Print Results → A Surge Cycle? — Yes → All Surges Over? — No / Yes → End

Description of Program Symbols

Arrays

AJ, AR, AL, AM = Cell boundary cross-sectional area, array number indicates cell number at any given time line.

ZJ, ZR, ZL, ZM = Cell boundary cumulative infiltration.

AEX = Area exchange variable for interchanging area from one time line to the next.

ZEX = Infiltration exchange variable.

ZRL = Cumulative infiltration at time cell recedes to less than or equal 5% of inlet area (continuous flow).

ZZZ = Cumulative infiltration at time cell recedes to less than or equal 5% of inlet area (surge flow).

ARJ = Area at time cell recedes to less than or equal 5% of inlet area (continuous flow).

AAA = Area at time cell recedes to less than or equal 5% of inlet area (surge flow).

ATOT = Average cell flow area at any time.

DX = Incremental value $\delta x/\delta t$ (continuous flow).

DK = Incremental value $\delta x/\delta t$ (surge flow).

DH = Incremental δx (continuous flow).

DS = Incremental $\delta \bar{x}$ (surge flow).

Z = Cumulative infiltration over $\delta \bar{x}_i$ (continuous flow).

ZSUR = Cumulative infiltration over δx_i (surge flow).

ZS = Interpolated infiltrated array variable for surge cumulative infiltrated volume.

Non-Arrays

NF = Status indicator for continuous or surge flow.

NSURGE = Number of surge cycles.

Q = Furrow inflow rate.

SO = Field slope.

FN = Mannings n.

$F = \rho_2$

$D = \rho_1$

$ETA = \theta$

$PHI = \phi$

KT = Time at which inflow is cut off.

SK = K, infiltration parameter, continuous flow).

A = a, infiltration parameter, continuous flow.

$FO = f_o$, infiltration parameter, continuous flow.

$Rl = K'$, infiltration parameter, surge flow.

$Al = a'$, infiltration parameter, surge flow.

$R2 = f_o'$, infiltration parameter, surge flow.

L = Maximum time for program run.

$AET = \alpha\theta$

$CON = 1-\phi-\theta/\alpha\theta$

$P = m+1$

$C = \alpha$

$AO = A_o$

$ZO = Z_o$

IJ, JN = Status indicators.

CUMZ = Cumulative infiltration over whole advance.

TR = Dummy argument for Newton-Rhapson procedure.

N = Number of interior cells at any time.

Cl = C_1

C2 = C_2

DL = Cumulative advance length, continuous or first surge.

TINFLO = Total inflow.

AH = 5% of AO.

DLS = Cumulative advance length, surge 2 and on.

JJJ = Status indicator.

LL = Status indicator.

KB = Time count for dry advance during surge.

NS = Number interior cells during surge.

ZLM, XYZ, XYH, HHH = Interpolation variables.

IHH = Surge cycle count.

FUNCTION RHAP = Newton-Rhapson procedure function.

X, Q1, Q2, P1 = Dummy arguments, Newton-Rhapson.

H, H1, R, Y = Newton-Rhapson procedure variables.

APPENDIX C

PROGRAM OUTPUT - CONTINUOUS FLOW

```
FURROW INFLOW IN M**3/SEC= .000442
FIELD SLOPE IN M/M         = .01
MANNINGS N                 = .04
CONTINOUS FLOW INFILTRATION PARAMETERS
                    K= .00357
                    A= .485
                    FO= .000169
SPATIAL AVERAGING FACTOR = .5
TEMPORAL  "        "     = .6
DELTA TIME IN MINUTES    = 1.0
MAXIMUM TIME OF RUN,MIN  = 185
TIME OF CUTOFF IN MINUTES= 180
FURROW GEOMETRY PARAMETERS
                 RHO1= .267
                 RHO2= 2.657
*TIME LIMIT*
ENTER T TO CONTINUE OR PRESS RETURN TO STOP:
T
```

CONTINOUS FLOW ADVANCE-RECESSION TRAJECTORY

TIME,MINUTES	ADVANCE,METERS	CUM. INFILTRATION,M**3/M
1	4.28	.07514
2	7.84	.07522
3	10.61	.07520
4	13.04	.07515
5	15.10	.07520
6	16.98	.07508
7	18.64	.07489
8	20.18	.07466
9	21.59	.07441
10	22.92	.07414
11	24.15	.07387
12	25.32	.07358
13	26.42	.07329
14	27.47	.07299
15	28.47	.07270
16	29.42	.07240
17	30.34	.07210
18	31.22	.07179
19	32.06	.07149
20	32.88	.07118
21	33.67	.07088
22	34.43	.07057
23	35.17	.07026
24	35.88	.06995
25	36.58	.06964
26	37.25	.06933
27	37.91	.06902
28	38.55	.06871
29	39.17	.06840
30	39.77	.06809
31	40.37	.06778
32	40.94	.06747
33	41.51	.06715
34	42.06	.06684
35	42.60	.06653
36	43.13	.06621
37	43.65	.06590
38	44.15	.06559

39	44.65	.06527
40	45.14	.06496
41	45.61	.06464
42	46.08	.06432
43	46.54	.06401
44	46.99	.06369
45	47.44	.06337
46	47.87	.06306
47	48.30	.06274
48	48.73	.06242
49	49.14	.06210
50	49.55	.06178
51	49.95	.06146
52	50.35	.06114
53	50.73	.06082
54	51.12	.06050
55	51.50	.06018
56	51.87	.05986
57	52.24	.05954
58	52.60	.05921
59	52.95	.05889
60	53.31	.05856
61	53.65	.05824
62	53.99	.05791
63	54.33	.05759
64	54.67	.05726
65	54.99	.05694
66	55.32	.05661
67	55.64	.05628
68	55.96	.05595
69	56.27	.05562
70	56.58	.05529
71	56.88	.05496
72	57.19	.05463
73	57.48	.05430
74	57.78	.05397
75	58.07	.05363
76	58.36	.05330
77	58.64	.05296
78	58.93	.05263
79	59.20	.05229
80	59.48	.05196
81	59.75	.05162
82	60.02	.05128
83	60.29	.05094
84	60.55	.05060
85	60.82	.05026
86	61.07	.04992
87	61.33	.04957
88	61.58	.04923
89	61.84	.04889
90	62.08	.04854
91	62.33	.04820
92	62.57	.04785
93	62.82	.04750
94	63.06	.04715
95	63.29	.04680
96	63.53	.04645
97	63.76	.04610
98	63.99	.04575
99	64.22	.04539
100	64.45	.04504
101	64.67	.04468

102	64.89	.04432
103	65.11	.04397
104	65.33	.04361
105	65.55	.04324
106	65.76	.04288
107	65.98	.04252
108	66.19	.04215
109	66.40	.04179
110	66.60	.04142
111	66.81	.04105
112	67.01	.04068
113	67.22	.04031
114	67.42	.03994
115	67.62	.03956
116	67.82	.03919
117	68.01	.03881
118	68.21	.03843
119	68.40	.03805
120	68.59	.03767
121	68.78	.03729
122	68.97	.03690
123	69.16	.03651
124	69.35	.03612
125	69.53	.03573
126	69.71	.03534
127	69.89	.03494
128	70.07	.03455
129	70.25	.03415
130	70.43	.03374
131	70.61	.03334
132	70.78	.03293
133	70.96	.03253
134	71.13	.03211
135	71.30	.03170
136	71.47	.03128
137	71.64	.03087
138	71.81	.03044
139	71.98	.03002
140	72.14	.02959
141	72.31	.02916
142	72.47	.02873
143	72.63	.02829
144	72.80	.02785
145	72.96	.02740
146	73.12	.02695
147	73.27	.02650
148	73.43	.02604
149	73.59	.02558
150	73.74	.02512
151	73.90	.02465
152	74.05	.02417
153	74.20	.02369
154	74.35	.02321
155	74.50	.02271
156	74.65	.02222
157	74.80	.02171
158	74.95	.02120
159	75.10	.02068
160	75.24	.02015
161	75.39	.01962
162	75.53	.01908
163	75.67	.01852
164	75.82	.01796

165	75.96	.01738
166	76.10	.01679
167	76.24	.01619
168	76.38	.01558
169	76.52	.01494
170	76.65	.01429
171	76.79	.01362
172	76.93	.01292
173	77.06	.01219
174	77.19	.01144
175	77.33	.01064
176	77.46	.00979
177	77.59	.00889
178	77.72	.00790
179	77.86	.00680
180	77.98	.00552
181	78.11	.00390

RECESSION COMPLETE AT T= 182 MINUTES

VOLUME BALANCE
          TOTAL INFLOW=   4.77 M**3
          TOTAL INFILT=   4.77 M**3
    37.908 CP SECONDS EXECUTION TIME.

APPENDIX D

PROGRAM OUTPUT - 1:3 CYCLE RATIO SURGE FLOW

```
FURROW INFLOW IN M**3/SEC= .000442
FIELD SLOPE IN M/M        = .01
MANNINGS N                = .04
CONTINOUS FLOW INFILTRATION PARAMETERS
                      K= .00357
                      A= .485
                      FO= .000169
SPATIAL AVERAGING FACTOR = .5
TEMPORAL  "       "   "  = .6
DELTA TIME IN MINUTES    = 1.0
MAXIMUM TIME OF RUN,MIN  = 31
TIME OF CUTOFF IN MINUTES= 15
FURROW GEOMETRY PARAMETERS
                  RHO1= .267
                  RHO2= 2.657
SURGE FLOW INFILTRATION PARAMETERS
                      K= .00175
                      A= .1003
                      FO= .00008
```

ADVANCE-RECESSION TRAJECTORY FOR SURGE 1

TIME,MINUTES	ADVANCE,METERS	CUM. INFILTRATION,M**3/M
1	4.28	.01653
2	7.84	.01640
3	10.61	.01640
4	13.04	.01588
5	15.10	.01785
6	16.98	.01732
7	18.64	.01656
8	20.18	.01600
9	21.59	.01557
10	22.92	.01506
11	24.15	.01429
12	25.32	.01351
13	26.42	.01312
14	27.47	.01231
15	28.47	.01161
16	29.38	.01079
17	29.93	.00990
18	30.38	.00918
19	30.75	.00818
20	31.89	.00708
21	32.64	.00572
22	32.91	.00397

RECESSION COMPLETE AT T= 23 MINUTES

```
VOLUME BALANCE
      TOTAL INFLOW=   .40 M**3
      TOTAL INFILT=   .48 M**3
```

ADVANCE-RECESSION TRAJECTORY FOR SURGE 2

0.

TIME,MINUTES	ADVANCE,METERS	CUM. INFILTRATION,M**3/M
1	6.18	.02021
2	12.21	.01989
3	18.05	.02031
4	23.78	.01929

5	29.38	.01615
6	34.88	.00585
7	40.27	.01479
8	41.79	.01472
9	44.44	.01364
10	45.54	.01275
11	47.47	.01210
12	48.91	.01134
13	50.23	.01077
14	51.48	.00980
15	52.64	.00883
16	53.74	.00834
17	54.77	.00706
18	55.66	.00560
19	55.95	.00425
20	56.41	.00220

RECESSION COMPLETE AT T= 21 MINUTES

VOLUME BALANCE
   TOTAL INFLOW=   .80 M**3
   TOTAL INFILT=   .85 M**3

ADVANCE-RECESSION TRAJECTORY FOR SURGE   3
0.

TIME,MINUTES	ADVANCE,METERS	CUM. INFILTRATION,M**3/M
1	6.18	.02392
2	12.21	.02345
3	18.05	.02381
4	23.78	.02279
5	29.38	.01965
6	34.88	.00935
7	40.27	.01829
8	45.56	.01721
9	50.76	.01482
10	55.87	.01143
11	60.89	.00710
12	65.83	.01260
13	66.91	.01269
14	69.30	.01156
15	70.37	.01058
16	72.09	.01013
17	73.36	.00912
18	74.55	.00796
19	75.65	.00684
20	76.41	.00598
21	77.72	.00413
22	78.66	.00210

RECESSION COMPLETE AT T= 23 MINUTES

VOLUME BALANCE
   TOTAL INFLOW=   1.19 M**3
   TOTAL INFILT=   1.25 M**3

ADVANCE-RECESSION TRAJECTORY FOR SURGE   4
0.

TIME,MINUTES	ADVANCE,METERS	CUM. INFILTRATION,M**3/M
1	6.18	.02763
2	12.21	.02701
3	18.05	.02731
4	23.78	.02628
5	29.38	.02314
6	34.88	.01285
7	40.27	.02179
8	45.56	.02086
9	50.76	.01866
10	55.87	.01490
11	60.89	.01047
12	65.83	.01623
13	70.69	.01521
14	75.46	.01263
15	80.16	.00647
16	84.78	.01001
17	85.55	.00887
18	87.77	.00762
19	88.81	.00626
20	90.33	.00448
21	91.22	.00236

RECESSION COMPLETE AT T= 22 MINUTES

VOLUME BALANCE
        TOTAL INFLOW=   1.59 M**3
        TOTAL INFILT=   1.63 M**3

ADVANCE-RECESSION TRAJECTORY FOR SURGE   5
0.

TIME,MINUTES	ADVANCE,METERS	CUM. INFILTRATION,M**3/M
1	6.18	.03135
2	12.21	.03056
3	18.05	.03080
4	23.78	.02978
5	29.38	.02664
6	34.88	.01634
7	40.27	.02528
8	45.56	.02433
9	50.76	.02214
10	55.87	.01830
11	60.89	.01387
12	65.83	.01934
13	70.69	.01832
14	75.46	.01575
15	80.16	.00982
16	84.78	.01351
17	89.32	.01061
18	93.79	.00661
19	98.18	.00907
20	98.75	.00849

21	100.79	.00702
22	101.39	.00589
23	101.90	.00407
24	104.22	.00203

RECESSION COMPLETE AT T= 25 MINUTES

VOLUME BALANCE
        TOTAL INFLOW=   1.99 M**3
        TOTAL INFILT=   2.03 M**3
        •

ADVANCE-RECESSION TRAJECTORY FOR SURGE   6
0.

TIME,MINUTES	ADVANCE,METERS	CUM. INFILTRATION,M**3/M
1	6.18	.03506
2	12.21	.03412
3	18.05	.03430
4	23.78	.03327
5	29.38	.03014
6	34.88	.01984
7	40.27	.02878
8	45.56	.02785
9	50.76	.02562
10	55.87	.02170
11	60.89	.01727
12	65.83	.02244
13	70.69	.02142
14	75.46	.01886
15	80.16	.01292
16	84.78	.01693
17	89.32	.01425
18	93.79	.00988
19	98.18	.01201
20	102.50	.00911
21	106.72	.00509
22	110.78	.00707
23	113.53	.00634
24	114.68	.00412
25	116.12	.00209

RECESSION COMPLETE AT T= 26 MINUTES

VOLUME BALANCE
        TOTAL INFLOW=   2.39 M**3
        TOTAL INFILT=   2.44 M**3

ADVANCE-RECESSION TRAJECTORY FOR SURGE   7
0.

TIME,MINUTES	ADVANCE,METERS	CUM. INFILTRATION,M**3/M
1	6.18	.03878
2	12.21	.03748
3	18.05	.03780
4	23.78	.03677
5	29.38	.03363
6	34.88	.02334
7	40.27	.03227

8	45.56	.03135
9	50.76	.02911
10	55.87	.02510
11	60.89	.02067
12	65.83	.02555
13	70.69	.02453
14	75.46	.02197
15	80.16	.01603
16	84.78	.02034
17	89.32	.01789
18	93.79	.01315
19	98.18	.01496
20	102.50	.01197
21	106.72	.00788
22	110.78	.00989
23	114.55	.00847
24	117.84	.00657
25	120.45	.00258

RECESSION COMPLETE AT T= 26 MINUTES

VOLUME BALANCE
        TOTAL INFLOW=   2.78 M**3
        TOTAL INFILT=   2.85 M**3

ADVANCE-RECESSION TRAJECTORY FOR SURGE   8
0.

TIME,MINUTES	ADVANCE,METERS	CUM. INFILTRATION,M**3/M
1	6.18	.04249
2	12.21	.04124
3	18.05	.04129
4	23.78	.04027
5	29.38	.03713
6	34.88	.02683
7	40.27	.03577
8	45.56	.03484
9	50.76	.03259
10	55.87	.02850
11	60.89	.02407
12	65.83	.02866
13	70.69	.02764
14	75.46	.02507
15	80.16	.01913
16	84.78	.02376
17	89.32	.02152
18	93.79	.01643
19	98.18	.01790
20	102.50	.01484

21	106.72	.01068
22	110.78	.01270
23	114.55	.01125
24	117.84	.00929
25	120.45	.00516

RECESSION COMPLETE AT T= 26 MINUTES

VOLUME BALANCE
        TOTAL INFLOW=   3.18 M**3
        TOTAL INFILT=   3.24 M**3
    6.448 CP SECONDS EXECUTION TIME.